



TEAM CEMENT3D

Final Project Report for MEAM 445/446

September 2017—April 2018

Submitted: April 30, 2018

Team Members

Sarah Allen

Karim Bolous

Miranda Cravetz

Krish Mehta

Chris Painter

Faculty Advisor

Dr. Jordan Raney

*Assistant Professor, Mechanical Engineering and Applied Mechanics, University of
Pennsylvania*

Technical Advisor

Dr. Bruce Kothmann

Senior Lecturer, Mechanical Engineering and Applied Mechanics, University of Pennsylvania

Instructor

Dr. Graham Wabiszewski

Senior Lecturer, Mechanical Engineering and Applied Mechanics, University of Pennsylvania

Abstract

Recent advances in additive manufacturing have made it possible for nearly anyone to participate in the so-called “maker movement”. However, projects are limited by restrictions on size and material. For large home projects, or those which require strong parts, homeowners must rely on more costly and time-intensive, traditional processes. To address this need, Team CEMENT3D is developing a user-friendly, portable, 3D printer that can build highly customizable structures.

To undertake this challenge, CEMENT3D first began by testing and analyzing the mechanical and material properties of cement to validate the feasibility of 3D printing concrete at the human scale. CEMENT3D then proceeded to design and prototype portable structures that were efficiently able to satisfy the systems’ loading, torsional and bending characteristics. Finally, the team designed an actuation system capable of precisely controlling a print head. The result is a 3D printer that enables a user to print structures comprised of multiple layers of concrete.

CEMENT3D’s final 3D printer weighs only 40lbs, despite having a relatively large print area of 1m x 1m x 0.5m. The printer fits in a 1.25m x 1.25m x 1.25m cube, can be assembled together within an hour by two people, and is anticipated to have a user rental price of \$200 over a period of 10 days. With this printer, CEMENT3D hopes to enable homeowners to conveniently build dog kennels, patios, or fire pits at the simple push of a button.

Table of Contents

1 Executive Summary.....	4
2 Statement of roles and external contributions.....	6
3 Background.....	8
3.1 Market.....	8
3.2 Printing.....	11
4 Objectives and Standards.....	12
4.1 Objectives.....	12
4.2 Design impact of standards.....	13
4.2.1 Concrete standards.....	13
4.2.2 Ingress Protection.....	16
5 Design and Realization.....	18
5.1 System-level Concept Solution.....	18
5.2 Structural Mechanics of System.....	20
5.3 Print Head.....	23
5.4 Cable Selection.....	26
5.5 Capstan.....	26
5.6 Motor Mount.....	28
5.7 Extrusion.....	30
5.7.1 Concrete Mixture Composition.....	30
5.7.2 Concrete Flow Characterization.....	31
5.7.3 Time between layer formation.....	33
5.7.4 Flow Rate.....	35
5.7.5 Tube.....	36
5.7.6 Linear Actuator Pump.....	39
5.7.7 Nozzle.....	40
5.8 Electronics.....	40
5.8.1 Basic Overview.....	40
5.8.2 Motor Selection.....	41
5.8.3 Motor Driver Selection.....	41
5.8.4 Power Supply Selection.....	42
5.8.5 Arduino Selection.....	42
5.8.6 Wiring.....	43
5.9 Programming.....	47
5.9.1 Basic Overview.....	47
5.9.2 Pre-Processing.....	48
5.9.3 Arduino Code.....	49

5.10 Non-critical systems.....	50
5.10.1 Pulley.....	50
5.10.2 Turntable / Lazy Susan.....	51
5.10.3 Surface Area Fins.....	52
5.10.4 Universal Joints.....	52
5.10.5 Tube Ring.....	53
6 Validation and testing.....	54
6.1 Validation of Concrete.....	54
6.1.1 Deformation of concrete layers.....	54
6.1.2 Compressive strength test of concrete.....	55
6.1.3 Compressive strength test of different concrete ratio mixes.....	56
6.1.4 Extrusion.....	57
6.2 Validation of Actuation.....	58
6.2.1 Virtual Validation.....	58
6.2.2 Real System Validation.....	65
7 Discussion.....	66
7.1 Target versus accomplished performance.....	66
7.2 Recommendations.....	67
8 Budget, donations, and resources.....	67
References.....	71
Appendix.....	75

1 Executive Summary

The Landscaping Services industry in the U.S. is worth approximately \$82 billion, and has grown by 4.8% annually over the past five years. In this \$82 billion industry, 13.8% of revenues are driven by design-build-installation services. Considering that 42.3% of this market is residential, the total addressable market for landscapers to build structures in residential areas is at least \$4.9 billion [1]. Homeowners currently address their landscaping needs by building structures themselves, by ordering pre-manufactured products, or by hiring contractors. However, each of these methods has drawbacks: building structures requires homeowners to input time and develop their skills, pre-manufactured products are rarely customizable, and hiring contractors can be expensive.

Given that 87% of the 112 homeowners surveyed by CEMENT3D feel that they lack either the time or the capabilities to build structures that they want for their homes, there is a need for a highly customizable, affordable, easy-to-use method which addresses homeowner's landscaping needs. To address this market need, CEMENT3D developed a user-friendly and portable, 3D printer, BUILDER, that can build highly customizable structures. BUILDER is a delta-style 3D printer designed to offer homeowners, interested in building customizable structures in a convenient manner, a more affordable solution compared to existing solutions such as contracting.

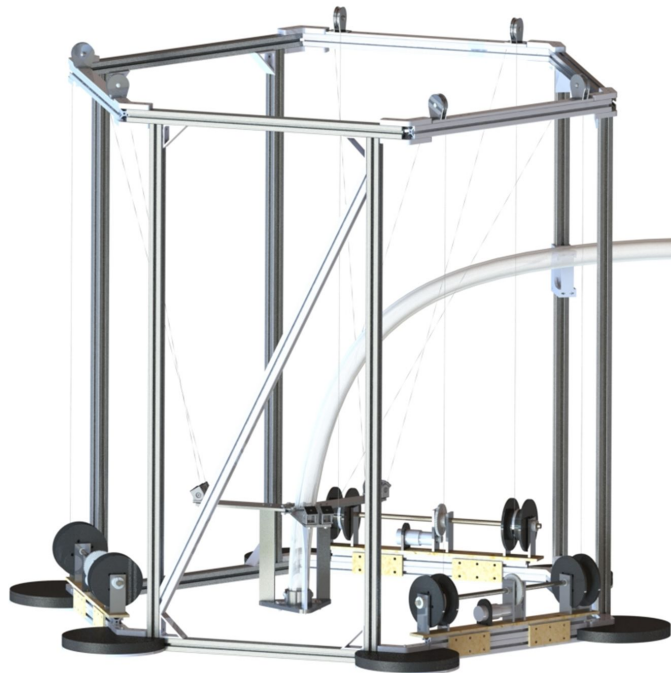


Figure 1.1: BUILDER: Delta-style, concrete 3D printer

A system of this type, a delta style 3D printer, was identified as the best solution because of the customizability of designs realizable by 3D printers, the relative convenience of transport and assembly of a delta design when compared to a cartesian alternative, and the ability to scale the print space, should someone decide to build upon the team's work for other highly-deployable concrete printers. A prototype that demonstrated the feasibility of controlling nozzle actuation and concrete extrusion, BUILDER, was designed to act as a proof-of-concept for commercial delta-style concrete printers.

Aside from the frame-based superstructure of the system, BUILDER is comprised of three main subsystems: actuation, extrusion, and print head. The actuation subsystem makes use of cables that change length according to the angular position of the capstans to which they are anchored. The relative lengths of these cables fully determine the position of the end-effector and the print head in three-dimensional space. The print head also interfaces with the extrusion system to provide concrete delivery, which makes use of a linear actuator acting as a positive displacement pump, in order to drive concrete flow through a 1.5" tube (the end of which is connected to a nozzle). The print head itself was designed with a wide arm space and a center of actuation close to the center of mass, keeping the nozzle in a stable orientation.

In seeking to present a useful product to address this market need, CEMENT3D focused on a set of seven performance objectives, arrived at via a Quality Function Deployment that can be seen in **Appendix B**. These metrics were: a print area of 0.5 m³, a cost of production less than \$1400, 12 pieces before assembly, a system weight of less than 445 Newtons, less than 25 user operations per print, a print resolution of 6cm, and a standard object print time under 20 minutes. Of these, the part count, user operations, print resolution, and print time objectives were exceeded, while the others were met with varying degrees of success.

Statement of roles and external contributions

Team Members



Sarah Allen
Controls | Manufacturing | Simulation



Karim Bolous
Extrusion | Mechanical Analysis | Assembly



Miranda Cravetz
Mechanical Design | Manufacturing



Krish Mehta
Extrusion | Documentation



Chris Painter
Mechanical Design | Assembly

Advisors



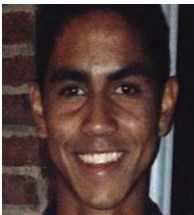
Dr. Jordan Raney, *Faculty Advisor*
Pumping and extruding concrete | Concrete fluid properties



Dr. Bruce Kothmann, *Technical Advisor*
Controls and electronics | print head stability



Dr. Graham Wabiszewski, *Instructor*
Design guidance | Project management



Dan Harris, *TA Advisor*
Design guidance | Controls and electronics | Documentation

Other Contributors

Chris Cecil, *RepRap Community*
Donated smoothieboard | Guidance on controls and electronics

Brett Harned, *Student*
Guidance on controls and electronics

Brian Zhang, *Student*
Project management advice

3 Background

3.1 Market

The U.S. landscaping industry has grown annually by 4.8%, over the past five years [1]. This growth is driven by increases in per capita disposable income, and increases in the number of households earning more than \$100,000 [1]. In this \$82 billion dollar industry, 13.8% of revenues are driven by design-build-installation services, as seen in **Figure 3.1**. Considering that 43.9% of this market is residential, as seen in **Figure 3.2**, the total addressable market for landscapers to build structures in residential areas is at least \$4.9 billion. This figure does not take into consideration the economic value of many Americans who build landscaping structures for their own homes.

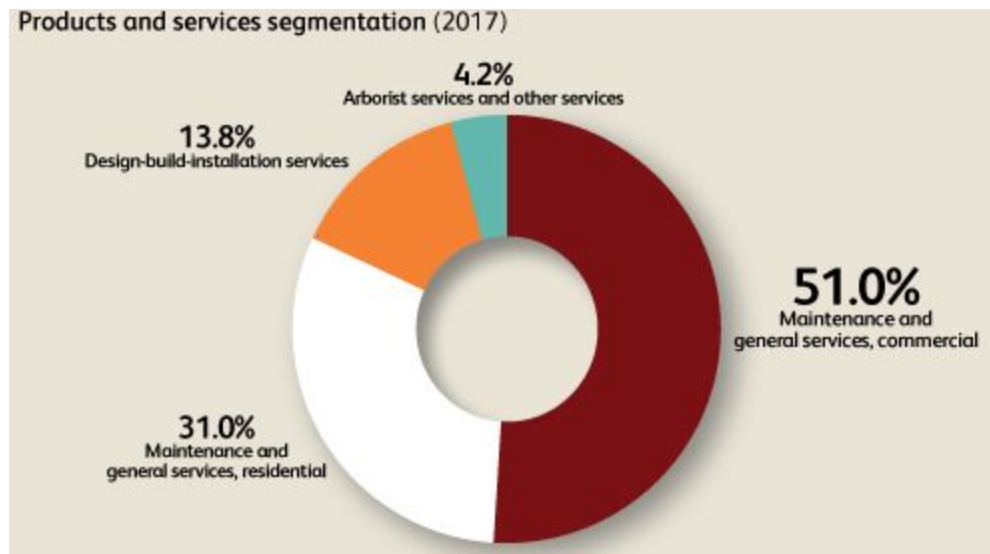


Figure 3.1: Landscaping industry segmentation by products and services [1]

Major Markets

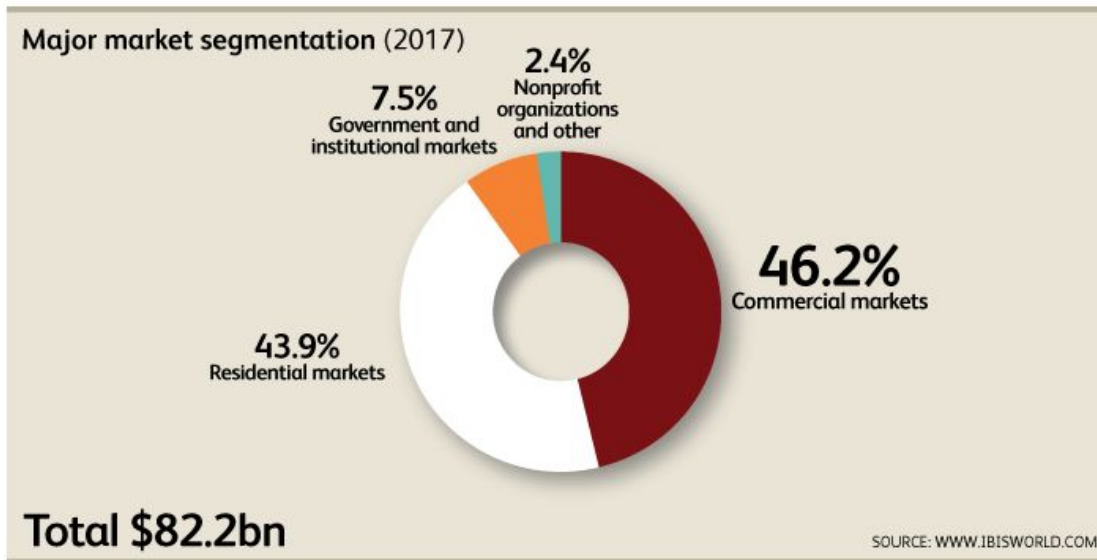


Figure 3.2: Major market segments in the landscaping industry [1]

To further understand this market, CEMENT3D sent out a survey to 112 homeowners that had backyards. The results of this survey revealed that 87% of respondents felt that they lacked either the time or the capabilities to build the features that they wanted for their houses. This was especially noteworthy given that 38% of respondents attempted to build something for their backyards, at least once a year. The team therefore sought to explore the options available to homeowners, and to isolate the aspects that prevented some homeowners from implementing them, in hopes of creating a more desirable alternative for these individuals. It was determined that homeowners currently meet their landscaping needs by either building structures themselves, purchasing prefabricated structures, or hiring contractors, each of which have their own drawbacks.

Do-It-Yourself (DIY)

As the name suggests, the process of “Do-It-Yourself” is one where the homeowner is directly involved in the construction of his or her structure. To build one’s own structure, a homeowner would have to invest the necessary time, and have the necessary skills to address his or her landscaping needs. The benefit of DIY is that homeowners are able to construct customizable structures that cater to their preferences.

Prefabricated Products

On the other end of the spectrum from DIY, homeowners can order a prefabricated, finished product. This offers homeowners a solution that is highly convenient, but one that does not give them the ability to benefit from customizable structures. Compared to the other solutions in this space, ordering a product typically takes the least amount of time, as the homeowner does not participate in the creation of the product.

Hiring Contract Workers

Within the small-scale construction solution space, contracting offers a solution that is both highly convenient for homeowners and would allow them to benefit from highly customizable structures. However, the main drawback behind contracting is its cost: a customized fire pit can cost up to \$1400 [2].

The benefits and costs of each of these methods is summarized in **Figure 3.3** below.

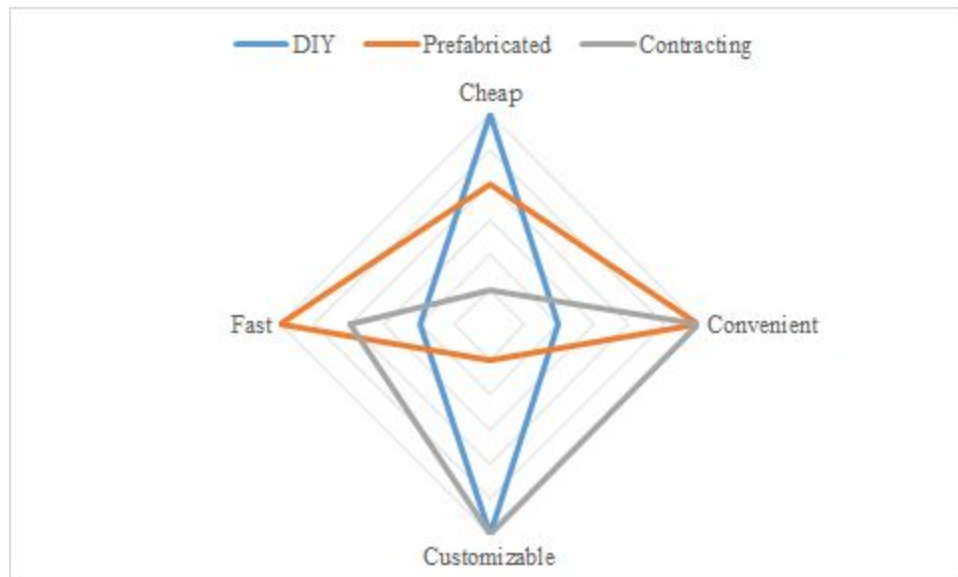


Figure 3.3: Relative comparison of existing solutions in the small-scale construction space

Figure 3.3 highlights the lack of solutions in the small-scale construction domain that offers homeowners a solution that is affordable, is convenient to use, can build customizable structures, and involves a low time investment.

Given the needs of the customer base, Team CEMENT3D set out to create a device that can automate the process of building landscaping structures. More specifically, the team set out to build a portable, 3D printer, that can print concrete structures. The team's device, BUILDER, not only taps into the \$4.9 billion market, but also increases the market size by including the DIY project space that was previously unaccounted for.

3.2 Printing

3D printing is a form of additive manufacturing used to create 3-dimensional objects layer-by-layer. One of the primary advantages of 3D printing is that it enables easy manufacturing of customized designs.

Broadly, there are four main types of 3D printing: Fused Deposition Modeling, Material Jetting, Stereolithography, and Laser Sintering. Team CEMENT3D chose to emulate Fused Deposition Modeling, a type of 3D printing where a material is made to flow and sent through a nozzle. Once the material passes through the nozzle, it solidifies and forms a layer. The team chose this type of 3D printing as it was most suited to 3D printing concrete.

The team further believes that, a portable, concrete 3D printer not only has relevant applications in the residential homeowner space, but also in the contracting, architectural, and infrastructure industries. Specifically, the team has spoken to contractors that have indicated interest in such a device to replace employees that may otherwise be required to build the landscaping structures for homeowners. Further, architecture companies have indicated in such a device to design prototypes for housing structures. Finally, the former President of the Metropolitan Transportation Agency in New York, Mysore Nagaraja, indicated that there is “potential scope” for such a device, as it would enable “lean construction” since “most of the public construction is very conventional”.

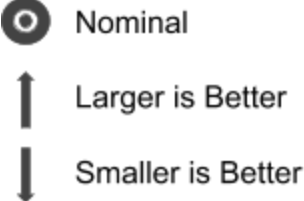
Thus, this portable, concrete 3D printer serves as a proof-of-concept that 3D printing concrete at a relatively small scale (1m^3) is a possibility.

4 Objectives and Standards

4.1 Objectives

As discussed above, the primary objective of CEMENT3D was to create a system that could fabricate concrete structures in a way that was desirable to its intended customers. In order to develop criteria that could measure the extent to which this objective was achieved, CEMENT3D compiled customer needs from the survey discussed in **Section 3** and performed a quality function deployment (QFD) to transform them into engineering characteristics. Only a single phase of QFD was performed, as determining part worth for cost-worth analysis, the task of later phases, was outside the scope of the project. A summary of the goals generated by this process is provided below. For more details on the process itself, see **Appendix B**.

Specification	Relative Importance	Desired Value	Direction of Increased Worth
Print Size	1	0.5 [m ³]	
Cost	2	\$1400 [USD] (based on user rental price of \$200)	
Pieces Before Assembly	2	12	
Weight	4	445 [N]	
User Operations per Print	5	25	
Print Resolution	6	6 [cm]	
Print Time	7	20 [min]	



 Nominal
 Larger is Better
 Smaller is Better

Table 4.1: QDF Objectives

4.2 Design impact of standards

4.2.1 Concrete standards

Team CEMENT3D identified standards to regulate the process for sampling freshly mixed concrete, for sampling hardened concrete, and for carrying out tensile strength tests on the concrete. All the concrete standards presented below were found from the ASTM International website, and are included in the References folder [3].

Standard Practice for Sampling Freshly Mixed Concrete: C172/C172M – 17

Standard C172/C172M - 17 highlights several industry standards for the sampling of concrete to carry out tests. Specifically, the standards listed below define the sample quantity and the time required between samples:

- 4.1 - ‘The elapsed time shall not exceed 15 min. Between obtaining the first and final portions of the composite sample’
- 4.1.1 - ‘Transport the individual samples to the place where fresh concrete tests are to be performed or where test specimens are to be molded. They shall be combined and remixed with a shovel the minimum amount necessary to ensure uniformity’
- 4.1.2 - ‘Start molding specimens for strength tests within 15 min after fabricating the composite sample.’
- 5.1 - ‘Make the samples to be used for strength tests a minimum of 28 L [1 ft³].’ ‘The size of the samples shall be dictated by the maximum aggregate size.’
- 6.3.2 - ‘Receptacle—A container of suitable size having nonabsorbent surface.’
- 6.3.4 - ‘Hand Tools—Shovels, hand scoops, plastering trowels, and rubber gloves as required.’

These standards guided the team’s procedure when sampling freshly mixed concrete for tests. This was especially relevant when carrying out the layer tests and when finding the optimal concrete:water ratio for the concrete mixture. Specifically, CEMENT3D concertededly took samples within 15 minutes of first mixing the concrete and the water. Further, with time (on the order of 5 - 10 minutes), the concrete mixture would begin to settle and so would be mixed using a hand scoop. Unfortunately, standard 5.1 was not adhered to due to logistical reasons of handling such large volumes of concrete; 6L of concrete was used for each of the tests. However, the size of the sample is dictated by the maximum aggregate size; given that the team used

concrete with only fine particle, the mixture is likely homogeneous, although this has not been formally validated.

Standard Practice for Examination and Sampling of Hardened Concrete in Constructions: C823/C823M – 12

Standard C823/C823M - 12 highlights certain standards regarding obtaining hardened concrete samples which were necessary to carry out tensile and shear tests:

- 13.1 - When hardened samples are extracted, ‘Caution should be used to avoid or to minimize fracturing the concrete or contamination of the sample with foreign substances. Use of sledges, chisels, and similar tools should be avoided.’

Standard 13.1 from C823/C823M was important when collecting hardened samples for the shear tests. To eliminate the fear of fracturing the concrete, and given the limitation of not using sledges, chisels or other tools, the team created small samples that could be tested in whole when undertaking compressive strength tests.

Standard Test Method for Density (Unit Weight), Yield, and Air Content (Gravimetric) of Concrete: C138/C138M – 17a

- 7.2 - Theoretical Density—Calculate the theoretical density as follows:
 $D = M / V$; Where M = total mass of all materials, V = total absolute volume of components
- 7.5 - Cement Content—Calculate the actual cement content as follows:
 $C = C_b / V$; Where C_b = mass of cement

C138/C138M - 17a provided the above standards that are useful for calculating the density of the concrete mixture and to better evaluate the efficiency of the use of cement as a material.

Standard Test Method for Compressive Strength of Cylindrical Concrete Specimens: C39/C39M – 18

- 1.1 - ‘This test method ... is limited to concrete having a density in excess of 800 kg/m³ [50 lb/ft³].’
- Apparatus:

- 6.1 - ‘Testing Machine—The testing machine shall be of a type having sufficient capacity and capable of providing the rates of loading stress rate on the specimen of 0.25 ± 0.05 MPa/s’
- 6.1.2.1 - The machine must be power operated and must apply the load continuously rather than intermittently, and without shock.
- 7.1 - ‘Specimens shall not be tested if any individual diameter of a cylinder differs from any other diameter of the same cylinder by more than 2 %.’
- 7.2 - ‘Prior to testing, neither end of test specimens shall depart from perpendicularity to the axis by more than 0.5° (approximately equivalent to 1 mm in 100 mm [0.12 in. in 12 in.]). The ends of compression test specimens that are not plane within 0.050 mm [0.002 in.] shall be sawed or ground to meet that tolerance’
- 8.3 - ‘Tolerances for specimen ages are as follows

Test Age	Permissible Tolerance
24 h	$\pm 0.5h$
3 days	$\pm 2h$
7 days	$\pm 6h$
28 days	$\pm 20h$
90 days	± 2 days

Table 4.2: Tolerance of time between samples at different test ages

- 8.5.3 - ‘Make no adjustment in the rate of movement (platen to crosshead) as the ultimate load is being approached and the stress rate decreases due to cracking in the specimen’
- 8.6 - ‘Apply the compressive load until the load indicator shows that the load is decreasing steadily and the specimen displays a well-defined fracture pattern

Standards outlines in C39/C39M – 18 constrained the methods by which CEMENT3D undertook compressive strength tests on the concrete samples. Given that the team is building layers of concrete, layers were tested rather than the cylindrical shapes described in C39/C39M. To ensure correct testing procedure, the Team followed the specifications outlined in 6.1, 6.1.2.1 and 8.5.3 and so used an MTS machine to carry out compressive strength tests. The compressive plate used, and the speed calibration of the machine, was made in accordance with the requirement of 0.25MPa/s, applying pressure at an average rate of 0.28MPa/s.

To ensure the samples adhere to the specifications outlined in 7.1 and 8.3, the samples used were built within a mould, rather than laid out, to ensure the width of any two samples was not off by more than 2%, as detailed in 7.1. A calliper was used to measure the width of each of the samples and samples that were not within 2% of the average width were discarded. Prior to testing the samples, a file and sandpaper was used to flatten each sample to ensure flatness on the base. Finally, the samples that were tested were created within an hour of one another. These samples were tested for their compressive strength after 3 days and after 6 days of curing.

Standards were investigated for site characterization of construction through standards as, Standard Guide for Site Characterization for Engineering Design and Construction Purposes: D420 – 18. These standards informed the team that construction site standards were primarily relevant when the ground underneath is dug, a case the team does not anticipate over normal use of the product.

4.2.2 Ingress Protection

Many consumer devices, particularly indoor and outdoor consumer electronic devices, like smartphones, outlets, and speakers, are given ingress protection ratings, or scores that rate them on their ability to prevent dust or liquids from entering their cases and causing damage to their electronics or internal contents generally. In this code, “IPXY” the first number, “X” corresponds roughly to a 1-10 (with 10 being best) scale of how resistant the device is to dust, while the second number, “Y” corresponds to a 1-10 scale of how resistant the device is to fluid penetration [4].

Unfortunately, a primary source on this topic was not found that was accessible at the University of Pennsylvania. Thus, secondary sources were referred to to find an approximation of what the standard would prescribe for BUILDER.

Many outdoor consumer electronics, like outdoor speakers, are rated IP44 [5]. This rating, when applied to BUILDER, would require the following:

- The system must be resistant to the entrance of particles any larger than 1mm.
- Water splashing against the enclosure from any direction must have no harmful effect during a test duration of 5 minutes, with water volume of 10 liters per minutes and pressure of 80-100 kPa.

Since 1mm is quite a bit larger than the typical seven thousandths of an inch used in making pressfits, this standard constrains the team’s design only insofar as it requires to have a very tight entrance area for the system wiring into the press fit box where the electronics are held. The same is roughly true of the liquid requirement, except that it may also be important to wrap the

electronics in something waterproof or deliberately put the microcontrollers in an electronics box somewhat distant from the entrance to the box.

5 Design and Realization

5.1 System-level Concept Selection

When deciding between a Delta and Cartesian 3D printing system, the team made a continued effort to relate each of the system's advantages and disadvantages to the needs of the customer. The most significant difference between the two types of printing is the method of actuation: Cartesian printers use a linear system and actuate in the x-y plane, while Delta printers actuate based on trigonometric functions and are naturally suited towards printing circular structures, which may be taller in height [6].

	Delta	Cartesian
Relative ease of assembly	High	Low
Relative scalability	High	Low
Relative expected frame deployability	High	Low
Relative ability to print tall structures	High	Low
Actuation system	Circular	Linear
Relative Precision	Low	High

Table 5.1: Key considerations of Delta and Cartesian 3D printers [6, 7]

As such, the Delta 3D printer was most suited towards printing common landscaping structures, like firepits and garden beds, which are often designed with organic curves. More importantly, the Delta 3D printer also met two of CEMENT3D's key, initial objectives: scalability and portability [7]. The moving rails of a cartesian printer are quite heavy, and therefore difficult to support on a light-weight, low-profile, deployable structure. Additionally, it may be difficult for the user to lift such rails into position, and to remove them after printing. These problems are exacerbated with scale, since the rails of a cartesian printer need to be as long as the print space is wide.

After down-selecting to a Delta 3D printing mechanism (using **Table 5.1**), the team further narrowed the design based on actuation mechanism. Typically, Delta 3D printers are designed in one of two configurations: linear or rotational (revolute) [8]. Linear deltas are the simpler design, with rigid arms that connect via universal joints to both the frame of the printer and at the

print head. The connection to the printer frame is able to translate vertically along designated rails, controlling the vertical position by translation and the horizontal planar position by the joint angles. The rotational version is more complex, with each arm of the printer comprised of a revolute-universal-universal linkage. As these two designs are used for a majority of delta-style robots, there exists open-source firmware for the control of such systems, and their kinematics are well understood. However, both of these designs depend on the use of rigid actuation members, and the team was concerned about the weight and bulk such members would add to the system. Additionally, both configurations require a mechanically complex connection between the frame itself and the actuation members, forcing the product to have a more integrated architecture. This is an undesirable trait for deployability, as it would be difficult to separate the system into easily assemblable parts if every subsystem had high complexity interfaces.

CEMENT3D therefore chose to forsake the benefits of well-established delta designs in favor of a novel cable-driven mechanism. The cables in this system would act as telescoping members with extremely large extension ratios, with the lengths of the cables determining the location of the print head. Such a design also offered a solution that more closely matched the team’s initial objective of scalability. There are potential drawbacks of this design, such as the potential of cable tangling during transport and the potential for more frequent maintenance, but overall it was the solution most consistent with the team’s objectives (see **Table 5.3** for the considerations and tradeoffs between a telescoping and rigid mechanism).

Telescoping (cables)	Rigid (bars)
Need to write firmware for system actuation	Firmware exists for actuation mechanism
Tangling	Bending
More scalable	Require better sliders (prismatic joints)

Table 5.3: Down-selection process of connection mechanism to print head

Lastly, in order to reduce mechanical error within the system, the team chose to use a rigid frame to support and position BUILDER’s subsystems. Although the design of a more deployable superstructure would be necessary for BUILDER to become a consumer product, it was in the best interest of proving feasibility to omit this aspect of the design from the project.

5.2 Print Head

One of the main components of BUILDER is the print head, which offers a mechanism by which to connect the extrusion system with the positioning cables. A significant concern that the team had to address was the orientational stability of this component. Because the lateral forces acting on the print head (inertia, friction, etc.) are not always balanced, the end-effector of any delta design is naturally inclined to pitch and roll as it changes position, and since BUILDER would utilize cables, which have zero stiffness, the system was also likely to yaw. Such unintentional angular displacements could cause concrete to be mis-deposited, leading to layer or print failure. CEMENT3D therefore sought to design a highly stable system in which the print head does not yaw and stays parallel to the ground.

In order to quantify the print head's resistance to tilting moments a metric was employed called the Tilt Effector Stability (TES) constant, given by the following equation [8]:

$$TES = \frac{Arm\ Space^2}{b|c|} \quad (\text{Equation 5.1})$$

Where:

Arm Space = distance between parallel actuation members

b = distance between centers of articulation (joints) of adjacent arms

c = vertical distance from arm convergence to center of mass

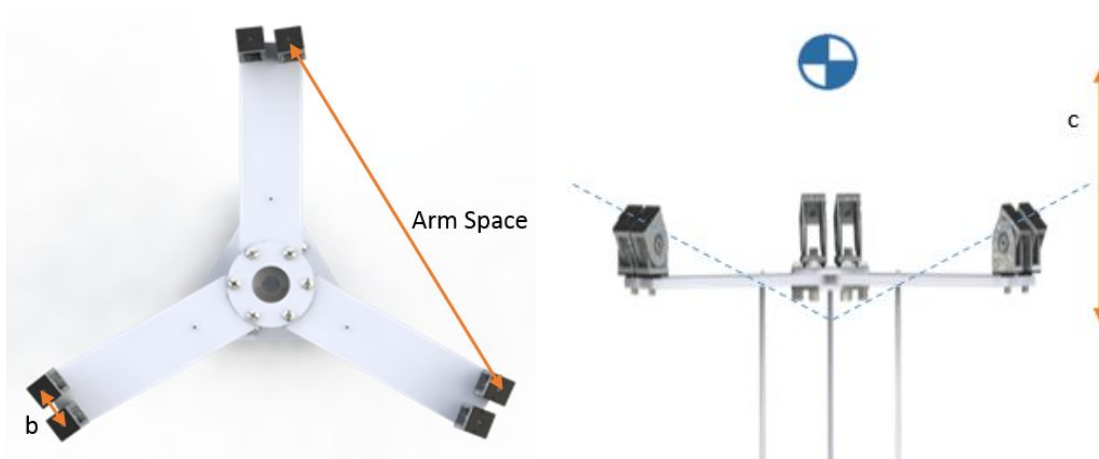


Figure 5.1: Print head schematic outlining TES metrics [8]

It is important to note that this metric is an informal one used by hobbyists, and that in practice these dimensions are determined by testing and adjusting the geometry. However, the TES

constant describes well the mechanical intuition behind what makes a stable system, and proved extremely useful in determining initial dimensions for BUILDER.

Because the joints connecting the print head to the cables had to be able to bear load, the design was constrained by a minimum value of $b = 30$ cm. Additionally, the center of mass of the print head, when integrated with the extrusion system, changes according to the height of the print head. This is because the print head supports a longer section of concrete-filled tube at the bottom of the print space than at the top. The vertical distance to the center of mass of the head, c , is therefore also physically limited - by the difference between the most extreme center of mass locations. That is, a “perfect” c value, $c = 0$, in the center of the print area still leads to c values of 250 mm at the top and bottom of the print area. Therefore the only parameter which could be tuned for greater stability was the arm space. The team set a goal of $TES = 50$, based on TES values of commercial and successful hobby printers, calculated from online poll responses [9]. Using the average value of c , 125 mm, the TES formula (**Equation 5.1**) becomes:

$$TES = 50 = \frac{Arm\ Space^2}{3750 [cm]}$$

Solving for Arm Space, a value of 433 mm is obtained. For the convenience of the team, this value was rounded up to 450 mm (corresponding to the distance between two pulleys) for the final design, which corresponds to a TES of 54.

It should be noted that this is not the true mathematical average of the TES function for the system, but rather a representative value, for which the value of the TES function is higher for half of the domain and lower for half of the domain. Such a value was considered more representative than the mathematical average because of the blow-up to infinity at $c = 0$. For clarity, this phenomenon is represented graphically in **Figure 5.2**.

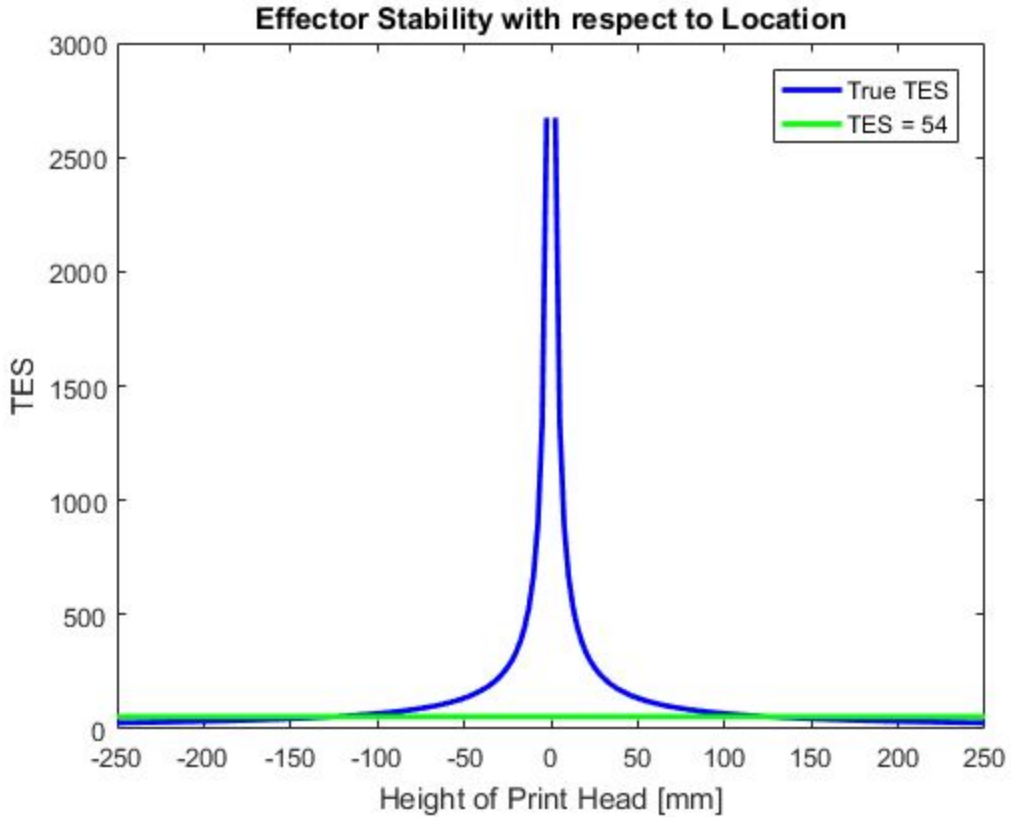


Figure 5.2: Comparison of True TES vs Height of print head and that of BUILDER

In order to validate that the print head would not undergo significant bending, an FEA was carried out on the print head. Three point loads (each with a magnitude of 250N) were modelled to act vertically upwards, each of which was located at the center of each arm and represented the combined tension of 250N in two cables.

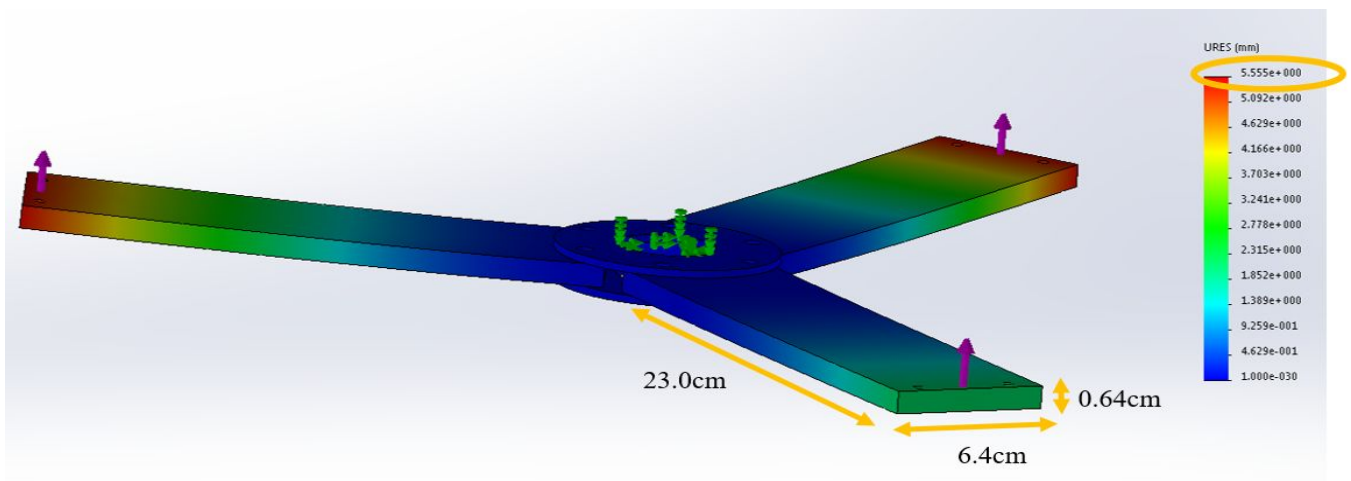


Figure 5.3: FEA of print head and corresponding vertical displacement

In order to validate the displacement given by the FEA in **Figure 5.3**, the following beam bending calculation was carried out:

$$\delta_{max} = \frac{Pl^3}{48EI} \text{ (Equation 5.2)}$$

$$I = \frac{1}{12}wt^3 \text{ (Equation 5.3)}$$

Where:

P = force acting on one arm of the print head = 250N

l = length of arm = 23m

E = young's modulus = 68.9 GPa

w = width of arm = 6.4cm

t = arm thickness = 0.64cm

Carrying out the beam calculations using Equations **5.2** and **5.3** yields a maximum displacement of 4.25mm, compared to the FEA in **Figure 5.3**, which yields a maximum displacement of 5.56 mm. Since both methods yielded displacement values on the same order of magnitude, the team was relatively confident that the print head would not undergo significant bending.

5.3 Structural Mechanics of System

The first step in the designing the superstructure of the system was to determine its dimensions. Since the target print area was 1m in diameter, the intersection between the theoretical arm centers and the cage needed to be at least 1m apart from one another. Furthermore, the pulleys had to be placed 45cm apart to yield the desired arm space. These considerations, along with space budgets for joints, determined the dimensions of the top and bottom of the cage, which is illustrated by **Figure 5.4**.

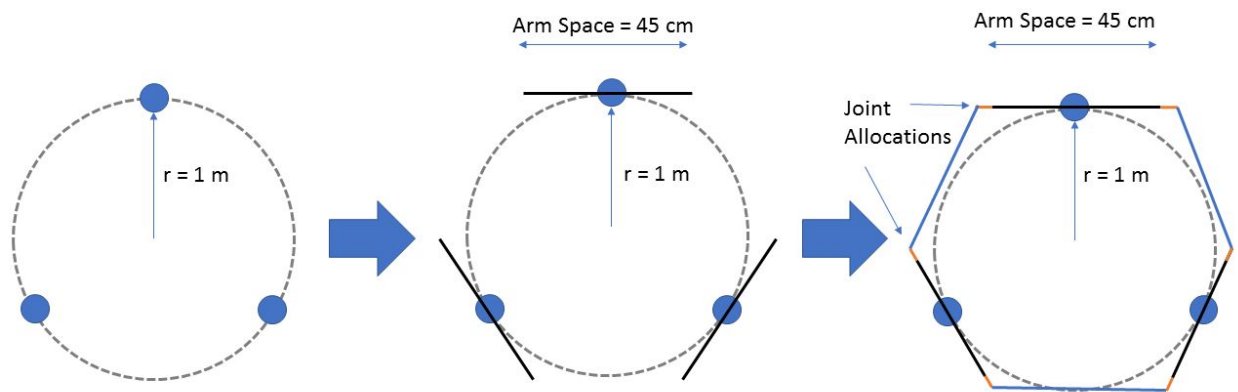


Figure 5.4: Arm space dimensions

The height of the cage was determined by putting a limit on the allowable tension in each of the cables. If the cage were the same height as the top of the print head at its highest position, the tension in the cables when the print head is positioned there would be infinite. The cage must therefore be taller than this height. Since tensions equal to the weight of the concrete are possible even when the print head is at the bottom of the print space (consider, for instance, the case where the print head is at the edge of the cage, directly under a set of pulleys), the team decided to use this value as the cutoff, thus avoiding an unnecessary increase in maximum cable load for the system. As can be seen in **Figure 5.5** below, the height of the nozzle can reach approximately 65% before it exceeds the desired wire tension. Thus for the team’s desired height of ~75 cm (nozzle height of 50 cm plus a print head height of ~25 cm including joints), a cage height of 125 cm is appropriate. **Figure 5.6** illustrates the full BUILDER cage dimensions.

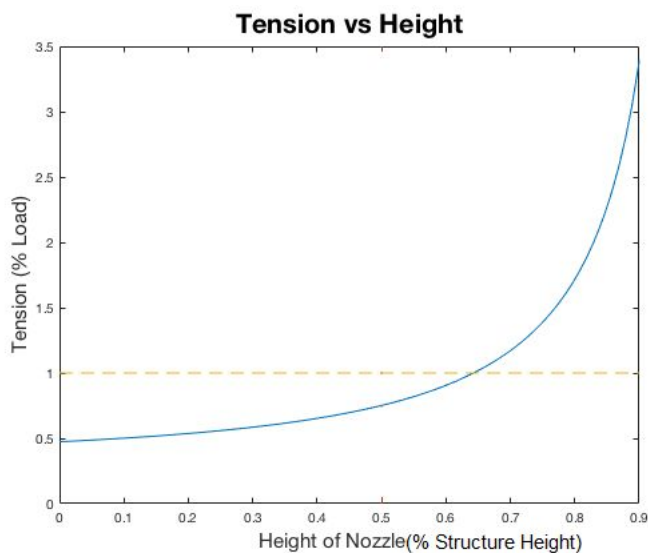


Figure 5.5: Normalized Tension vs Normalized Height of Nozzle produced by MATLAB simulation



Figure 5.6: BUILDER cage dimensions

In order to satisfy CEMENT3D's initial objective of ease of assembly for the consumer, 80-20 was chosen as the material to construct the cage from. Since twisting of the overall cage was one

of CEMENT3D’s main concern, cross members were added on every other y-z plane (on members that did not have motor mounts attached to them).

5.4 Cables Selection

0.038” diameter, Kevlar thread was used as cables to actuate the print head. The breaking strength of this kevlar is 580N and so is 3.8x stronger than the magnitude of the largest tension force (150N) exerted on any cable in the system, at any position. The possible cable choices that the team considered are outlined in **Table 5.4** below.

Cable choice	Diameter (cm)	Tensile strength (N)	Cost (\$/m)	Minimum Bend Radius (cm)
Rope [10]	0.48	2,445	\$2.16	0.75 [14]
Wire [11]	0.48	2,670	\$9.77	7.0
Steel wire [12]	0.20	1,565	\$0.60	1.8 [15]
Kevlar [13]	0.10	580	\$0.45	0.15 [14]

Table 5.4: Outline of characteristics for different cable materials

Kevlar thread was chosen because it had the smallest minimum bend radius and so could be used with small pulleys, thus further reducing the cost and weight of the system. This was possible because of Kevlar’s high strength at thin radii’. By virtue of being thin, the kevlar is also light and easy for consumers to use and makes for a compact actuation system.

5.5 Capstan

To actuate the amount of cable that extends from the system’s pulley to the print head, the system needs the ability to roll and unroll the cable, which was achieved with a capstan illustrated in **Figure 5.7**. This capstan was made of stacked sheets of MDF compressed together

by four long screws, as this would be cheaper than purchasing solid capstans and the design could then be changed rapidly as other parts of the system were redesigned.

The diameter of this capstan has no effect on the velocity at which the system is able to actuate its cables. The velocity at which cable leave the capstan is a function of the capstan's radius and the rate at which it is turned (see **Equation 5.4**) and the system torque is a function of force and radius (see **Equation 5.5**). From these relationships it follows that the system's torque and velocity actually have no radial dependence.

$$V = r \times \Omega \text{ (Equation 5.4)}$$

$$\tau = r \times F \text{ (Equation 5.5)}$$

$$\text{Therefore: } \Omega \propto \frac{1}{\tau} \text{ and } V \propto \frac{1}{F}$$

The cable was anchored in the capstan by lasering an angled channel into one of the plates that make up the capstan, and then placing one end of the kevlar cable in the channel during capstan assembly. This end of the kevlar was then tied off with a knot.

Since the speed at which the cables is actuated is independent of the capstan radius, any radius is feasible so long as it exceeds the minimum bending radius of the cable. The team chose to use a radius of 1.5 inches in order to fit all the full length of cable without it doubling over, making the release of cable on the physical system more similar to the team's model. In the future, this dimension could be reduced for the sake of cost and weight reductions.

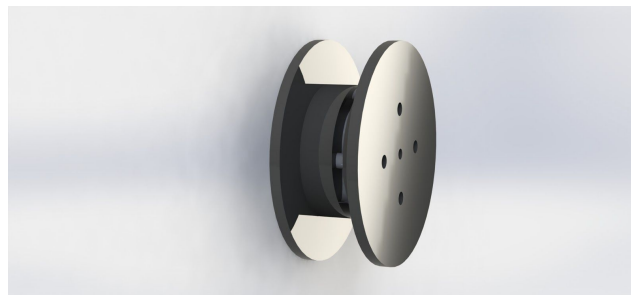


Figure 5.7: Render of capstan

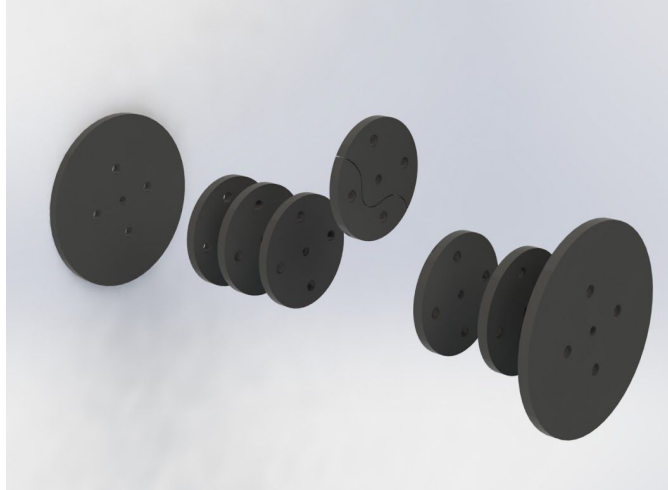


Figure 5.8: Exploded view of capstan with channeled plate raised for clarity

5.6 Motor Mount

It was necessary to provide a mechanism to drive the system's capstans in accordance with the planned positions from the actuation code. To accomplish this, an assembly was designed that allowed for synchronous motor actuation of the capstans reliable enough (e.g. communicating torques from the system motors to the capstans with a high enough resolution) that the length of the cables could be reasonably counted upon. A motor mount was designed that had a capstan associated with each of the two cables, all of which would be controlled by a single motor actuating through a pair of gears from the center of a 22 inch carbon steel rod, as is illustrated in **Figure 5.9**.

There were several mechanical concerns that needed to be addressed when designing this subsystem. Lateral bending in the carbon steel rod would potentially cause the capstans to move vertically, and torsional strains and twisting might cause decoupling of the motor driver and the system capstans. The distance required between the center of the two capstans, or the distance between the points at which the kevlar cable was released, was determined by the capacity of the kevlar cables to stay firmly connected to the pulleys. The ability of the entire motor mount, including the motor itself and both capstans, to communicate the vertical load from supporting the print head and concrete filled tube into the system frame beneath it, had to be assured. Lastly, the torque required to actuate the kevlar cables while bearing the print head and concrete would need to be provided for by designing for the correct gear ratio between the motor and the carbon steel rod.

To find the lateral bending that occurred in the rod responsible for turning the capstans, the follow calculation was made using Euler-Bernoulli Equation:

$$I = \frac{\pi(1/2)^4}{64} = 0.00307 \text{ (Equation 5.6)}$$

$$\delta_{max} = 48 \frac{LF}{3EI} = \frac{(2.25)(33.72)}{48(29.0e6)(0.00307)}$$

$$\delta_{max} = (1.775e - 5) \text{ inches}$$

To address the risk of the kevlar cable sliding off of the side of the pulley, the kevlar cables were pulled back and forth over the system pulleys at varying angles. It was determined that the kevlar would most securely rest on the pulleys if the capstans were arranged so that their centers were as far apart from each other as the pulleys are, such that the cables would be vertical while loaded. Fortunately, with the material strength in carbon steel, making a rod this long would not cause problems with lateral bending or torsion in the rod.

In designing the gear attachment between the system motors and the loaded kevlar cables, the maximum necessary torque was found to be 4.75 Nm based on a capstan radius of 1.5 inches as described above and a maximum load per cable of 250N. Thus, a gear ratio of 4.8:1 was found to be suitable for the team's selected motor, with a stall torque of 9.5 Nm.

To ensure that the motor driver could be relied upon to not suffer inaccuracies in reporting the motion of the capstans due to twisting in the capstan axle, the following calculation was made to determine the amount of twisting that would occur in the rod.

$$\theta = L \frac{T}{JG} \text{ (Equation 5.7)}$$

$$\theta = (0.2794m) \frac{(4.75Nm)}{(\pi(D^4)/32)(G)}$$

$$\theta = (0.2794m) \frac{(4.75Nm)}{(\pi(D^4)/32)(G)}$$

$$\theta = (0.2794m) \frac{(4.75Nm)}{(\pi(0.0127m^4)/32)(80e9Pa)}$$

$$\theta = (0.2794m) \frac{(4.75Nm)}{204.32 N}$$

$$\theta = 0.0065 \text{ radians deflection}$$

To ensure that the carbon steel rod wouldn't split in torsional shear, **Equations 5.8** and **5.9** were used:

$$J = \frac{\pi}{2}(c_2^4) \text{ (Equation 5.8)}$$

$$\tau_{max} = \frac{T\rho}{J} \text{ (Equation 5.9)}$$

$$J = \frac{\pi}{2}((0.25in)^4) = 0.006 \text{ in}^4$$

$$\tau_{max} = \frac{4.75Nm \cdot 0.25in}{0.006 \text{ in}^4} = \frac{4.75Nm \cdot 0.00635m}{2.50e-9 m^4} = 0.012 \text{ GPa}$$

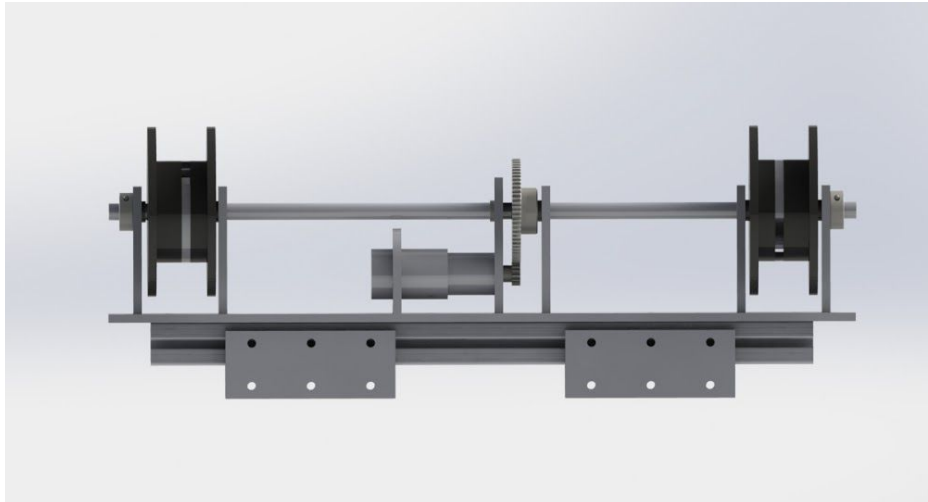


Figure 5.9: Render of motor mount system

5.7 Extrusion

To effectively print concrete, it was important for CEMENT3D to better understand the properties of concrete, characterize the flow of the concrete used, and finally, design a mechanism to extrude the concrete.

5.7.1 Concrete Mixture Composition

One of the challenges of 3D printing using Fused Deposition Modeling, is that the material must easily flow in a tube, but must solidify when extruded through a nozzle. The team experimented using concrete with different concrete of particulate compositions and finally chose to use Quikrete Sand Topping Mix. This type of concrete was chosen given that the sand topping mix was made of fine particulates which enables the concrete mixture to be homogenous, the layers that are printed to be smooth and the pumping of concrete to be easy.

To identify the ideal concrete:water mixture ratio, the team carried out spread tests to identify how concrete behaves at different concrete:water ratios. As seen in **Table 5.5** below, the team identified a concrete:water ratio of around 3.5:1 to be favorable when building layers. This

concrete to water ratio is used throughout when characterizing the flow of the concrete and when pumping the concrete.

Concrete: Water	Initial Width (cm)	Final Width (cm)	Spread (cm)	Comments
3.0	-	-	-	Too liquid to use
3.3	3.8	9.0	5.2	
3.4	4.6	4.6	0	
3.5	4.3	4.3	0	
4.0	-	-	-	Too solid to use

Table 5.5: Table displaying the spread for different concrete:water ratios

5.7.2 Concrete Flow Characterization

In order to characterize the flow of concrete and determine the pressure differential required to pump concrete through a PVC tube with given length and radius, the Hagen-Poiseuille law below was used:

$$\Delta P = \frac{8\mu L Q}{\pi r^4} \text{ (Equation 5.10)}$$

Where:

ΔP = pressure differential
 μ = dynamic viscosity
 r = pipe radius

L = length of pipe
 Q = volumetric flow rate

Equation 5.10 makes two key assumptions: the flow is laminar and concrete is assumed to behave similar to a Newtonian fluid. Since the flow rate corresponding with the target print time objective is relatively low, the laminar flow assumption was fairly reasonable to make since the velocity is fairly low. The rheology of concrete can be best described by the Bingham model [16]. Under this model, a fluid or substance behaves like a rigid body at low stress, but acts like a fluid at high stress [17]. The Bingham model suggests that the relationship between shear rate and shear stress is linear and identical to that of a Newtonian fluid, once the yield stress is exceeded (see **Appendix A.1**). As such, the second assumption of concrete behaving as a Newtonian fluid in Equation 5.1 is justified--provided that the shear stress applied is greater than

the yield stress--which is necessarily the case since the concrete is flowing at that point and does not act like a rigid body.

Density

The density of the team's 3.5:1 concrete to water mixture was measured to be, on average, 2094 kg/m³. This measurement was made in line with the Standard highlighted in **Section 4.2.1** in that the absolute volume of the water and of the concrete was used.

Viscosity

In order to approximate the viscosity of concrete, the Hagen-Poiseuille law was used (**Equation 5.10**). By rearranging **Equation 5.10**, the viscosity can be rewritten as:

$$\mu = \frac{\frac{mg}{v^2}\pi r^2 r^2}{8Lv\pi r^2} = \frac{r^2 \rho g m \pi r^2}{8v\pi r^2} = \frac{r^2 \rho g}{8v} \quad (\text{Equation 5.11})$$

Where:

μ = dynamic viscosity

v = velocity

r = inner pipe radius

Two key steps were taken to rewrite **Equation 5.10** as **Equation 5.11**. The pressure differential term was first decomposed into a force and area term, which was necessarily the case for the tests carried out in **Table 5.6**, where concrete was allowed to freely flow in a 0.75m long tube with gravity as the only force acting on it. Secondly, the volumetric flow rate term was decomposed into a product of velocity and area.

Length of tube (m)	Time (s)	Velocity (m/s)	Radius of tube (m)	Viscosity (kg/s or Pa.s)
0.75	4.48	0.27	0.013	2.48
0.75	7.12	0.11	0.013	3.94
0.75	4.15	0.18	0.013	2.29
Average Viscosity				2.90

Table 5.6: Measurements used to calculate viscosity

By plugging in the values for velocity, radius, density (from the calculated value of 2094 kg/m^3) and gravity into **Equation 5.2**, an average dynamic viscosity value of $2.90 \text{ Pa}\cdot\text{s}$ was calculated for the Quikrete mixture of concrete.

The viscosity value calculated was cross-checked with literature to ensure its validity. Bouvet et. al (2010) calculated empirical dynamic viscosity values for two different mixtures of concrete (one with and one without a plasticizer)---the mixture without the plasticizer had a dynamic viscosity of $1.4 \text{ Pa}\cdot\text{s}$ [18]. The value obtained from literature is likely lower than the value that CEMENT3D obtained due to the significant difference in water composition of both mixtures. CEMENT3D used a 3.5:1 concrete to water ratio, while Bouvet et. al (2010) used an approximate ratio of 2.7:1 concrete to water. This makes intuitive sense since using less concrete and more water will likely decrease the concrete's viscosity and increase its workability. Moreover, the large difference in magnitude is likely due to the fact that concrete is very sensitive to water, as the team's empirical tests have shown.

5.7.3 Time between layer formation

The time between placing one layer of concrete on top of another is important because, if the layers are placed on top of one another too quickly, the underlying layers may not be strong enough to support the structure, while, if the layers are placed on top of one another after too large a time interval, the underlying layers may not bond well.

The team carried out tests placing layers of concrete on top of another with intervals of 15 seconds between adding each layer. As illustrated through **Figure 5.10**, with a time interval under 30 seconds, it was not possible to place over 4 layers of concrete, without the bottom layers deforming and losing shape.



Figure 5.10: Illustration of multiple layers placed on top of one another given different time intervals

To determine the maximum time over which layers should be placed on top of one other, tests were undertaken to determine the maximum shear stress required to shear layers off of one another, given different time intervals between placing the layers.

The experimental setup, using an MTS machine, is illustrated in **Figure 5.11**. The concrete sample is placed on a flat plate at the bottom. A chisel is then axially loaded into the ridge between the layers. The team took care to ensure that the bottom of the sample is flat, by using a chisel, and to ensure that the chisel is directly perpendicular to the sample, by using a mount to attach the chisel to the MTS test.

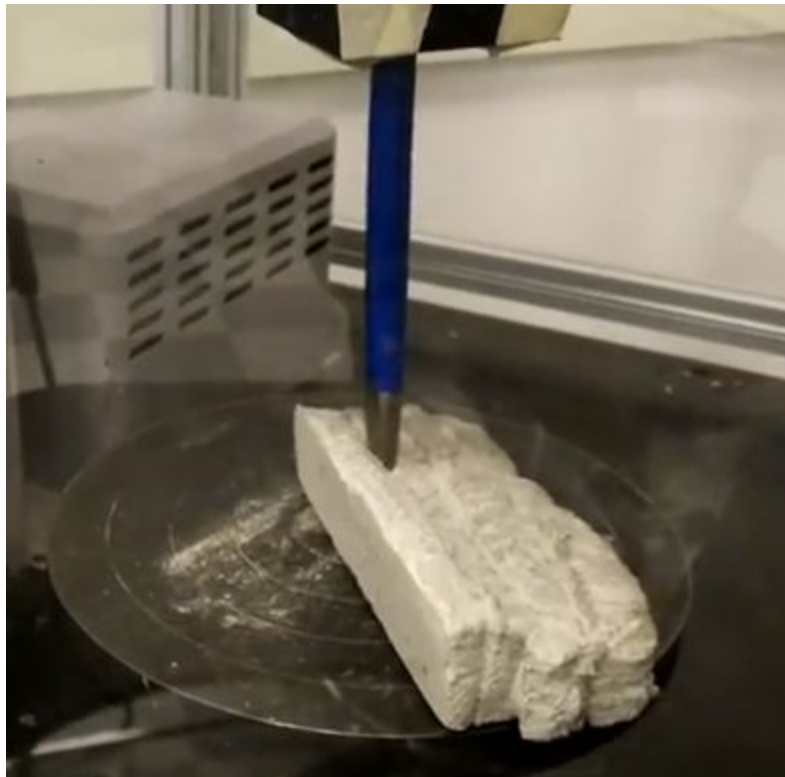


Figure 5.11: Testing setup for layer shear tests

Given these tests, it was found that the average maximum shear stress to break samples was 15% stronger when the time interval between placing one layer on top of another was 45 seconds as compared to 60 seconds, as seen in **Figure 5.12**. This informed the team that the optimal time between placing one layer on top of another is about 45 seconds.

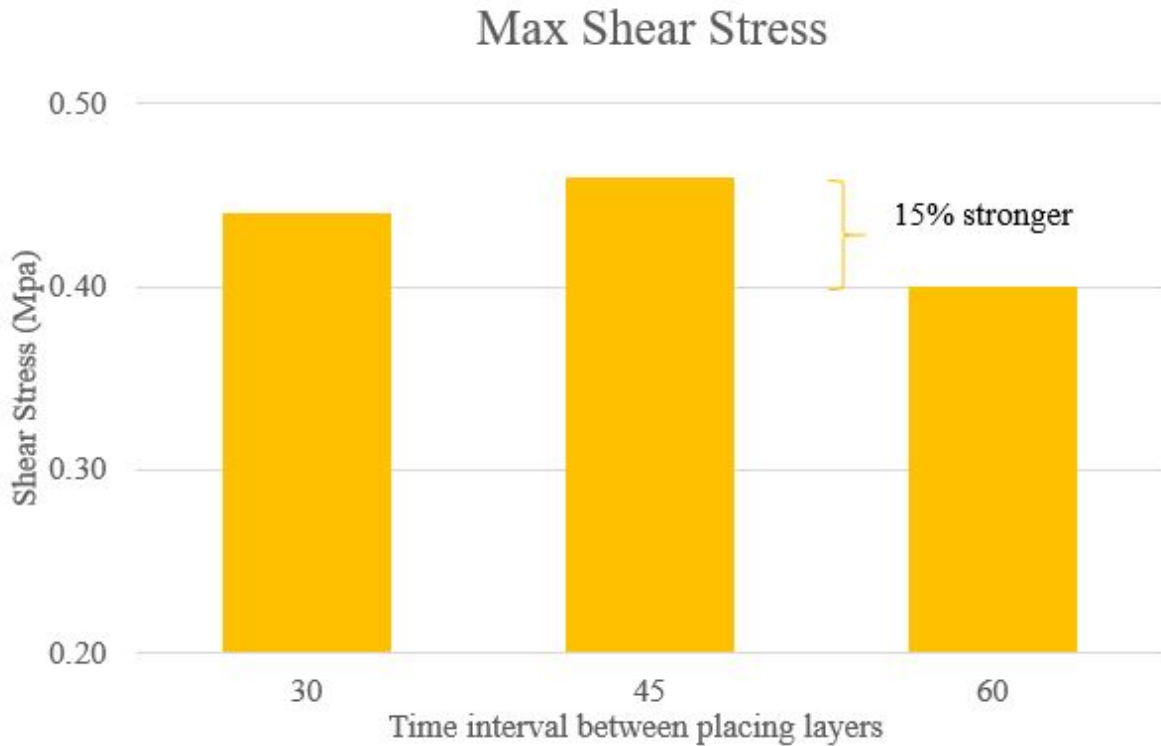


Figure 5.12: Shear stress needed to crack layers given different time intervals

5.7.4 Flow Rate

The flow rate required was calculated based on tests undertaken to determine the optimal time required before placing one layer of concrete on top of another (see **Section 5.7.3**). The team determined that 45 seconds was the optimal time after which a layer of concrete should be placed on top of another. Assuming that the printer must ‘wait’ 45 seconds before applying one layer on top of another, the flow rate was calculated by taking the volume of concrete extruded when building one layer, and dividing it by 45 seconds. The team thus calculated that the pumping mechanism should aim to deliver an average flow rate of $3.5 \times 10^{-5} \text{ m}^3/\text{s}$ (2.1 lpm) (see **Appendix C.1**).

The team validated that the actuation system can feasibly move the print head to match this flow rate. To do so, the team calculated that the optimal speed of the print head to ensure one layer is built on top of another in 45 seconds is 4 cm/s, as calculated in the **Appendix C.2**. At the chosen gear ratio for the motors, of 4.8:1, the print head can be moved at maximum of 7cm/s, and so the print head can be actuated to match the 4 cm/s requirement (see **Appendix C.3**).

5.7.5 Tube

Length of Tube

The required length of the tube was calculated to be 1.77m long based on **Equations 5.12** and **5.13**.



Figure 5.13: Parameters for **Equation 5.12**

$$l_{tube\ in\ cage} = (a^2 + b^2)^{\frac{1}{2}} \quad \text{(Equation 5.12)}$$

$$l_{tube} = l_{tube\ in\ cage} + l_{to\ pump} \quad \text{(Equation 5.13)}$$

Where:

a = vertical distance from base to tube holder

b = horizontal distance between two sides, intersecting the midpoint of each side

$l_{to\ pump}$ = length of tube to the pump

$l_{tube\ in\ cage}$ = length of tube in the cage

l_{tube} = length of tube

Tube Material

The material of the tube was selected based on two criteria: cost and flexibility. **Table 5.7** below shows the down-selection process that revolved around minimizing cost and bending radius (all bending radii comparisons were based on a benchmark, 1” inner diameter, 10ft long tube):

Type of Tube	Outer Diameter (in.)	Bending Radius (in.)	Cost per ft (\$)
Masterkleer PVC [19]	1.25	5	1.47
Polyurethane [20]	1.25	7.5	4.06
Tygon PVC [21]	1.25	5.13	7.95
EVA [22]	1.32	9	3.26

Table 5.7: Down-selection process for tube

Based on the considerations around minimizing cost and bending radius due to increased flexibility, the Masterkleer PVC tube type was selected.

Tube Diameter

After characterizing the properties of concrete, namely the density and the viscosity of the 3.5:1 concrete to water ratio mixture, Team CEMENT3D proceeded to calculate the delivery tube diameter for delivering the concrete.

The tube diameter was sized based on two competing factors: the pressure required to drive the flow, and the weight of the tube. The tube should not be made too small as the pressure required to pump the cement would be large. However, the tube should not be made too large as the weight of the tube, along with the concrete, would require stronger rope and more powerful

motors to actuate the nozzle. More specifically, the pressure difference required and the weight of the tube, was plotted against given tube diameters in **Figure 5.14** below.

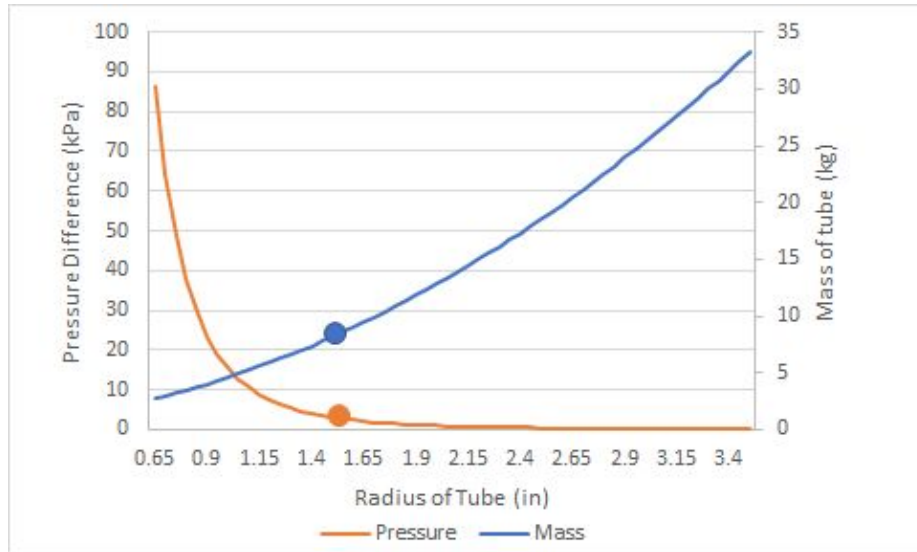


Figure 5.14: Plot of pressure differential required vs tube radius for different tube weights

The pressure difference required was calculated using the Hagen-Poiseuille equation (**Equation 5.10**) above and a characterized viscosity of 2.90Pas. A length of 1.77m was used for the tube, which was the maximum required length of the tube needed pump the concrete, as calculated using **Equation 5.13**, while the flow rate used was $3 \times 10^{-5} \text{ m}^3/\text{s}$, which was the calculated flow rate based on the needs of the consumer and the drying time of the concrete layers, as calculated in **Section 5.7.4**.

The weight of the tube, along with the concrete, was calculated by taking the calculating the volume of the concrete and the volume of the tubing material, assuming an inner wall density of 0.4in (as specified by manufacturers), and multiplying them by the density of concrete and the density of PVC respectively.

Given these calculations, a tube diameter of 1.5” was chosen, corresponding to an upper end for the mass the motors could drive at 8.16kg, and a pressure difference required of 3.04kPa (0.43 psi). This assumes that the pump is placed at a height and would not need to push the concrete against gravity when pumping.

5.7.6 Linear Actuator Pump

Reservoir choice

When making a pump, a reservoir was to be made for the concrete. A reservoir was chosen such that there would be enough concrete to print 3 full layers along the circumference of the print bed. Given this requirement, it was noted that $4.7 \times 10^{-3} \text{ m}^3$ of concrete was needed for the layers as calculated in **Appendix Section C.4**. Additionally, $2.0 \times 10^{-3} \text{ m}^3$ of concrete was present in the tube that was not extruded. This implied that the total minimum concrete required to be stored in the reservoir was $6.7 \times 10^{-3} \text{ m}^3$. The reservoir was a 1.25m high and 4" wide PVC tube that can hold $10.1 \times 10^{-3} \text{ m}^3$, which corresponds to 1.5x the concrete required.

Motor Choice

Based on this tube diameter, and the necessary pressure requirements, the team then proceeded to make a linear actuator to pump the concrete. To select the appropriate motor for the actuator, the torque required to pump the concrete was calculated.

The torque required was calculated by assuming that the linear actuator pushes the concrete horizontally. This assumption is valid given that the reservoir will be placed horizontally on a table. To calculate the torque required, first, the mass of the concrete was calculated to be 21kg, given the density of $2,094 \text{ kg/m}^3$, second, the distance required to push the concrete is 1m given that with a 1m push, enough concrete would be extruded out, third, the coefficient of friction was assumed to be 0.4 [23]. Thus, the torque required for the motor was calculated at 0.04Nm using **Equations 5.14 - 5.17**.

$$F_{friction} = \mu mg \text{ (Equation 5.14)}$$

$$F_{pressure} = A\Delta P \text{ (Equation 5.15)}$$

$$F_{total} = F_{friction} + F_{Pressure} \text{ (Equation 5.16)}$$

Where:

$F_{friction}$	= Force of friction needed to overcome	μ	= Coefficient of friction
m	- Mass of Concrete	ΔP	= Pressure differential required
$F_{pressure}$	= Force needed to overcome pressure difference	A	= Area of pump

Taking the pitch off the screw available on McMaster, the torque required can be calculated as:

$$T = \frac{F_{total}P}{2\eta\pi} \text{ (Equation 5.17)}$$

Where:

η = efficiency of motor

p = Pitch of screw

Thus, for the linear actuator, CEMENT3D chose to use a motor with a stall torque of 4.8Nm, since it easily satisfied the torque requirements of 0.04Nm [24].

5.7.7 Nozzle

For the nozzle, the team chose a linear profile based on the recommendation of Dr. Jordan Raney. In order to determine the nozzle size, there were four main considerations that CEMENT3D focused on: resolution, pressure differential required, resistance to dripping, and repeatability constraints. A smaller nozzle diameter increases the resolution and prevents dripping, but the repeatability of the system, its ability to reliably reach the same physical point in space for the same target coordinates, needs to be better for the layers to be deposited on top of each other. There is also a risk for exceeding the force capabilities of the pump for small nozzle diameters. After carrying out extrusion tests, the team found that a 1-inch diameter nozzle yielded the best results given the team's pumping system, which corresponds to a resolution of 0.5cm (half of the nozzle diameter).

5.8 Electronics

5.8.1 Basic Overview

The electronics system for the device contains the following subsystems. First, there are three motors, fit with encoders, which individually control two pulleys each. Second, there are two motor drivers; one driver controls one motor, while the second motor driver controls the other two. These motor drivers each have a power supply that powers the motors. Finally, there is an Arduino that controls the motor drivers and reads in information from each of the motor's encoders. In addition, there is an Adafruit microSD card reader that allows for a series of positions derived from G-code to be sent to the Arduino. The following sections explain how the team selected each of these electrical components and how the system is wired together.

5.8.2 Motor Selection

In order to pick a motor, multiple factors needed to be considered. First, the motors must be able to support high torques due to the weight of the concrete. Next, the motors must be able to handle dynamic loads, as the amount of torque the motor must withstand will vary depending on where the nozzle head is at any given moment. In addition, the motors should be cheap as to reduce the overall price of the system, and preferably be easy to control.

Based on these criteria, the team looked at three types of motors: servo motors, stepper motors, and gear motors. The types of motors were then compared against one another, as seen in the **Table 5.8** below:

Type of Motor	Servo	Stepper	Gear
High Torque Application?	Yes	No	Yes
Handles Dynamic Loads?	Yes	No	Yes
Relative Cost	Medium	High	Low
Easy to Control?	No	Yes	Yes

Table 5.8: Down-selection process of motor

From this examination, the gear motor became the desired choice. The main negative with the gear motor was its difficulty to control. However, since the complexity of the controls is only a problem for the designers, not the user, the team found the trade off reasonable.

At this point, the team decided on purchasing the 84 RPM HD Premium Planetary Gear Motor with Encoder, available for purchase from Servo City. These motors had the highest torque that the team could find at a stall torque of 1347.1 oz-in (9.51 Nm) and came equipped with incremental rotary encoders. Each motor costs approximately \$60.

5.8.3 Motor Driver Selection

Next, the motor driver needed to be selected. These motor drivers needed to satisfy two characteristics determined by the team's motor choice: first, they needed to supply 12 V, the voltage requirement of the motor, and second they needed to be able to handle high current, as the stall current of the chosen motors is 20 A. In addition, it would also be preferable for the motor drivers to be able to be easily connected to an Arduino.

Based on these criteria, the team selected the Polulu Dual G2 High-Power Motor Driver 18v18 Shield for Arduino. This motor driver supports an operating range of 6.5 V to 30 V, which satisfies the 12 V requirement. It also can handle up to 18 A of continuous current without additional heat sinks. CEMENT3D felt that this maximum current was high enough for CEMENT3D's purposes, as the user would never attempt to drive the motors at their stall current. Finally, as the motor driver is a shield for the Arduino, it can be easily connected and controlled by one. The motor driver costs \$49.95 each.

5.8.4 Power Supply Selection

As mentioned above, each motor requires a voltage supply of 12 V as well as, at maximum, 20 A of current. For the motor driver that controls two motors, this means that theoretically the power supply must support a maximum of 40 A. However, since the team will not run the motors at their stall current, as this could cause damage to the motor, the full 40 A is not required.

Thus, the team decided on purchasing two BMOUO 12V 30A DC Universal Regulated Switching Power Supplies, one for each power supply. Each of these power supplies costs \$18.56.

5.8.5 Arduino Selection

Finally, the Arduino needed to be chosen. The Arduino needed to have both enough pins for all of the connections to the motor drivers and motors as well as interrupt pins required for accurate reading of the encoders. As will be explained in the following sections, the two motor drivers require a total of six digital pins, three of which must be able to support PWM, and the motor encoders require six interrupt pins. An additional digital pin is needed to read inputs for the microSD card reader.

While the Arduino Uno was used for preliminary tests of the system, it only contained two interrupt pins, which was not enough for the system. Ultimately the team chose the Arduino Due. The Due comes with 54 digital pins, 12 of which support PWM. In addition, all of the digital pins can be used as interrupt pins. An Arduino Due costs \$37.40.

5.8.6 Wiring

Basic Overview

The wiring consists of the following components: three motors, two motor drivers, an Arduino, a microSD card reader, and two power supplies. Below is a diagram of the entire system without a power supply. The associated table shows the relationship between wire color and type of connection as is illustrated in **Figure 5.15** and **Table 5.9**:

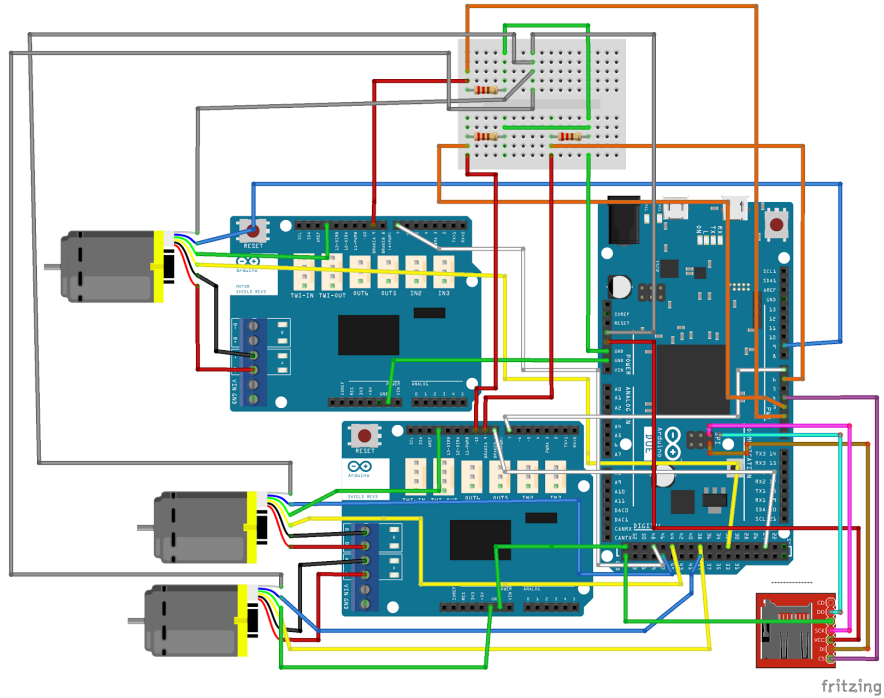


Figure 5.15: Circuit drawing of the entire system

Type of Connection	Color
Motor +	Red
Motor -	Black
Ground	Green
Encoder Channel A	Yellow
Encoder Channel B	Blue
Encoder Voltage	Grey

Motor Direction	White
Motor PWM (Motor Driver)	Red
Motor PWM (Arduino)	Orange
CLK-SCK	Pink
DO-MISO	Cyan
DI-MOSI	Brown
CS-SS	Purple

Table 5.9: Wire Color Meaning

Motors

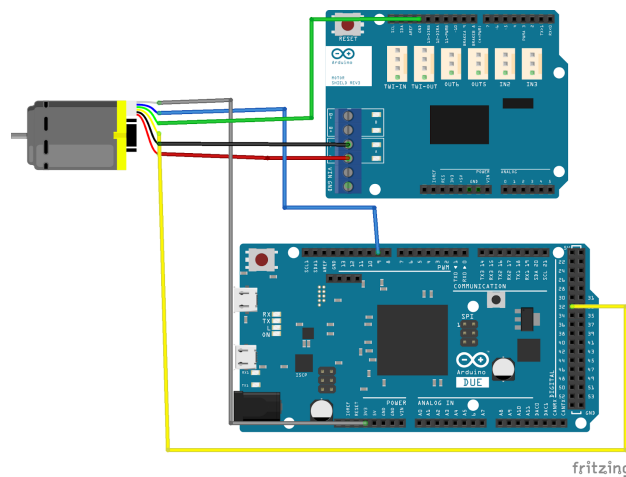


Figure 5.16: Motor Connections for Motor 1. Red and black are motor positive and negative, yellow and blue are Channels A and B of the encoder, green is ground, and grey is encoder supply

Each motor contains six wires: two for powering the motor (positive and negative leads), and four for the encoder (channel A, channel B, ground, and supply voltage), as can be seen from **Figure 5.16**. The positive and negative power wires connect directly into the motor driver. The ground wire for the encoder is connected to the ground pin of the Arduino, and the supply voltage is connected to the 3.3V of the Arduino.

As mentioned above, the encoders require attachment to interrupt pins to allow for the fastest and most accurate reading of the encoders (see **Table 5.10** below).

Motor Number	Channel A	Channel B
Motor 1	32	9
Motor 2	38	39
Motor 3	44	47

Table 5.10: Description of how channels A and B for each of the encoders were attached to the encoders

Motor Drivers

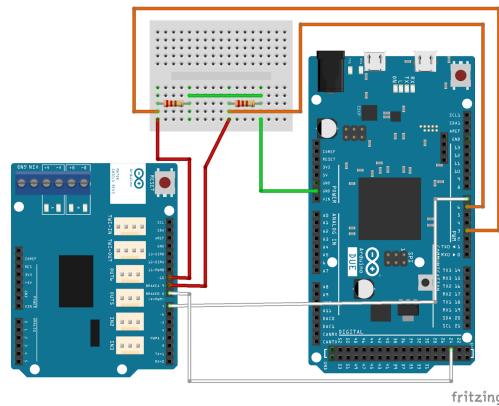


Figure 5.17: Connections for Motor Driver 2. White is direction, orange is the PWM signal from the Arduino, red is the PWM signal to the motor driver, and green is ground. Motor connections have been removed for ease of viewing

As is illustrated in **Figure 5.17**, the motor driver wiring has two main components: power and control. Each motor driver connects to a power supply, which powers the motor driver itself as well as the motors, and has terminals available for powering up to two motors. These terminals have been designated as either “Left” or “Right” in the circuit drawings. For one motor driver (named Motor Driver 1), there is only one motor connected to the motor driver; for the second motor driver (named Motor Driver 2) there are two motors.

Each motor driver also has various connections required for controlling the motor. First, the motor driver is connected to the ground pin from the Arduino. Second, each motor has a respective DIR pin, standing for “Direction,” which controls the direction the motor spins. Each direction pin must connect directly to a pin on the Arduino. Finally, each motor has a respective PWM pin, which controls the speed of the motor. These PWM pins each connect to a 2.2 kΩ pull-down resistor, which prevents the motors from spinning while the Arduino is starting up, which then connects to a PWM pin available on the Arduino (see **Table 5.11** below).

Motor Number	Motor Driver Number	DIR Pin (Motor Driver)	DIR Pin (Arduino)	PWM Pin (Motor Driver)	PWM Pin (Arduino)
1	1	7	48	9	2
2	2	7	7	9	6
3	2	8	24	10	3

Table 5.11: Pin connections from the motor driver to the Arduino

microSD Card Reader

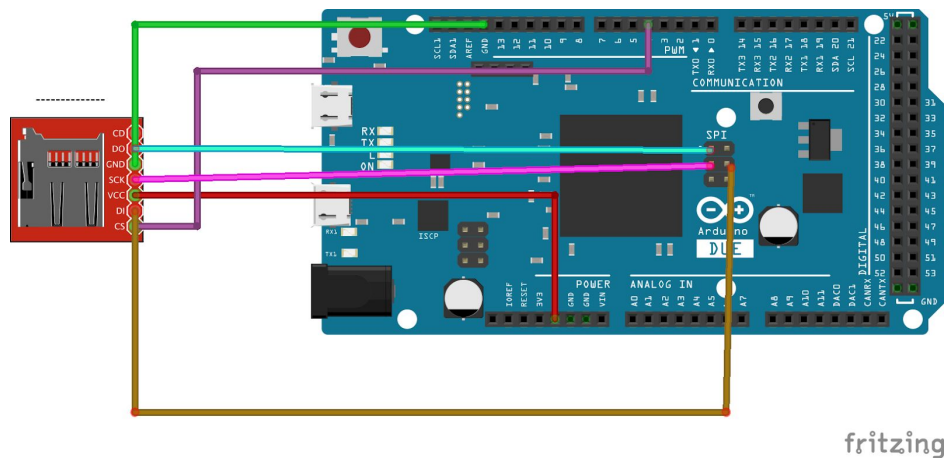


Figure 5.18: MicroSD Card Reader Wire Connections. Red is voltage in, green is ground, pink is the CLK-SCK connection, cyan is the DO-MISO connection, brown is the DI-MOSI connection, and the CS-SS connection is purple.

Finally, there is a microSD card reader similar to the one illustrated in **Figure 5.18**. The reader has six pins: 5V, GND, CLK, DO, DI, and CS. Each of these pins has a respective pin on the Arduino. 5V connects to the 5V pin, GND to the common ground, CLK to the SCK pin, DO to the MISO pin, DI to the MOSI pin, and CS to the SS pin, chosen to be pin 4.

5.9 Programming

5.9.1 Basic Overview

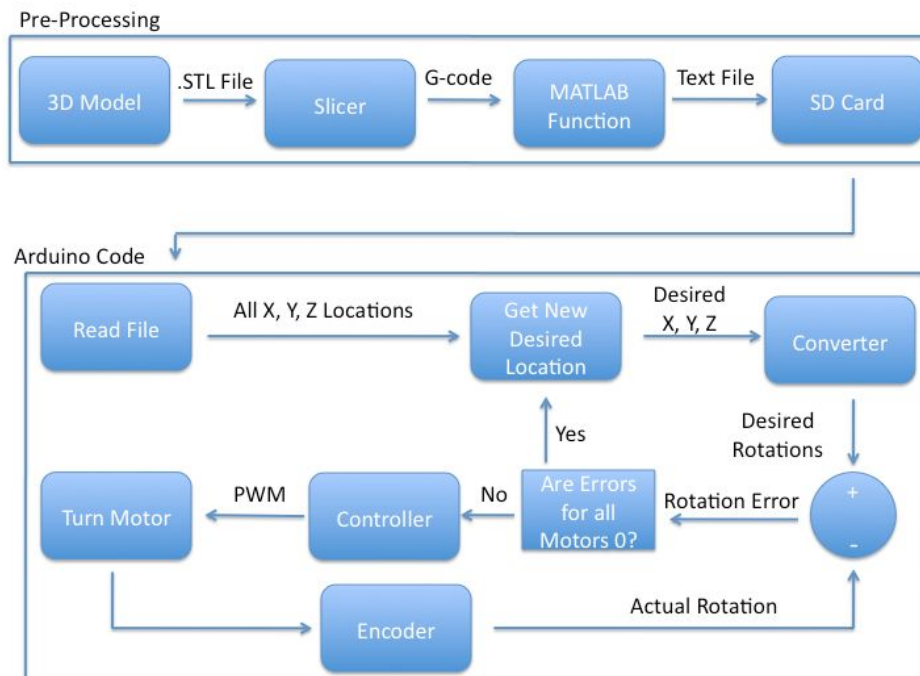


Figure 5.19: Flowchart of code structure. “Pre-Processing” denotes steps done outside of the system, and “Arduino Code” describes the control structure on the Arduino itself

There are two major steps of the code as is illustrated in **Figure 5.19**. First is pre-processing, which describes how the desired part is transferred into a series of positions that the nozzle must reach. Next is the controller itself, done on the Arduino, which reads in these desired positions and drives the nozzle to the desired position.

5.9.2 Pre-Processing

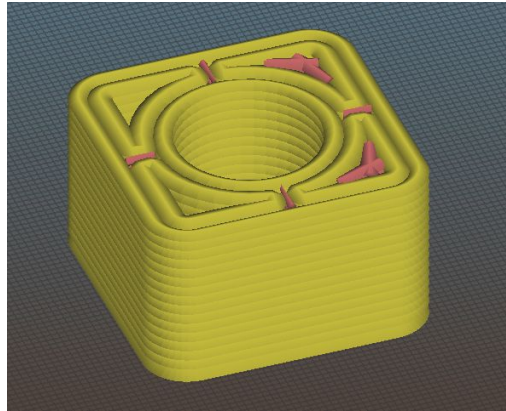


Figure 5.20: Example 3D model passed through the slicer

First, the 3D model of the desired part is saved as a .STL file, similar to the one in **Figure 5.20**. This file is then given to a slicer, which takes the model and produces a series of commands known as G-code. As developing a slicer was outside of the scope of this project, the group utilized the free software known as Slic3r. Slic3r allows for critical information, such as print area, nozzle diameter, and layer height to be defined, which was critical for the team's atypical 3D printer. To force the layer heights to be a constant, thicker distance, the "Layer Height Table" property in Slic3r was used. For example, the 3D model shown in the figure above has a height of 10 inches (254 mm), and the desired layer height is 0.6 inches (15.24 mm). If the table is filled out in the way seen below, then each layer will be the desired height for the entire print:

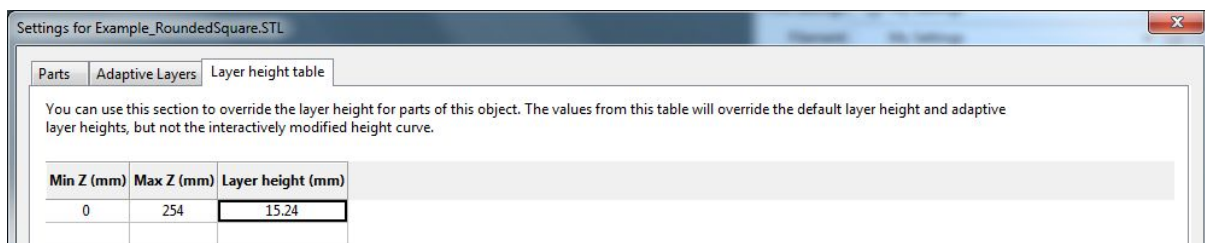


Figure 5.21: Setting layer height

Once the parameters have been set, the Slic3r outputs a G-code file like the one in **Figure 5.21**. The G-code produced contains a list of commands for 3D printers. These commands describe operations such as moving to a specific location, heating the extruded material, changing the extruded material, etc. In order to produce a series of commands that the Arduino can understand, this G-code is inserted into a Matlab Function known as `convertingGCode.m`.

First, the function reads in the provided G-Code. Next, it searches for the first line where the commands begin. The code then reads in the commands line by line and processes its meaning.

For BUILDER, the only important commands are G0 and G1, which describe rapid and controlled movement of the nozzle respectively. Both of these commands follow a similar structure, which can be seen in **Equation 5.18** below:

$$G1 X \# Y \# Z \# \text{ (Equation 5.18)}$$

Where:

= position that the nozzle must move to along that specific axis (mm). If one of these axes is missing (e.g. the line states “G1 X # Y #”) then the missing axis should remain the same as the previous command. Often this omission exists for the Z axis, as the height for a single layer should remain the same.

The code takes each of the above lines, extracts the X, Y, and Z locations, and saves these values into a nx3 matrix, where n is the number of positions. Finally, the function saves this matrix into a text file, where each new line is a new row in the matrix. This text file is then placed on a microSD card, which is inserted into the microSD card reader of the Arduino.

5.9.3 Arduino Code

To begin, the Arduino reads in the inserted text file. It then extracts each line of the text file and saves those values in a matrix. The controller will access this matrix of X, Y, Z locations to determine what the new desired position of the nozzle is.

To control the location of the nozzle, the code examines the current location of the nozzle and the next desired location of the nozzle. For each of those positions, the code determines the length of the wire for each of the three motors using **Equation 5.19**:

$$l = \sqrt{(x_{pulley} - (x_{nozzle} + x_{offset}))^2 + (y_{pulley} - (y_{nozzle} + y_{offset}))^2 + (x_{pulley} - (z_{nozzle} + z_{offset}))^2}$$

(Equation 5.19)

Where:

$x_{pulley}, y_{pulley}, z_{pulley}$ = location of the pulley

$x_{nozzle}, y_{nozzle}, z_{nozzle}$ = location of the center of the nozzle

$x_{offset}, y_{offset}, z_{offset}$ = offset from the center of the nozzle to the location that the wire actually attaches to

While there are two wires connected to each motor, this calculation is only performed once per motor as the lengths of the two wires should always be the same. Next, the code determines how many revolutions each motor should turn by using **Equation 5.20**:

$$rev = \frac{(l_{new} - l_{old})}{2\pi r} \quad \text{(Equation 5.20)}$$

Where:

l_{new} = length of the wire for the new position l_{old} = length of the wire for the old position
 r = radius of the pulley

This revolution is then turned into an associated encoder value the motor must reach using **Equation 5.21**:

$$Encoder \ Value = C_{ideal} * rev \quad \text{(Equation 5.21)}$$

Where:

C_{ideal} = ideal number of encoder counts associated with a single rotation, which for the chosen encoders is 4776.384.

Next, the code determines how fast the motors should spin. The code examines the three desired encoder values and determines which one is the largest. The motor associated with the largest encoder value must move the furthest, and therefore must spin the fastest to end up at the desired position at the same time as the other motors. Thus, this motor will spin at the maximum set speed and the other two motors will move at some proportion of that speed.

As the motors are spinning, the code reads in encoder values from the encoder. Once the encoder has reached its desired value, the code informs the associate motor to stop. When all three motors have reached their desired spot, the code finds the next desired position by performing the same calculation as above. This process continues repeatedly until all desired positions have been met.

5.10 Non-critical systems

5.10.1 Pulley

The dimensions of the pulleys used to route the cables was arbitrary, though thin pulleys were preferred for positional accuracy. The team chose to use the smallest size of mounted pulley

available from the supplier McMaster Carr for logistical convenience. Replacing these pulleys with equivalent parts from a cheaper supplier could cut costs for a future iteration of BUILDER.

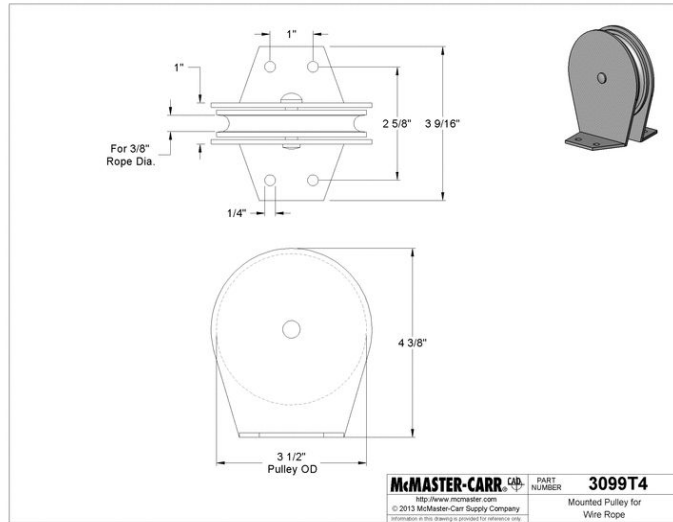


Figure 5.22: Engineering drawing of pulley [25]

5.10.2 Turntable / Lazy Susan

Since the pulleys needed to be able to angle themselves in order to achieve the desired cable angles without slipping, they were separated from the frame by a small lazy susan style bearing. Once again, a convenient part was ordered from McMaster Carr.

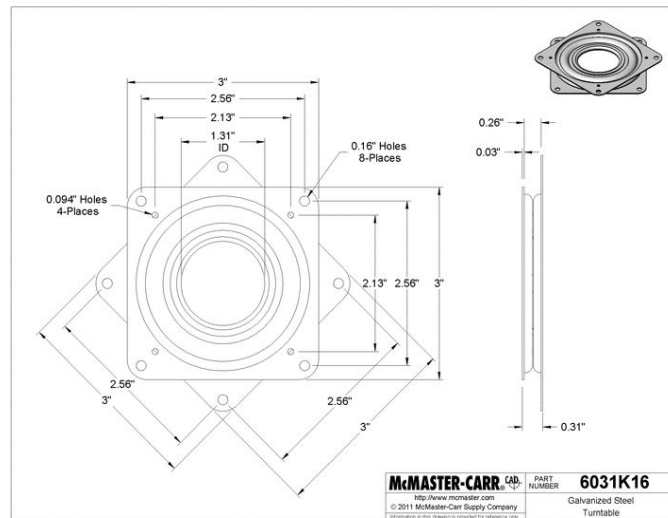


Figure 5.23: Engineering drawing of lazy susan [26]

5.10.3 Surface Area Fins

Since the system is much taller than it is wide and is subject to human-scale inertial forces, tipping was an area of concern. To ensure that the system remained upright, a series of fins were added to the base of the superstructure, as is illustrated in the Engineering drawing in **Figure 5.23**.

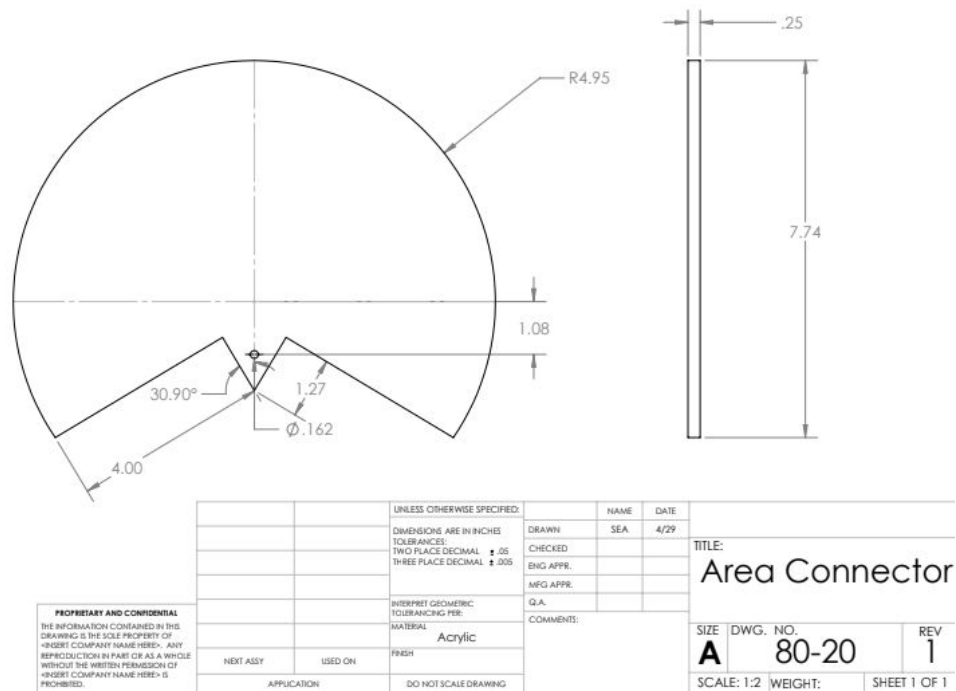


Figure 5.24: Engineering drawing of surface area fin

5.10.4 Universal Joints

It is necessary for the orientation of the print head to be isolated from the orientations of the actuation cables. CEMENT3D therefore chose to connect the two using universal joints. These joints were comprised of pre-fabricated pivot joints from 80-20 allowed to spin freely on M5 shoulder bolts attached to the print head.



Figure 5.25: Render of universal joints pictured on system

5.10.5 Tube Ring

In order to support the weight and provide a connection mechanism for the concrete tube and the print head, a tube ring assembly was attached to one of the cross-members in the y-z plane as is illustrated in **Figure 5.26** below. As mentioned in **Section 5.3**, the design considerations surrounding print head stability and structural mechanics led the team to attach the tube ring at a vertical distance of 0.75m from the base.



Figure 5.26: Tube ring from different orientations

6 Validation and testing

6.1 Validation of concrete

6.1.1 Deformation of concrete layers

It was important for Team CEMENT3D to validate whether there would be any deformation of the structure due to the addition of multiple layers. To address this concern, the team built layered structures using a mould, dimensioned 0.6”x1”x5”, as representative of a single layer. Upon curing, the height of these layered structures were recorded and mapped below along with the theoretical height of these structures, in **Figure 6.1**.

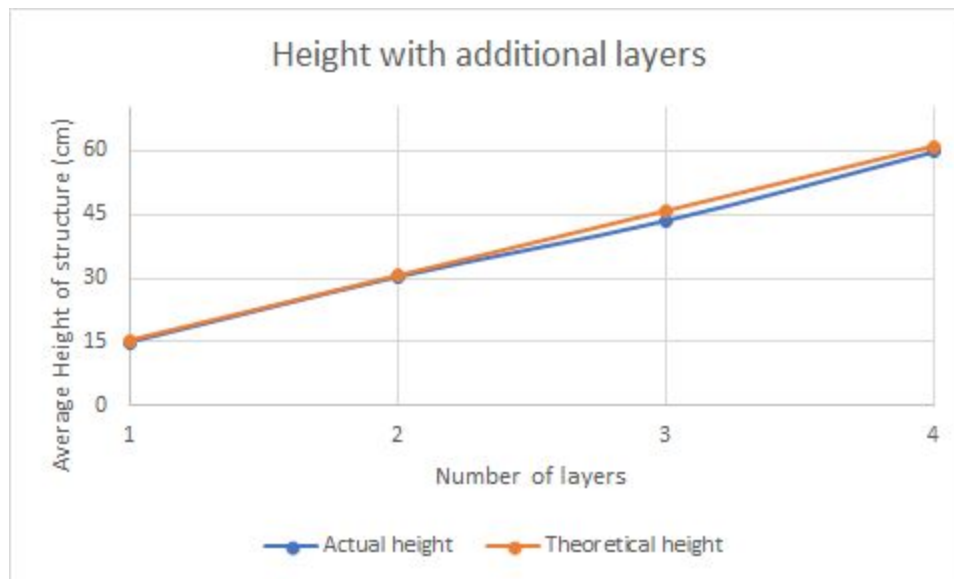


Figure 6.1: Height of the structure given multiple layers

The results show that there was no significant deformation of the structure when additional layers were added. These layers were placed on top of one another, between time intervals of 45 seconds, due to the reasons outlined in **Section 5.7.3**.

A key limitation of this test is that the maximum height tested is only approximately 7cm, whereas CEMENT3D’s print space is expected to be up to 50cm and so further validation may be needed to conclusively prove that no deformation within the structure will take place.

6.1.2 Strength of Layered Concrete

Team CEMENT3D validated whether placing the concrete layer on layer, as opposed to conventional means where the concrete would have no layers, would significantly weaken the structural integrity of items printer.

The team undertook tests similar to those outlined in **Section 5.7.3**, where an axial load was applied by a chisel, onto the ridge between layers of the concrete samples. The maximum stress required to crack the layers, assuming a 45 second interval between placing the layers on top of one another, was compared to the maximum stress required to crack a solid block. The results indicated in **Figure 6.2** show that the layered concrete was 12% weaker than the concrete with no layers.



Figure 6.2: Max shear stress to crack between the layers of concrete as compared to no-layers



Figure 6.3: Cracks along layers after maximum shear stress is reached

As seen above, **Figure 6.3** illustrates the cracks forming along the layer as anticipated.

6.1.3 Compressive strength test of different concrete ratio mixes

Given that BUILDER uses a concrete:water ratio of 3.5:1, which is higher than the recommended 2.6:1 [27], it was important for the team to validate that this new concrete to water ratio does not adversely affect the mechanical properties of the concrete.

For this reason, Team CEMENT3D measured the shear stress required to fracture the concrete given the optimal concrete to water ratio as compared to that used by the team. As seen in **Figure 6.4**, there is no significant difference between the shear stress required to crack concrete blocks with different concrete to water ratios. Thus, the team is not heavily concerned with the possibility that the team's chosen mixture may be weaker than a standard mixture.



Figure 6.4: Cracks along layers after maximum shear stress is reached

6.1.4 Extrusion

In order to validate that the linear actuator CEMENT3D used was able to pump concrete given the 1" nozzle, as well as to test for possible complications with layer adhesion, hand tests were carried out with one person supporting the tube, as concrete was extruded. **Figure 6.5** below shows that the team was able to extrude concrete successfully using the linear actuator. The variations in width are attributed to the non-constant speed at which the nozzle was moved.



Figure 6.5: Extruded concrete using linear actuator

6.2 Validation of Actuation

6.2.1 Virtual Validation

The team validated the system in two ways: first in virtual simulation, and then on the actual device. The virtual simulation was performed using MATLAB, as is given in **Figure 6.6**.

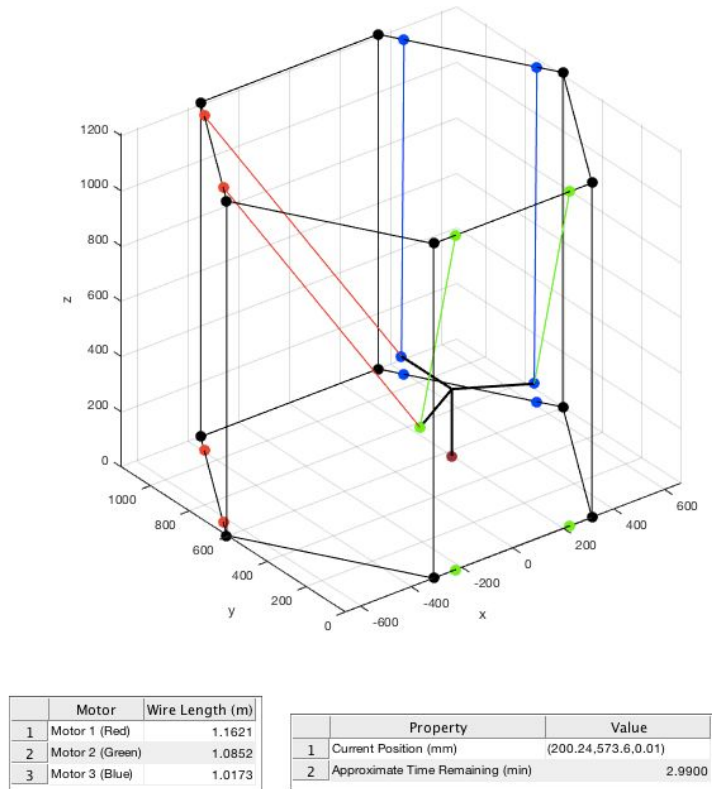


Figure 6.6: Sample image of the simulation. The red, green, and blue wires correspond to motor 1, motor 2, and motor 3 respectively

First, the MATLAB code plots a simplified version of the system, removing the cross members, the wires that go from the base to the respective pulley, the attachment on the cage for the tubing, and the tubing itself. The print head and motor mounts are also simplified.

Next, the code uses the `convertingGCode.m` function described in section 5.10.2 to take a provided G-Code file produce a matrix of X, Y, and Z locations for the nozzle to move. Then, using the equations described in section 5.10.3, the code finds the new desired wire lengths in order to produce the next nozzle position. This process repeats until all of the desired locations have been reached.

The simulation also records information in two tables located at the bottom of the figure. The table on the left describes the current length of the wires connected to each of the three motors. The table on the right contains two pieces of information: first, the current location of the print nozzle, and second the estimated time remaining for the print to finish.

The estimated remaining print time was calculated by first calculating the estimated print time. The code calculates this number by first finding the distances between each point. Then, it assumes that the nozzle will be able to move at the maximum speed between each point. Finally, the estimated print time is found using **Equation 6.1**:

$$t_{print} = \frac{\sum d}{v_{max}} \text{ (Equation 6.1)}$$

Where:

d = vector containing all of the distances between points

v_{max} = maximum speed

The estimated remaining print time is then found by subtracting the estimated print time by the current simulation time. Based on how the estimated print time is calculated, the estimated remaining print time will always be an underestimate, as the nozzle will not be moving at maximum speed at all times.

In addition, as the nozzle moves from one position to another, the code leaves a brown dot to represent the printer extruding concrete. **Figure 6.7** below show example patterns drawn from G-Code files:

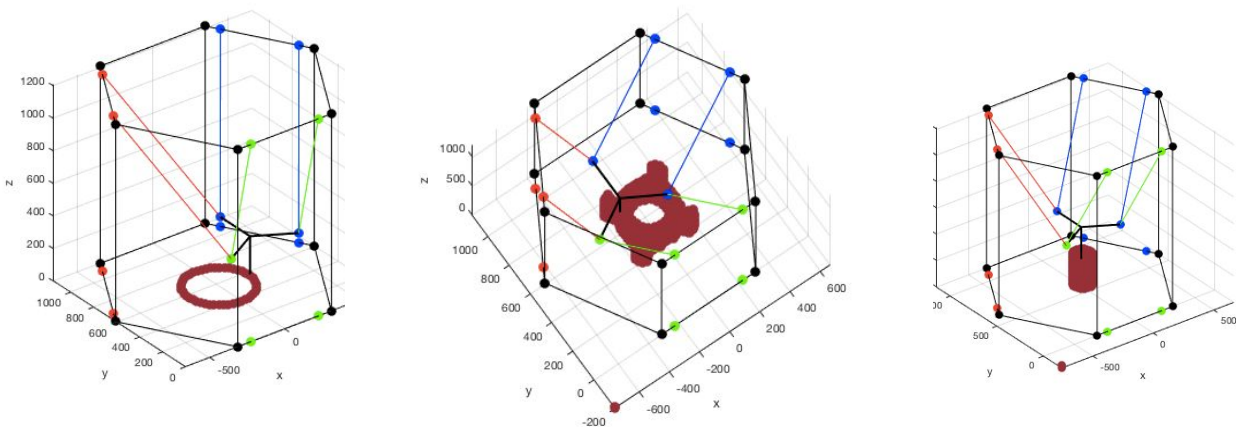


Figure 6.7: Example shapes drawn from G-Code. From left to right: a circle, a rounded square with a hole, a cylinder

Another characteristic of the simulation is implementation of Forward Kinematics on the system. As opposed to the Inverse Kinematics shown above and in section 5.10.3, which finds the wire lengths for each of the cables based on the desired location of the print nozzle, Forward Kinematics finds the location of the print nozzle based on the current wire lengths. By implementing Forward Kinematics, the controller is able to drive errors in X, Y, and Z to zero, whereas Inverse Kinematics can only drive errors in θ_1 , θ_2 , and θ_3 (the angles of the motor) to zero.

To do this, the simulation requires knowledge of the wires lengths for all of the motors. Next, it looks at wire “pairs,” where two wires from two different motors connect to the same point.

Wire Pair	1st Wire Name	2nd Wire Name	print head Location
1	Motor 1 Left	Motor 3 Right	+Y
2	Motor 1 Right	Motor 2 Left	-X, -Y
3	Motor 2 Right	Motor 3 Left	+X, -Y

Table 6.1: Description of which two wires connect to the print head. “Left” and “Right” denotes which pulley the wire is connected to when facing the pulleys from outside of the structure looking in. “Print Head Location” describes where the wires connect on the print head, denoted by the offset from the center

Each of these wire pairs describes the intersection of two spheres, where the center of the sphere is the pulley location and the radius is the wire length. The intersection of two spheres forms a circle. Since it is known that the two wires intersect on the print head, the location of that point of the print head must lie somewhere on the resulting circle.

To find this circle, first the two pulley locations are normalized such that the first pulley in the pair is located at $(0, 0, 0)$ and the second pulley is at $(d, 0, 0)$. The circle which describes the intersection of the two spheres must lie somewhere on this rotated x-axis in between the two points. To find this distance d along this rotated x-axis, one can use **Equation 6.2**:

$$d = \sqrt{\Sigma(P_1 - P_2)^2} \text{ (Equation 6.2)}$$

Where:

P_1 = location of the first pulley in the rotated frame

P_2 = location of the second pulley in the rotated frame.

Next, to find the center and radius of the circle, one can use the **Equations 6.3 - 6.5** below:

$$x_{center}^{Rotated} = \frac{d^2 - P_2^2 + P_1^2}{2d} \text{ and } r = \frac{1}{2d} \sqrt{((4d^2 P_1^2) - (d^2 - P_2^2 + P_1^2))^2} \quad \text{(Equation 6.3)}$$

However, the location of the center is in the rotated frame, not the world frame. The Z-value of this point is simply the height of the pulleys, as the heights are known to be the same. To find the X and Y value, first P_1 is rotated into the new frame. Then x_{center} is added to the rotated point. Finally, the point is rotated again to return it into the original world axis. **Equation 6.4** below shows the final result:

$$[x_{center}, y_{center}]^T = R^T (R * P_1 + [x_{center}^{Rotated}, 0]^T) \quad \text{(Equation 6.4)}$$

Where:

R = rotation from the world frame into the rotated frame, defined as the frame whose X-axis points in the direction of the second pulley.

The 2-D rotation matrix is defined using **Equation 6.5** below:

$$R = [\cos(\theta), -\sin(\theta); \sin(\theta), \cos(\theta)] \quad \text{(Equation 6.5)}$$

Where:

θ = angle from the world frame's X-axis to the rotated frame's X-axis.

For each of the three wire pairs, this angle is as follows:

Wire Pair	Angle (Degrees)
1	0
2	-60

3	60
---	----

Table 6.2: Angle in degrees for the rotation matrix of each wire pair

With the location of each of the centers of the circles and the corresponding radii, the three circles can be plotted, as seen in **Figure 6.8** below:

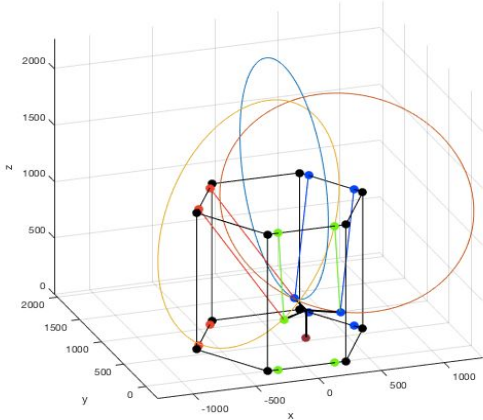


Figure 6.8: The three circles formed through the three sphere-sphere intersections. The blue circle corresponds to wire pair 1, the yellow to wire pair 2, and the red to wire pair 3

When the above image is projected onto the X-Y plane, an interesting observation is noted:

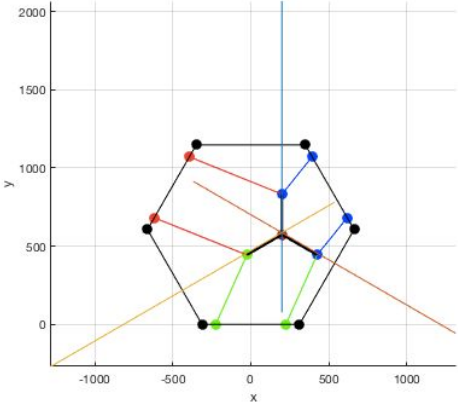


Figure 6.9: Figure 6.8 projected on the X-Y plane. The circles from the previous figure are now the blue, yellow, and red lines

The three circles, when projected onto the X-Y plane, turn into lines, which just so happen to intersect at the center of the nozzle in X and Y, as is seen in **Figure 6.9** above. The reason for this phenomenon is due to the angles described in **Table 6.2** above. The angle for the rotation matrices are 0, -60, and 60 respectively. The circles must be perpendicular to this rotated axis, which means the angle the circles will fall along are 90, -30, and 30 respectively. As the arms of the print head are separated by 120 degrees, these circles will have the proper angle to have the intersection point be at the center of the print head.

To find the location in X and Y of the center of the print nozzle, one must find the intersection of these three points. First, these lines are represented as **Equation 6.6**:

$$y - m * x = b \text{ (Equation 6.6)}$$

Where:

m = slope of the line, found to be $\tan(\theta)$ as described above

b = found through performing the above equation for a known point on the line: the center of the circle.

Next, the system of three equations is created by setting up the following matrices in **Equation 6.7**. Note that the A coefficient matrix is constant, as it is only dependent on the angles, which are always the same.

$$\begin{bmatrix} 1 & 0; & .5774 & 1; & - .5774 & 1 \end{bmatrix} * \begin{bmatrix} x_{intersect} & y_{intersect} \end{bmatrix}^T = \begin{bmatrix} y_{center_1} - m_1 x_{center_1} & y_{center_2} - m_2 x_{center_2} & y_{center_3} - m_3 x_{center_3} \end{bmatrix}^T \text{ (Equation 6.7)}$$

By using the pseudo-inverse, $\begin{bmatrix} x_{intersect} & y_{intersect} \end{bmatrix}^T$ can be found. To find the height in Z, the distance formula is utilized. The X and Y location of any of the nozzle head arms are known, since the location of the center is known, and the lengths of all of the wires are known. Thus, using the wire pair 1 point (offset from the center only in y), the wire length associated with motor 1, and knowledge that the print head must be below the pulley, the height is defined by **Equation 6.8**:

$$z_{intersect} = P_{1,z} - \sqrt{l^2 - (P_{1,x} - x_{intersect})^2 + (P_{1,y} - (y_{intersect} + y_{offset}))^2} \text{ (Equation 6.8)}$$

Where:

l = length of the wire associated with motor 1

To test the accuracy of the Forward Kinematic solution, the team ran simulations using the Forward Kinematic print head location and compared those values to the desired print head locations given into the simulation via the G-code, illustrated in **Figure 6.10**. The following graphs show the absolute value of the difference of the Forward Kinematic solution and the known nozzle location:

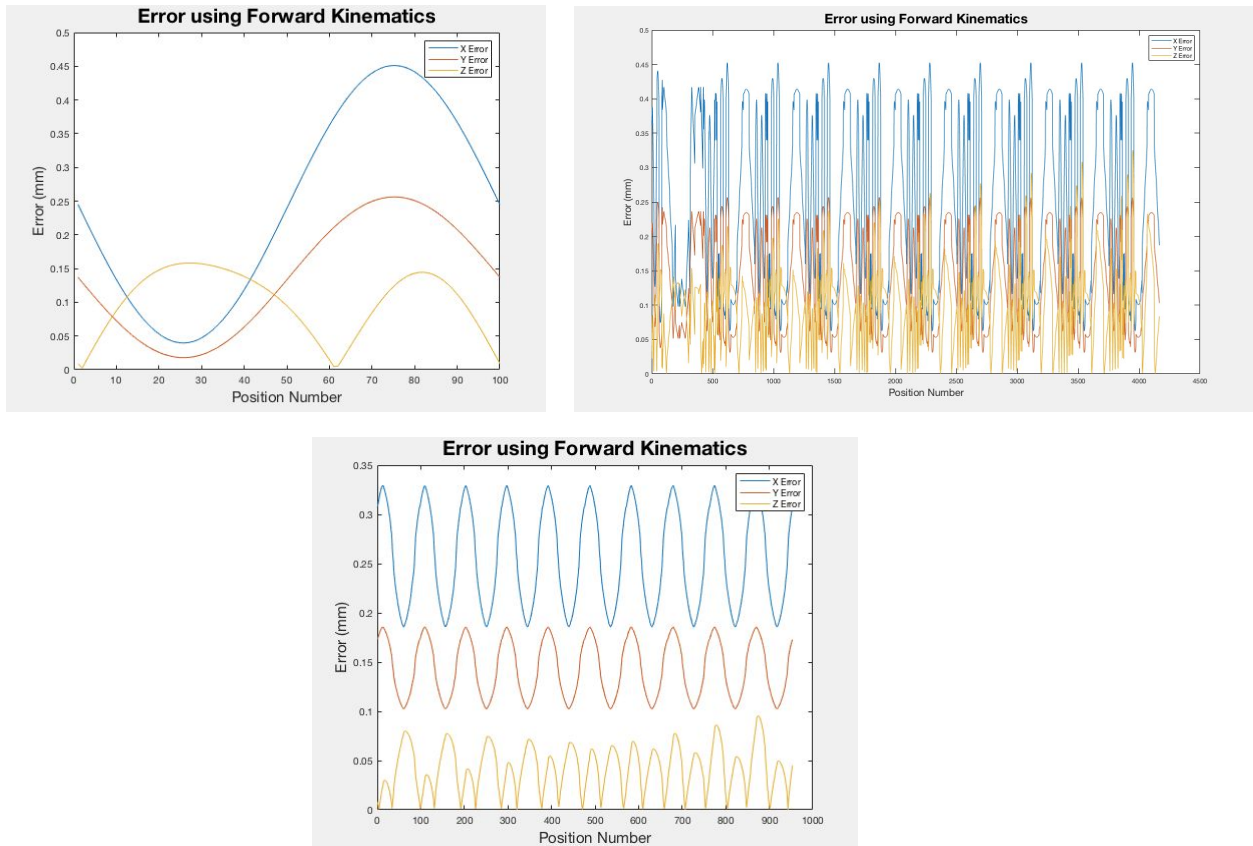


Figure 6.10: Error using Forward Kinematics for the following formations: circle (upper left), rounded square with a hole (upper right), and a cylinder (bottom). Blue represents error in X, red represents error in Y, and yellow represents error in Z

Though the error is not constant through the simulation, it remains less than 0.5 millimeters (.02 in) at all times. Based on this small error, the team observed that the Forward Kinematics is relatively accurate.

6.2.2 Real System Validation

On the real system, there were three main components. First, the Arduino needed to be able to read in the text file through the microSD card reader. This step was done through looping through every row of the text file and extracting out the X, Y, Z locations.

Next, code needed to be written to move the motors in an uncontrolled state. This was done by supplying a voltage to each of the motors via a PWM signal. Once the motors were spinning, the encoder values could also be read to ensure that they were working.

Finally, the actual controller code needed to be written. Unfortunately, while we were able to command the motors manually by supplying a specific PWM and direction, the controller did not work as desired. Due to the lengths of the wires connecting the motors to the box of the electronics there was a voltage drop and the motors did not spin at the same speed when the same PWM was given. Also, the controller did not move the motors the requested amount; for some reason, the amount moved was always shorter than expected. In order to solve these problems more time is required.

7 Discussion

7.1 Target versus accomplished performance

Below is a comparison of the completed system's performance on the set of key performance metrics identified at the project outset and the goals identified when the project was first undertaken (with justification for each value provided in **Appendix B**).

Specification	Relative Importance	Desired Value	Achieved Value
Print Size	1	0.5 [m ³]	0.69 [m ³]
Cost	2	1400 [USD] (based on user rental price of \$200 for 10 days)	1789.96 [USD]
Pieces Before Assembly	2	12	6
Weight	4	445 [N]	375 [N]
User Operations per Print	5	25	Not achieved
Print Resolution	6	6 [cm]	0.5 [cm]
Print Time	7	20 [min]	98 [min]

BUILDER's final characteristics fell short of meeting all the objectives of consumers. Specifically, BUILDER was more expensive and ran at a longer print time than initially targeted. However, CEMENT3D believes that, with large scale manufacturing, specifically by using non-branded electronics, using substitutes for 80-20, and by using large-scale manufactured gears, the cost for materials will be brought down substantially. This would enable consumers to rent BUILDER at a price that generates value for both the team and the consumer. It must be noted that the team does not believe print time can be reduced to meet target objectives, unless BUILDER is made more expensive. This is because reducing print time would involve having

more powerful motors, thicker kevlar cables, and a higher flow rate, each of which would involve a larger investment. This tradeoff is undesirable, since cost was a much more important factor than print time, based on customer need.

BUILDER exceeded the most salient objectives of consumers. The print area was designed such that it was larger than initially targeted. This is a great value add to consumers since most landscaping structures produced would require large print areas. Further, the weight of the system is lower than the OSHA standards for manual lifting by 2 people, enabling consumers to carry the system. Finally, the theoretical print resolution of the system is designed to be finer than targeted, allowing consumers to build more customizable products.

7.2 Recommendations

One of the biggest challenges that CEMENT3D faced was with integrating the concrete extrusion system with the rest of the printer. Specifically, despite being able to extrude concrete reliably and with a steady flow when the hose was detached, no flow was able to be achieved when the system was fully integrated. The team believes that because of the bends in the tube, air pockets formed during concrete loading, which obstruct the flow. Similar issues were experienced with air pockets during early concrete tests, which the team was able to resolve by tamping, since the tests were with a relatively short, straight tube. Additional thought needs to be put towards how to remove air from the integrated system before printing.

Had CEMENT3D had more funds available, the team would have likely purchased a Progressive Cavity pump. A Progressive Cavity pump transfers the concrete by means of twisting of a rotor, specifically designed to handle pumping high-viscosity fluids with large particulates at a controllable flow rate. Due to the lack of commercially available low-pressure, low flow-rate progressive cavity pumps (the pressure differential needed was only 0.43 psi as per **Section 5.7.5**), CEMENT3D would have had to purchase a Progressive Cavity pump that had more powerful specifications than needed. As such, the team would have purchased the lowest pressure-rated Grainger Progressive Cavity pump if the team had more funds--[28] in **References** shows one pump that CEMENT3D would have considered buying.

CEMENT3D also acknowledges that more design work is required to achieve optimal user interaction. The software, for instance, should be condensed to a user-friendly design application, which performs slicing and GCode formatting on the backend, and an on-board program that takes in the direct output of this application to produce a print. Additionally, an easy method of leveling the ground and the system and a more deployable frame would be needed to fully meet the needs of the user.

Lastly, CEMENT3D would have liked to further develop the design of the print head. Although the team carried out an FEA on the print head and cross checked that with a beam bending calculation in **Section 5.2**, the team would have liked to carry out more rigorous analytical validation by carrying out a mesh convergence study to ensure that the value reported from the FEA has stabilized. Alternatively, the team would have checked the conservation of strain energy relative to the load applied. Moreover, the team would have liked to further optimize the print head geometry for stability, potentially using dynamic simulations, or asking for advice from companies which have produced delta style printers. At the present moment, the dimensions are still approximate values derived from the TES constant, and although no problematic angular displacements were observed in the final system, a second iteration could potentially offer the advantage of being more compact.

8 Budget, donations, and resources

Item	Unit Price	Quantity	Total Price
84 RPM Gear Motor with Encoder	\$59.99	3	\$179.97
Dual G2 High-Power Motor Driver 18v18 Shield for Arduino	\$49.95	2	\$99.90
Arduino DUE	\$37.39	1	\$37.39
MicroSD Card Breakout Board+	\$7.50	1	\$7.50
12V 30A DC Universal Regulated Switching Power Supply	\$18.85	2	\$37.70
Metal Gear (14-1/2 Degree Pressure Angle, 32 Pitch, 20 Teeth)	\$25.40	6	\$152.40
Metal Gear (14-1/2 Degree Pressure Angle, 32 Pitch, 40 Teeth)	\$50.80	6	\$304.80
Pulley	\$7.38	6	\$44.28
180 inch aluminum (30mm X 30mm T-Slotted Profile)	\$45.15	4	\$180.60
Universal Joint	\$17.75	6	\$106.50
Aluminum Corner Bracket (for base)	\$17.75	12	\$213.00
M6 T-nut	\$0.27	160	\$43.20
M6 x 14.00mm Button Head Socket Cap Screw	\$0.39	200	\$78.00
M6 x 25.00mm Button Head Socket Cap Screw	\$0.32	120	\$38.40
M6 x 16.00mm Button Head Socket Cap Screw	\$0.24	16	\$3.84
Kevlar (0.038" High-Strength Temperature Thread)	\$27.17	2	\$54.34
1.5" Inner Diameter PVC tube	\$45.50	1	\$45.50
Concrete (Quikrete)	\$5.97	4	\$23.88
0.5" Carbon Steel D-Shaft	\$24.45	1	\$24.45
Linear Actuator	\$58.28	1	\$58.28
Aluminum Round Stock (for connecting print head)	\$15.41	1	\$15.41
Aluminum Sheet	\$25.50	1	\$25.50
Inside (30 degree) corner brackets	\$2.52	6	\$15.12

Total	\$1,789.96
--------------	-------------------

Table 8.1: Bill of Materials for parts required for BUILDER

References

[1] Proxy.library.upenn.edu. (2018). Shibboleth Authentication Request. [online] Available at: <http://proxy.library.upenn.edu:3880/reports/us/iexpert/default.aspx?entid=1497> [Accessed 25 Apr. 2018].

[2] Fixr.com. (2018). Cost to Install a Fire Pit - Estimates and Prices at Fixr. [online] Available at: <https://www.fixr.com/costs/fire-pit> [Accessed 25 Apr. 2018].

[3] Astm.org. (2018). ASTM International - Standards Worldwide. [online] Available at: <https://www.astm.org/> [Accessed 30 Apr. 2018].

[4] Okw.co.uk. (2018). IP Ratings | IP Rated Electronic Enclosures. [online] Available at: https://www.okw.co.uk/en/technical_data/IP-ratings.htm [Accessed 30 Apr. 2018].

[5] Connevanselectronics.co.uk. (2018). IP rated speakers | Connevans Electronics. [online] Available at: <https://www.connevanselectronics.co.uk/catalogue/7139696/IP-rated-speakers> [Accessed 30 Apr. 2018].

[6] Jorgenson, L. (2018). How to Choose Between Cartesian and Delta 3D Printers — Fargo 3D Printing. [online] Fargo 3D Printing. Available at: <https://www.fargo3dprinting.com/choose-cartesian-delta-3d-printers/> [Accessed 30 Apr. 2018].

[7] Build A 3D Printer. (2018). Why a Delta?. [online] Available at: <http://builda3dprinter.eu/information/why-a-delta/> [Accessed 24 Apr. 2018].

[8] Reprap.org. (2018). Delta geometry - RepRapWiki. [online] Available at: http://reprap.org/wiki/Delta_geometry [Accessed 24 Apr. 2018].

[9] Groups.google.com. (2018). Google Groups. [online] Available at: <https://groups.google.com/forum/#!topic/deltabot/iIAQ1cGgcWY> [Accessed 30 Apr. 2018].

[10] McMaster.com. (2018). McMaster-Carr. [online] Available at: <https://www.mcmaster.com/#3790t11/=1cmjsey> [Accessed 30 Apr. 2018].

[11] McMaster.com. (2018). McMaster-Carr. [online] Available at: <https://www.mcmaster.com/#3461t26/=1btq79f> [Accessed 30 Apr. 2018].

[12] McMaster.com. (2018). McMaster-Carr. [online] Available at: <https://www.mcmaster.com/#8872k49/=1cmjstf> [Accessed 30 Apr. 2018].

[13] McMaster.com. (2018). McMaster-Carr. [online] Available at: <https://www.mcmaster.com/#8800k43/=1cmjrtn> [Accessed 30 Apr. 2018].

[14] Rope User's Manual: Guide to Rope Selection, Handling, Inspection and Retirement. (n.d.). [ebook] Samson, p.37. Available at: http://www.samsonrope.com/Documents/Rope_Users_Manual_WEB.pdf [Accessed 30 Apr. 2018].

[15] Steel Rope Technical Information. (n.d.). [ebook] Bridon Oil and Gas, p.18. Available at: http://www.bridon.com/china/x/downloads/steel_technical.pdf [Accessed 30 Apr. 2018].

[16] Feys, D., Verhoeven, R. and De Schutter, G. (2009). Why is fresh self-compacting concrete shear thickening?. Cement and Concrete Research, 39(6), pp.510-523.

[17] En.wikipedia.org. (2018). Bingham plastic. [online] Available at: https://en.wikipedia.org/wiki/Bingham_plastic [Accessed 24 Apr. 2018].

[18] Bouvet, A., Ghorbel, E. and Bennacer, R. (2010). The mini-conical slump flow test: Analysis and numerical study. Cement and Concrete Research, 40(10), pp.1517-1523.

[19] McMaster.com. (2018). McMaster-Carr. [online] Available at: <https://www.mcmaster.com/#5233k72/=1cjxxmo> [Accessed 24 Apr. 2018].

[20] McMaster.com. (2018). McMaster-Carr. [online] Available at: <https://www.mcmaster.com/#5108k68/=1cjxx5k> [Accessed 24 Apr. 2018].

[21] McMaster.com. (2018). McMaster-Carr. [online] Available at: <https://www.mcmaster.com/#6516t34/=1cjxwpm> [Accessed 24 Apr. 2018].

[22] McMaster.com. (2018). McMaster-Carr. [online] Available at: <https://www.mcmaster.com/#5632k38/=1cjxy3n> [Accessed 24 Apr. 2018].

[23] Vinidex. (2018). PVC Properties - Vinidex. [online] Available at: <http://www.vinidex.com.au/technical/material-properties/pvc-properties/> [Accessed 30 Apr. 2018].

[24] Machine Design. (2018). How to Pick Motors for Linear Motion. [online] Available at: <http://www.machinedesign.com/motorsdrives/how-pick-motors-linear-motion> [Accessed 30 Apr. 2018].

[25] McMaster.com. (2018). McMaster-Carr. [online] Available at: <https://www.mcmaster.com/#3099t4/=1cmt4sx> [Accessed 30 Apr. 2018].

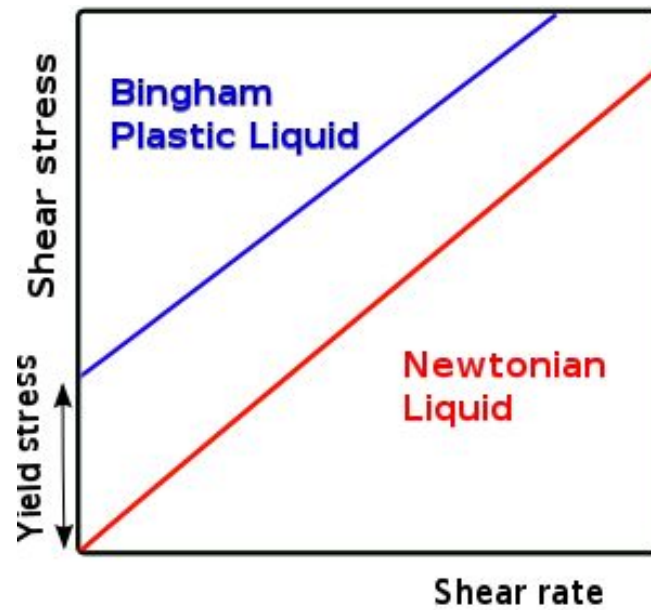
[26] McMaster.com. (2018). McMaster-Carr. [online] Available at: <https://www.mcmaster.com/#6031K16> [Accessed 30 Apr. 2018].

[27] D, A. (2018). SAND / TOPPING MIX DIVISION 3. [online] Available at: https://www.quikrete.com/pdfs/data_sheet-sand-topping%20mix%201103.pdf [Accessed 30 Apr. 2018].

[28] Grainger.com. (2018). MOYNO Motorized Progressive Cavity Pump,40 psi - 30EK56|34459 - Grainger. [online] Available at: <https://www.grainger.com/product/MOYNO-40-psi-Motorized-Progressive-30EK56> [Accessed 25 Apr. 2018].

Appendix

Appendix A: Miscellaneous Figures



A.1: Bingham plastic fluid behavior as a function of shear stress and shear rate [17]

Appendix B: Quality Function Deployment (QFD)

This QFD made use of the 1-3-9 standard to represent a low, medium, or high value or relationship, with 1 representing a weak value and 9 representing a strong value. Additionally, the shorthands LIB/NOM/SIB were used for “larger is better”, “nominal is better”, and “smaller is better”.

									+ Positive Correlation - Negative Correlation
MEAM446									
QFD Phase 1									
		Engineering Metrics							
Customer Needs	Customer Weights	Weight (Packaged)	Print Time	Print Area	# of user operations per print	# of pieces before assembly	Print resolution	Cost	
can create common landscaping features	9			9			1		
can be used without additional input or supervision	3		1	3	9		1		
can create objects quickly	1		9	3	1				
is affordable	9			1				9	
is easy to assemble	9	3		1		9			
is safe	9	3		3					
can create customized objects	3						3		
					non-dimensional	non-dimensional			
	Units	[N]	[min]	[m ²]			[cm]	[USD]	
	EM Direction	SIB	SIB	NOM	SIB	SIB	SIB	SIB	
Technical Benchmark	A: Ashland Concrete Firepit Kit	3470	60	0.38	77	37	N/A	200	
	B: Professional Stamped Concrete "Hardscaping" (Average National Cost):	N/A	1440	1.06	0	N/A	0.7	4493	
	C: Landmann USA 36-in W Brown Steel Wood-Burning Fire Pit	146	0	0.5	0	1	N/A	211	
	Raw Score	54	12	138	28	81	21	81	
	Relative Weight	13%	3%	33%	7%	20%	5%	20%	
	Rank	4	7	1	5	2	6	2	
Technical targets		445	20	0.5	25	12	5	1400	

B.1: QFD schematic

Justification of Technical Targets	
Target	Justification
Weight	Based on OSHA standards for manual lifting. Can be safely handled by 2 hardware store employees. Comparable to benchmarked products.
Print Time	Chosen for 3x performance of benchmarked products.
Print Area	Based on average project size and comparison to benchmarked products.
Operations Per Print	Chosen for 3x performance of benchmarked products.
Pieces Before Assembly	Chosen for 3x performance of benchmarked products.
Resolution	Resolution should be on the order of the tolerance of poured concrete in order to create comparable projects.
Cost	Based on a rental price of \$200 to be comparable to low-end methods. Rental period was approximated as 10 days, with profit generation at 6 months. This made the wholesaler price \$2400. A margin stack was applied using U&E Typical margins for industrial equipment, making the target cost for the manufacturer .

B.2: Justification of technical targets

Print Area	
Length of shortest side in cage (m)	0.6
Radius of inscribed circle within hexagon with smallest sides (m)	0.52
Percent radius used for print	90%
Print Area (m ²)	0.69

B3: Calculations for Print Area of the system

Weight of BUILDER	
Component	Mass (kg)
Concrete + tube	8.5
Top Cage	3.5
Bottom Cage	3.5
Vertical Members (6 total)	6.5
Cross Members (3 total)	3.1
Two Cap Mount	1.6
Bottom 80-20 members (3 total)	1.3
Printhead	1.3
Surface Area Enhancers (30 total)	2.7
Nozzle Rig Joints (6 total)	0.7
Pulleys (6 total)	1.2
Lasercut Connectors (48 total)	1.3
Other miscellaneous (approxima	3.0
Total Mass (kg)	38.3
Total Weight (N)	375

B4: Masses used to calculate the weight of BUILDER

Resolution of a printer is determined by calculating which of the following 3 factors is limiting: Repeatability, controllability and the nozzle.

Repeatability	
Not Measured	
Controllability	
Smallest angle control (deg)	1.9
Radius of Capstan (cm)	3.81
Smallest Movable distance (cm)	0.13
Nozzle	
Nozzle diameter (cm)	2.54
Nozzle radius (cm)	1.27

B5: Theoretical Resolution of Printer

Custom print in 0.69m ² print space	
Height of print space (m)	0.5
Volume of print space (m ³)	0.345
In-fill %	60%
Volume of concrete required	0.207
Volumetric flow rate (m ³ /s)	3.51E-05
Time (s)	5896
Time (min)	98
Time (hrs)	1.6

B6: Calculations used to determine the time required for a full print

Appendix C: Calculations

Printing 1 layer	
Circumference of Print Area	1.814
Height of layer	0.023
Wight of layer	0.038
Total Volume of Concrete (m ³)	0.002
Print time (s)	45
Flow rate (m ³ /s)	3.5E-05
Flow rate (lpm)	2.1

C.1: Figures and calculations used to determine Flow rate

Assumption: The flow rate was calculated assuming the print head must print a circle along the circumference of the print area within 45 seconds.

Printing 1 layer	
Circumference of Print Area (m)	1.814
Print time (s)	45
Speed of actuation (cm/s)	4.03

C.2: Figures and calculations used to determine average required speed of actuation

Assumption: The required print head speed was calculated assuming the print head must print a circle along the circumference of the print area within 45 seconds.

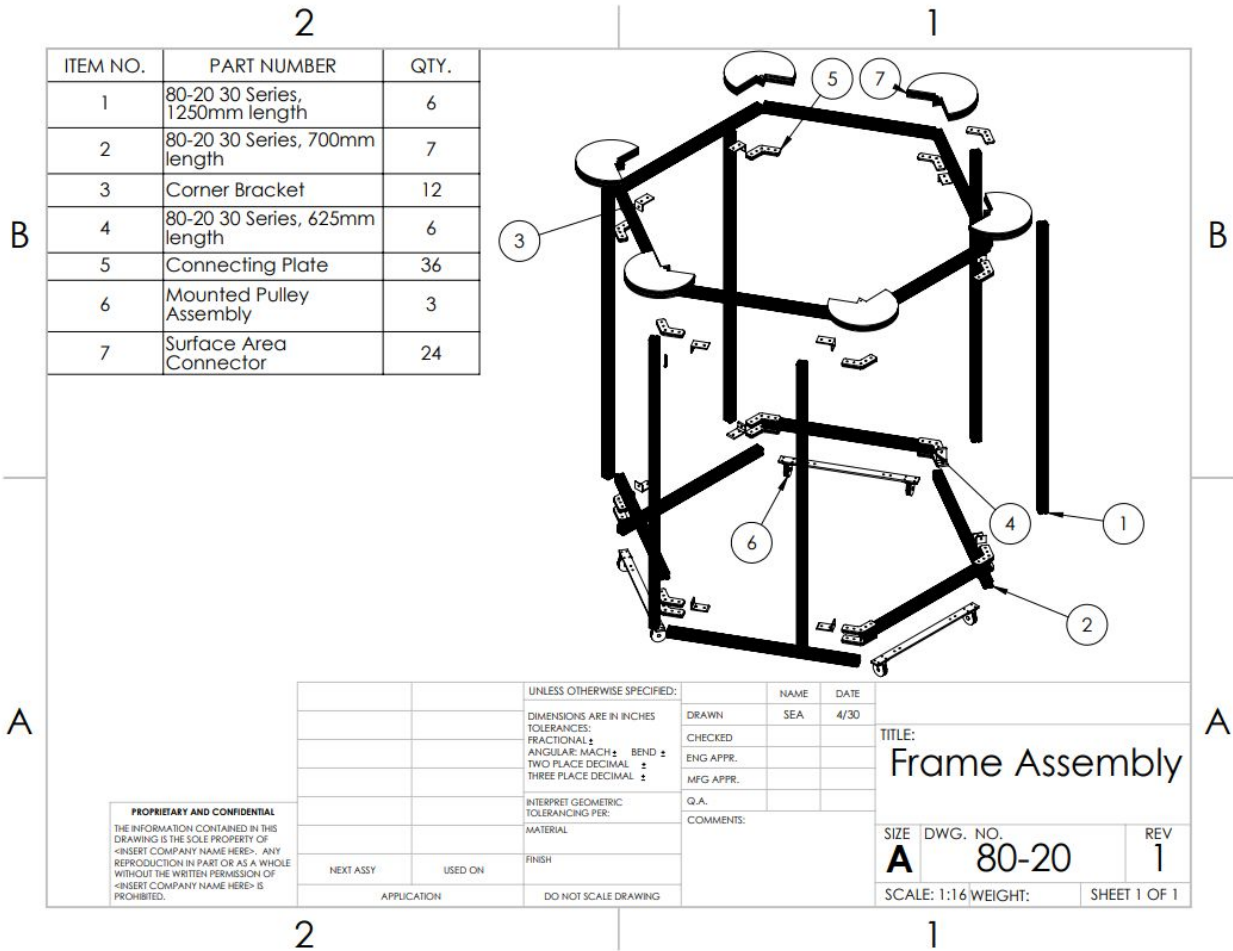
Max actuation speed of print head	
Max rpm of motor	84
Max rps of motor	1.4
Gear ratio	4.8:1
Radius of capstan (cm)	3.8
Max actuation speed (cm/s)	7.0

C.3: Figures and calculations used to determine the maximum actuation speed of the print head

Total Volume of Concrete (m3)	
Circumference of Print Area	1.814
Height of layer	0.023
Weight of layer	0.038
Number of layers	3
Total Volume of Concrete (m3)	0.0047

C.4: Figures and calculations to determine the volume of concrete required for printing 3 layers

Appendix D: Engineering Drawings



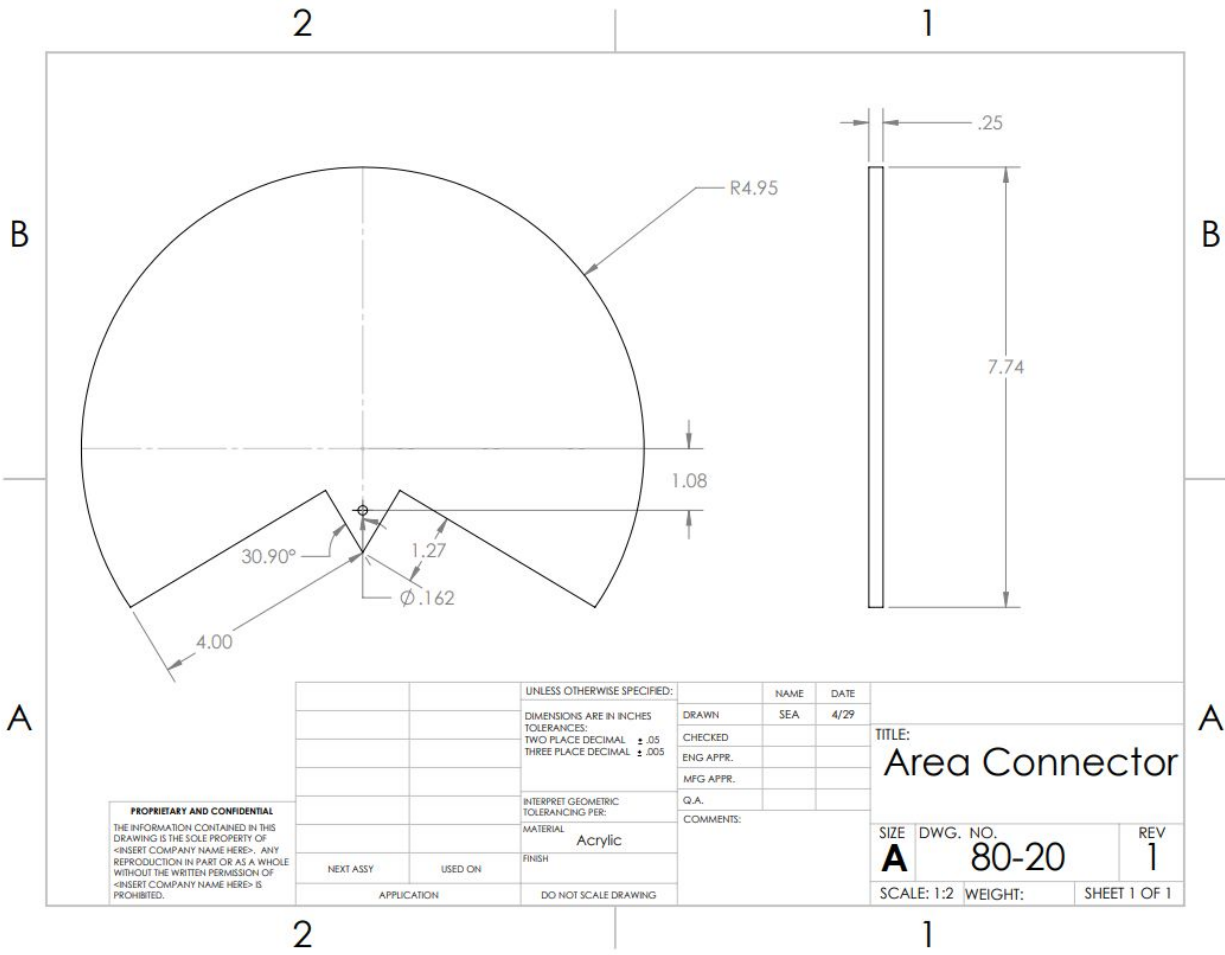
ITEM NO.	PART NUMBER	QTY.
1	Motor Base Plate	1
2	Spool	2
3	1/2" Diameter Carbon Steel Rod	1
4	Motor	1
5	Motor Holder	1
6	Motor Lifter	1
7	Aluminum Holder	5
8	24 Pitch 72 Teeth Gear	1
9	24 Pitch 15 Teeth Gear	1
10	5/8" OD 1/2" ID	6
11	Clamping Shaft Collar	2
12	80-20 30 Series, 19.5 in Length	1
13	Fastener	4

		UNLESS OTHERWISE SPECIFIED:		NAME	DATE
		DIMENSIONS ARE IN INCHES		DRAWN	SEA 4/30
		TOLERANCES:		CHECKED	
		FRACTIONAL: ±		ENG APPR.	
		ANGULAR: MACH ± BEND ±		MFG APPR.	
		TWO PLACE DECIMAL: ±		Q.A.	
		THREE PLACE DECIMAL: ±		COMMENTS:	
		INTERPRET GEOMETRIC TOLERANCING PER:			
		MATERIAL:			
		FINISH:			
NEXT ASSY	USED ON				
APPLICATION		DO NOT SCALE DRAWING			

TITLE: Motor Mount

SIZE	DWG. NO.	REV
A	MM	1

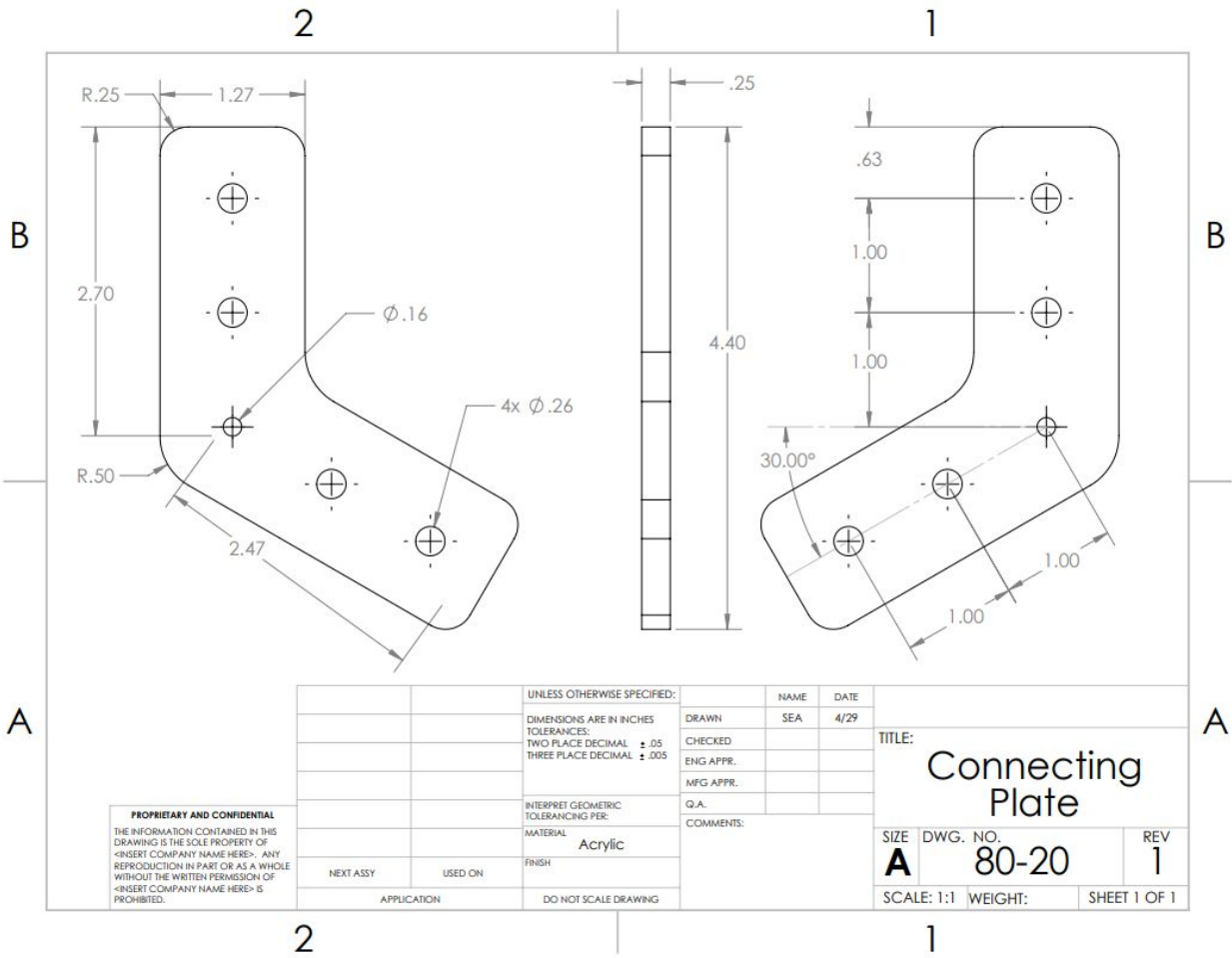
SCALE: 1:5 WEIGHT: SHEET 1 OF 1

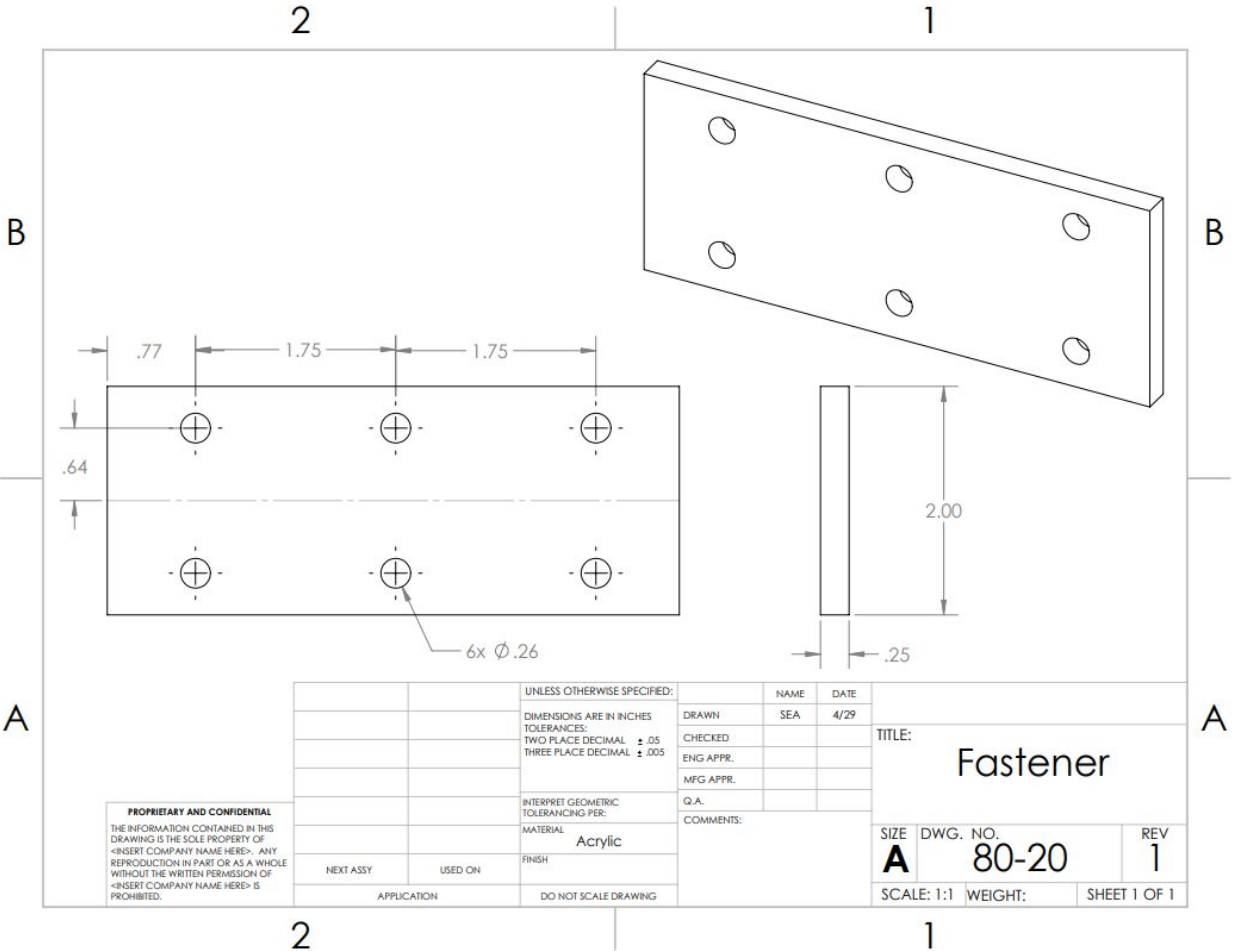


PROPRIETARY AND CONFIDENTIAL
 THE INFORMATION CONTAINED IN THIS DRAWING IS THE SOLE PROPERTY OF <INSERT COMPANY NAME HERE>. ANY REPRODUCTION IN PART OR AS A WHOLE WITHOUT THE WRITTEN PERMISSION OF <INSERT COMPANY NAME HERE> IS PROHIBITED.

		UNLESS OTHERWISE SPECIFIED:		NAME	DATE
		DIMENSIONS ARE IN INCHES		DRAWN	SEA
		TOLERANCES:		CHECKED	4/29
		TWO PLACE DECIMAL ± .05		ENG APPR.	
		THREE PLACE DECIMAL ± .005		MFG APPR.	
		INTERPRET GEOMETRIC TOLERANCING PER:		Q.A.	
		MATERIAL		COMMENTS:	
		Acrylic			
		FINISH			
NEXT ASSY	USED ON				
APPLICATION		DO NOT SCALE DRAWING			

TITLE:		
Area Connector		
SIZE	DWG. NO.	REV
A	80-20	1
SCALE: 1:2	WEIGHT:	SHEET 1 OF 1



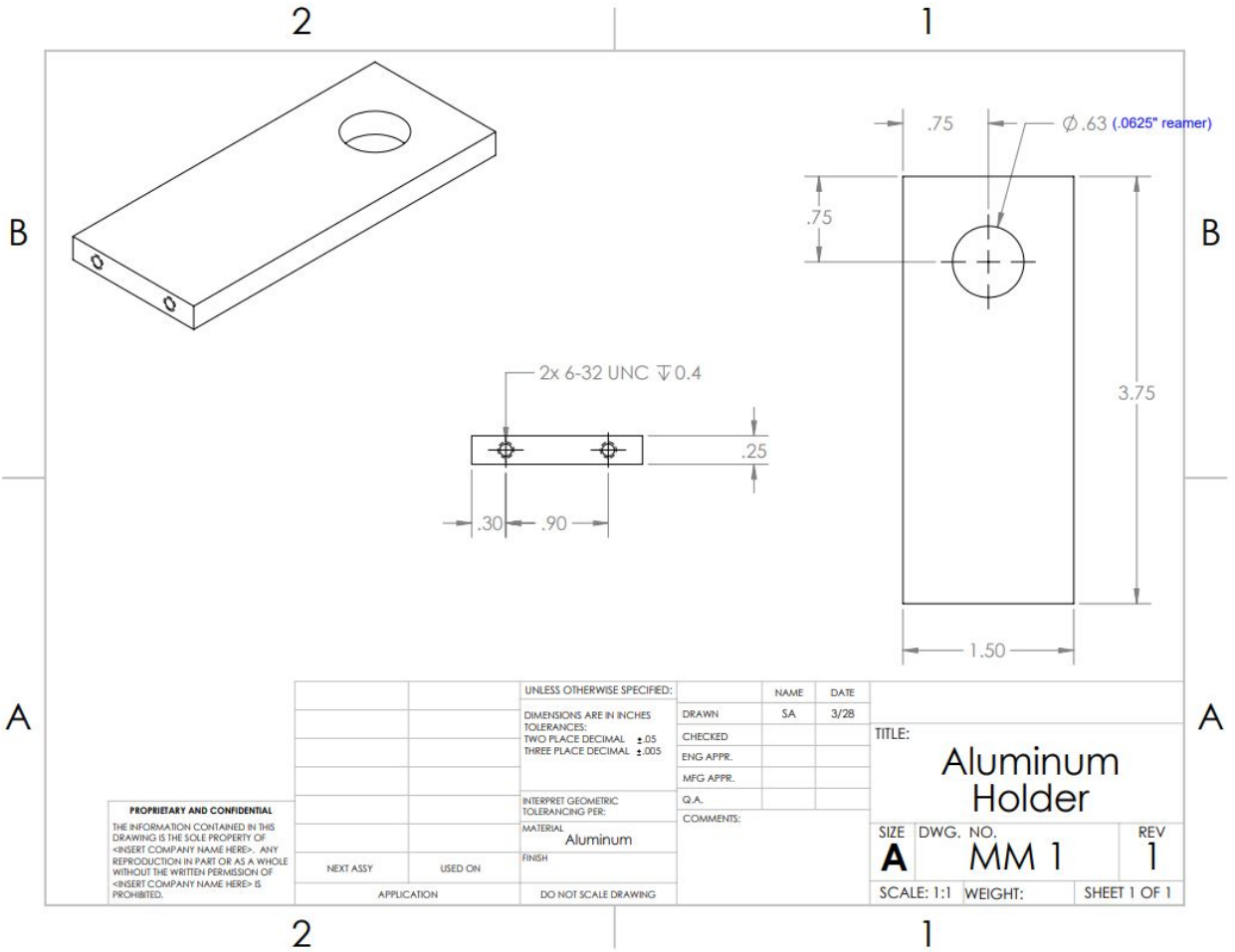


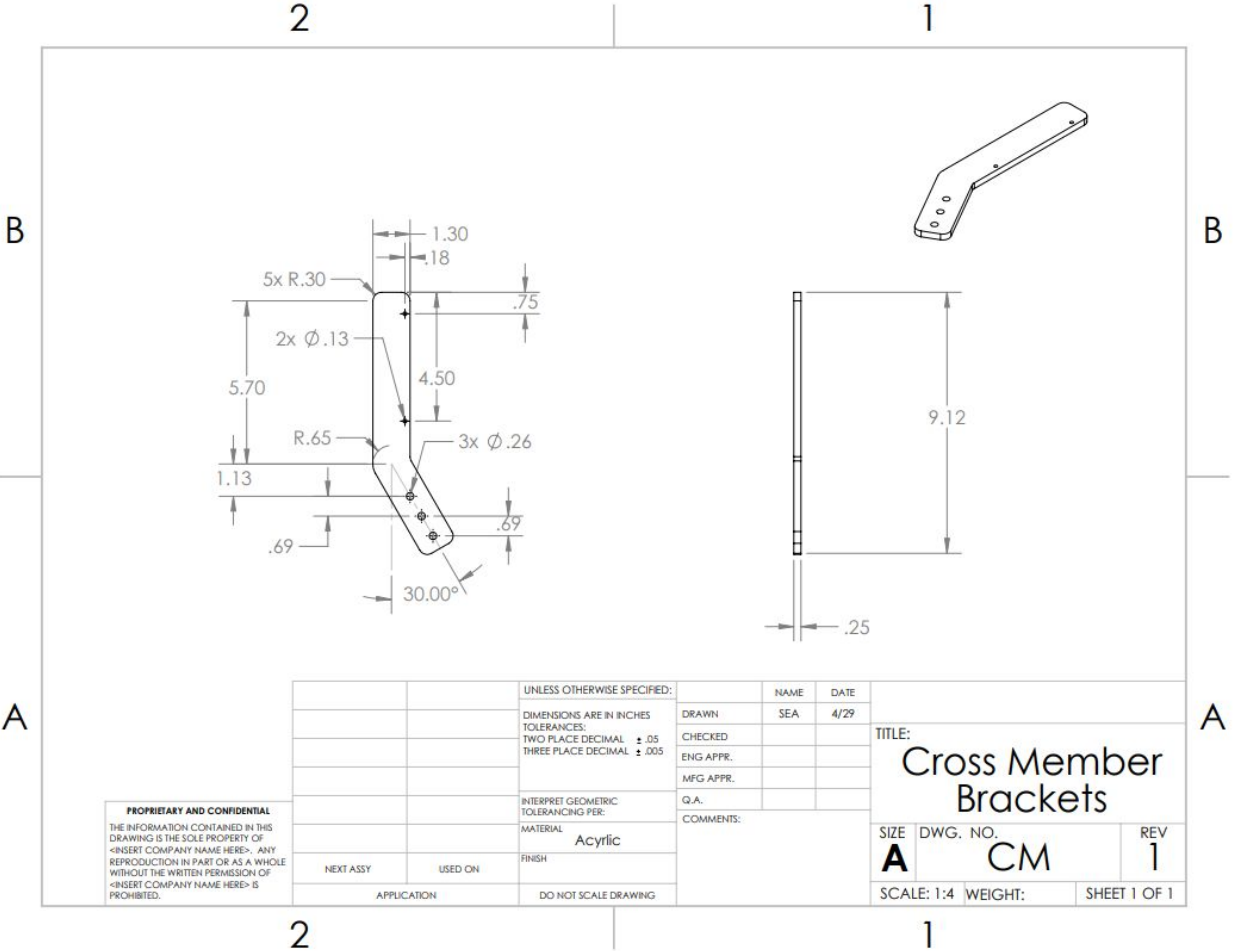
PROPRIETARY AND CONFIDENTIAL
 THE INFORMATION CONTAINED IN THIS DRAWING IS THE SOLE PROPERTY OF <INSERT COMPANY NAME HERE>. ANY REPRODUCTION IN PART OR AS A WHOLE WITHOUT THE WRITTEN PERMISSION OF <INSERT COMPANY NAME HERE> IS PROHIBITED.

		UNLESS OTHERWISE SPECIFIED:
		DIMENSIONS ARE IN INCHES
		TOLERANCES:
		TWO PLACE DECIMAL ± .05
		THREE PLACE DECIMAL ± .005
		INTERPRET GEOMETRIC TOLERANCING PER:
		MATERIAL Acrylic
		FINISH
NEXT ASSY	USED ON	
APPLICATION		DO NOT SCALE DRAWING

	NAME	DATE
DRAWN	SEA	4/29
CHECKED		
ENG APPR.		
MFG APPR.		
Q.A.		
COMMENTS:		

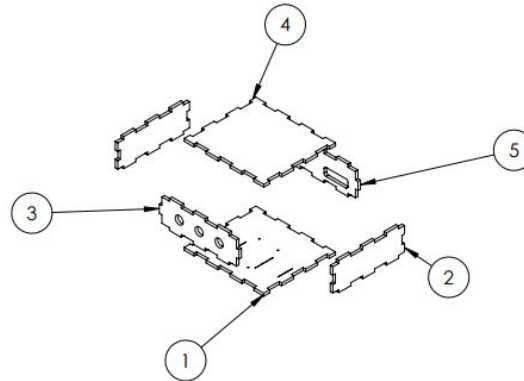
TITLE: Fastener		
SIZE A	DWG. NO. 80-20	REV 1
SCALE: 1:1	WEIGHT:	SHEET 1 OF 1



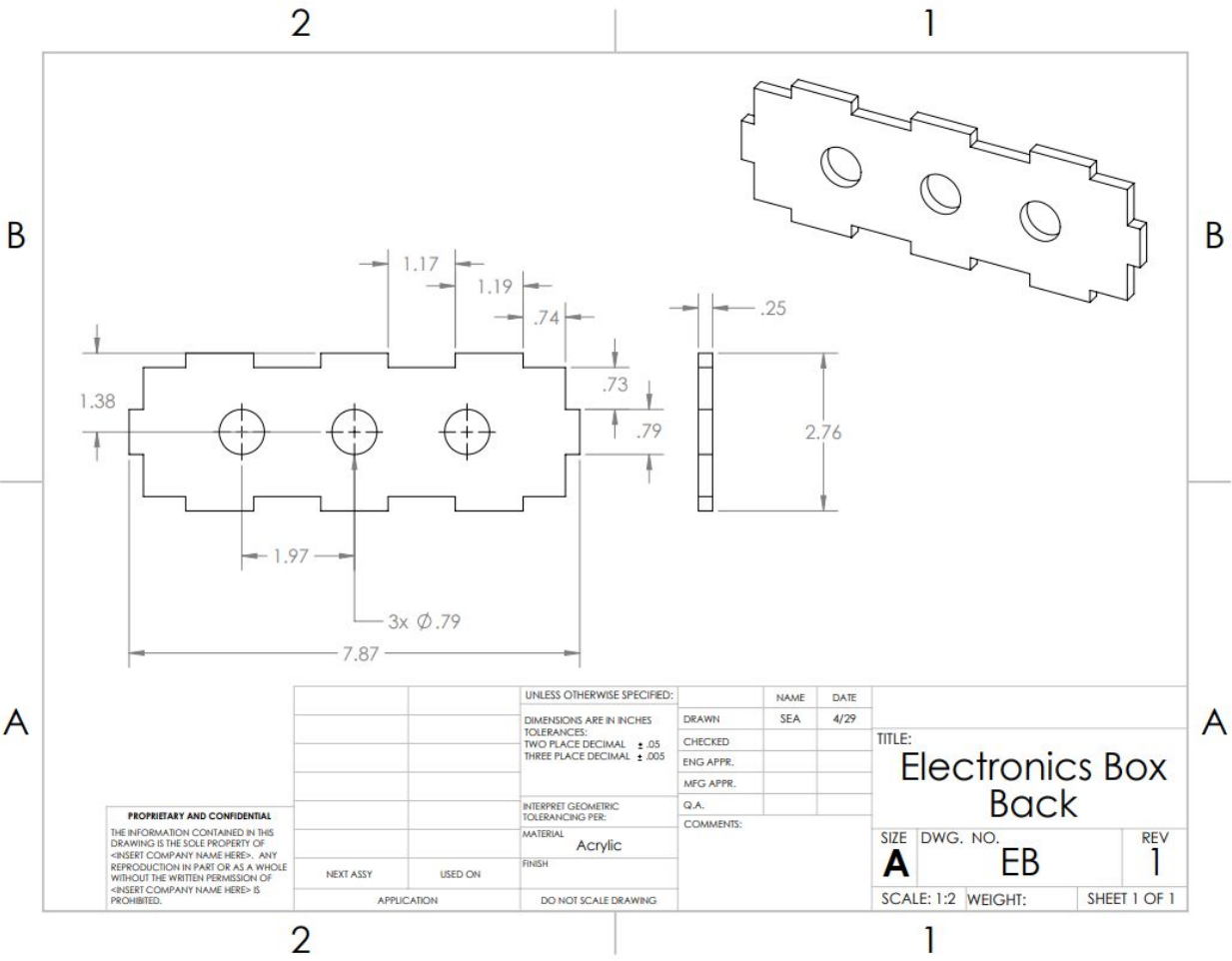


ITEM NO.	PART NUMBER	QTY.
1	Box Bottom	1
2	Box Side	2
3	Box Back	1
4	Box Top	1
5	Box Front	1





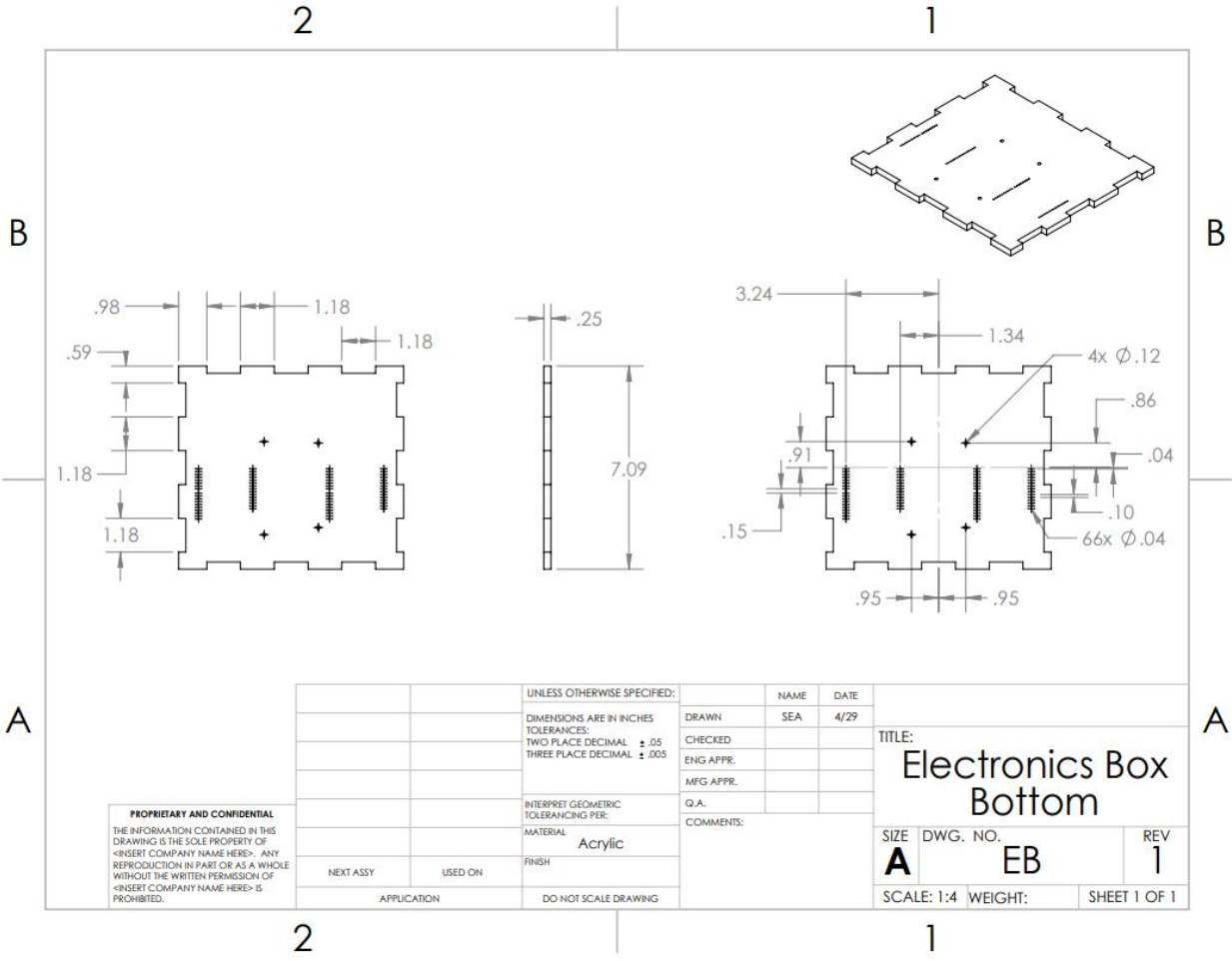
<p>PROPRIETARY AND CONFIDENTIAL</p> <p>THE INFORMATION CONTAINED IN THIS DRAWING IS THE SOLE PROPERTY OF <INSERT COMPANY NAME HERE>. ANY REPRODUCTION IN PART OR AS A WHOLE WITHOUT THE WRITTEN PERMISSION OF <INSERT COMPANY NAME HERE> IS PROHIBITED.</p>			UNLESS OTHERWISE SPECIFIED: DIMENSIONS ARE IN INCHES TOLERANCES: TWO PLACE DECIMAL ±.05 THREE PLACE DECIMAL ±.005	DRAWN CHECKED ENG APPR. MFG APPR. Q.A. COMMENTS:	NAME SEA	DATE 4/29	<p>TITLE:</p> <h2 style="margin: 0;">Electrical Box Assembly</h2>	
	NEXT ASSY	USED ON	MATERIAL Acrylic	FINISH	SIZE A	DWG. NO. EB		REV 1
	APPLICATION		DO NOT SCALE DRAWING		SCALE: 1:8 WEIGHT:			SHEET 1 OF 1



PROPRIETARY AND CONFIDENTIAL
 THE INFORMATION CONTAINED IN THIS DRAWING IS THE SOLE PROPERTY OF <INSERT COMPANY NAME HERE>. ANY REPRODUCTION IN PART OR AS A WHOLE WITHOUT THE WRITTEN PERMISSION OF <INSERT COMPANY NAME HERE> IS PROHIBITED.

		UNLESS OTHERWISE SPECIFIED:		NAME	DATE
		DIMENSIONS ARE IN INCHES		DRAWN	SEA
		TOLERANCES:		CHECKED	4/29
		TWO PLACE DECIMAL ±.05		ENG APPR.	
		THREE PLACE DECIMAL ±.005		MFG APPR.	
		INTERPRET GEOMETRIC TOLERANCING PER:		Q.A.	
		MATERIAL		COMMENTS:	
		Acrylic			
		FINISH			
NEXT ASSY	USED ON				
APPLICATION		DO NOT SCALE DRAWING			

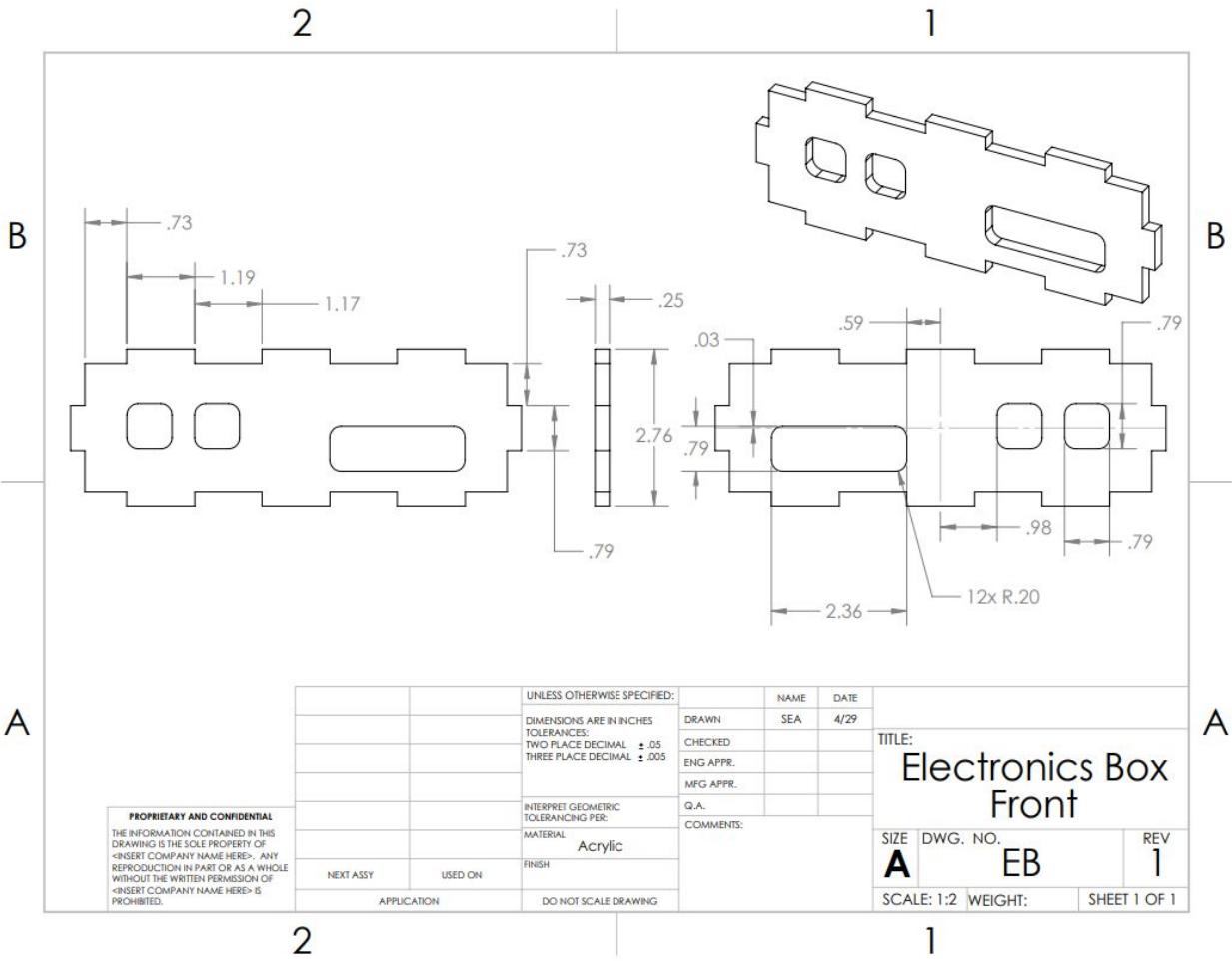
TITLE:		
Electronics Box Back		
SIZE	DWG. NO.	REV
A	EB	1
SCALE: 1:2 WEIGHT:		SHEET 1 OF 1



PROPRIETARY AND CONFIDENTIAL
 THE INFORMATION CONTAINED IN THIS DRAWING IS THE SOLE PROPERTY OF <INSERT COMPANY NAME HERE>. ANY REPRODUCTION IN PART OR AS A WHOLE WITHOUT THE WRITTEN PERMISSION OF <INSERT COMPANY NAME HERE> IS PROHIBITED.

		UNLESS OTHERWISE SPECIFIED:		NAME	DATE
		DIMENSIONS ARE IN INCHES		DRAWN	SEA
		TOLERANCES:			4/29
		TWO PLACE DECIMAL ± .05		CHECKED	
		THREE PLACE DECIMAL ± .005		ENG APPR.	
		INTERPRET GEOMETRIC TOLERANCING PER:		MFG APPR.	
		MATERIAL		Q.A.	
		Acrylic		COMMENTS:	
		FINISH			
NEXT ASSY	USED ON				
APPLICATION		DO NOT SCALE DRAWING			

TITLE:		
Electronics Box Bottom		
SIZE	DWG. NO.	REV
A	EB	1
SCALE: 1:4	WEIGHT:	SHEET 1 OF 1



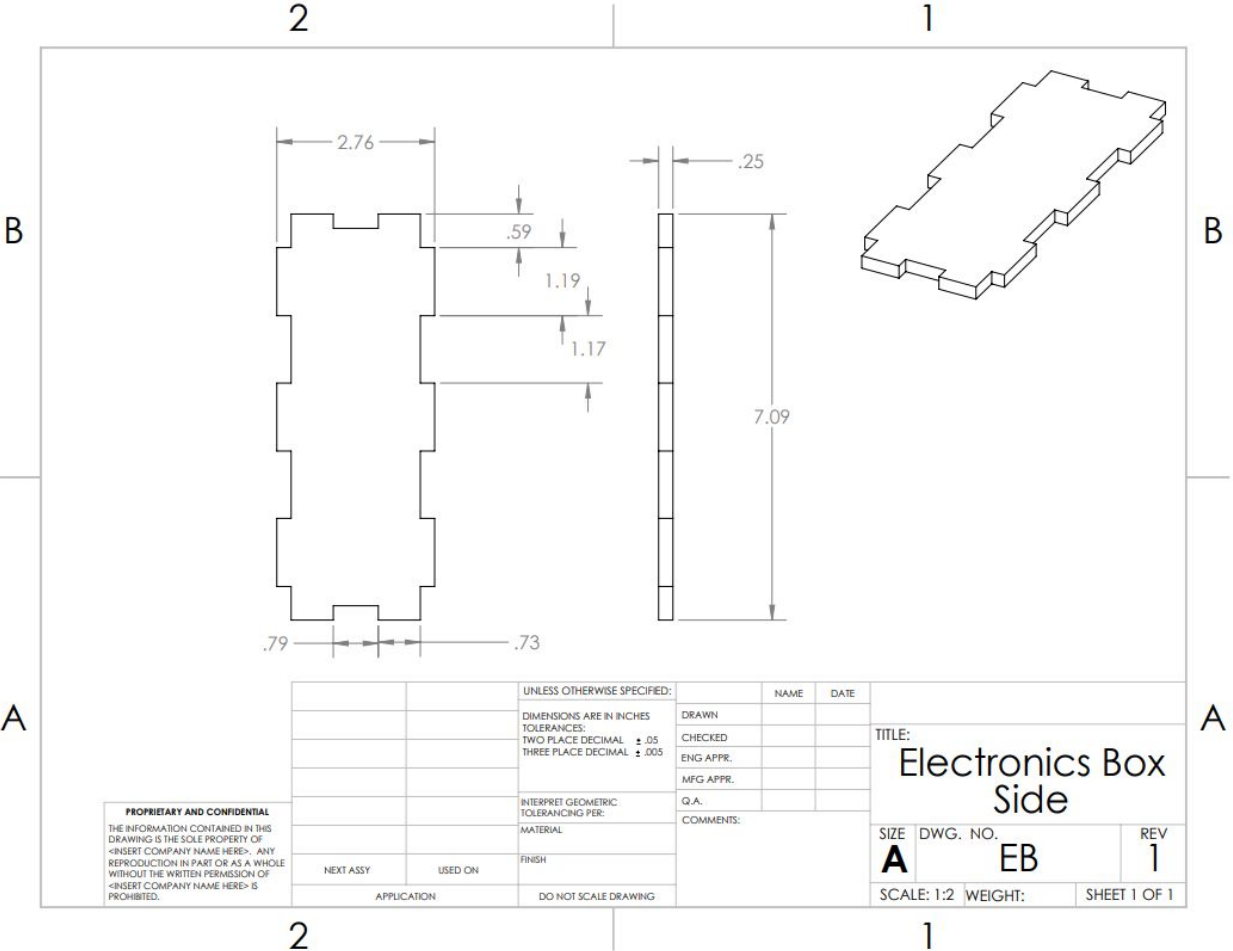
PROPRIETARY AND CONFIDENTIAL
 THE INFORMATION CONTAINED IN THIS DRAWING IS THE SOLE PROPERTY OF <INSERT COMPANY NAME HERE>. ANY REPRODUCTION IN PART OR AS A WHOLE WITHOUT THE WRITTEN PERMISSION OF <INSERT COMPANY NAME HERE> IS PROHIBITED.

		UNLESS OTHERWISE SPECIFIED:		NAME	DATE
		DIMENSIONS ARE IN INCHES		DRAWN	SEA
		TOLERANCES:		CHECKED	4/29
		TWO PLACE DECIMAL ± .05		ENG APPR.	
		THREE PLACE DECIMAL ± .005		MFG APPR.	
		INTERPRET GEOMETRIC TOLERANCING PER:		Q.A.	
		MATERIAL		COMMENTS:	
		Acrylic			
		FINISH			
NEXT ASSY	USED ON				
APPLICATION		DO NOT SCALE DRAWING			

TITLE:
Electronics Box Front

SIZE	DWG. NO.	REV
A	EB	1

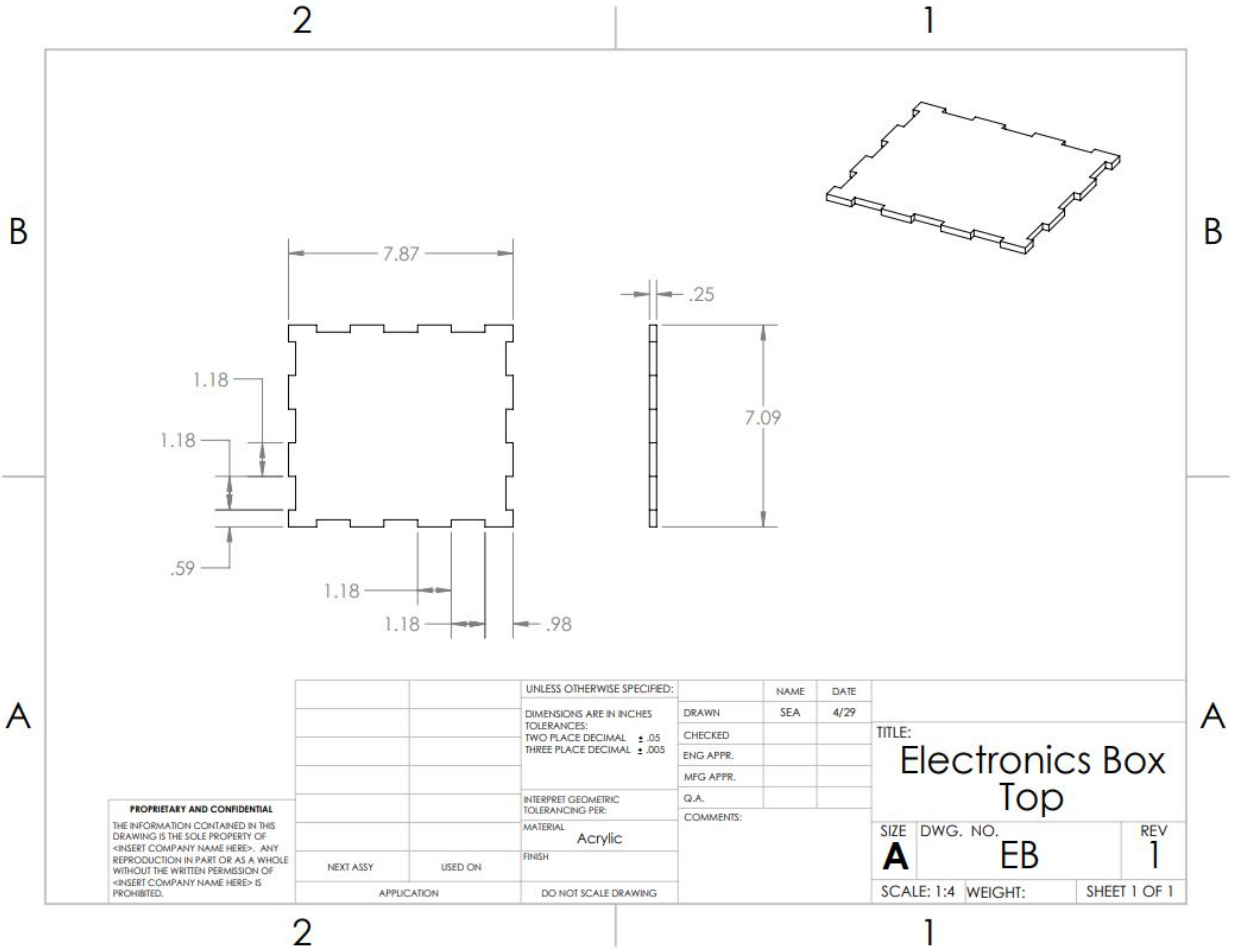
SCALE: 1:2 WEIGHT: SHEET 1 OF 1

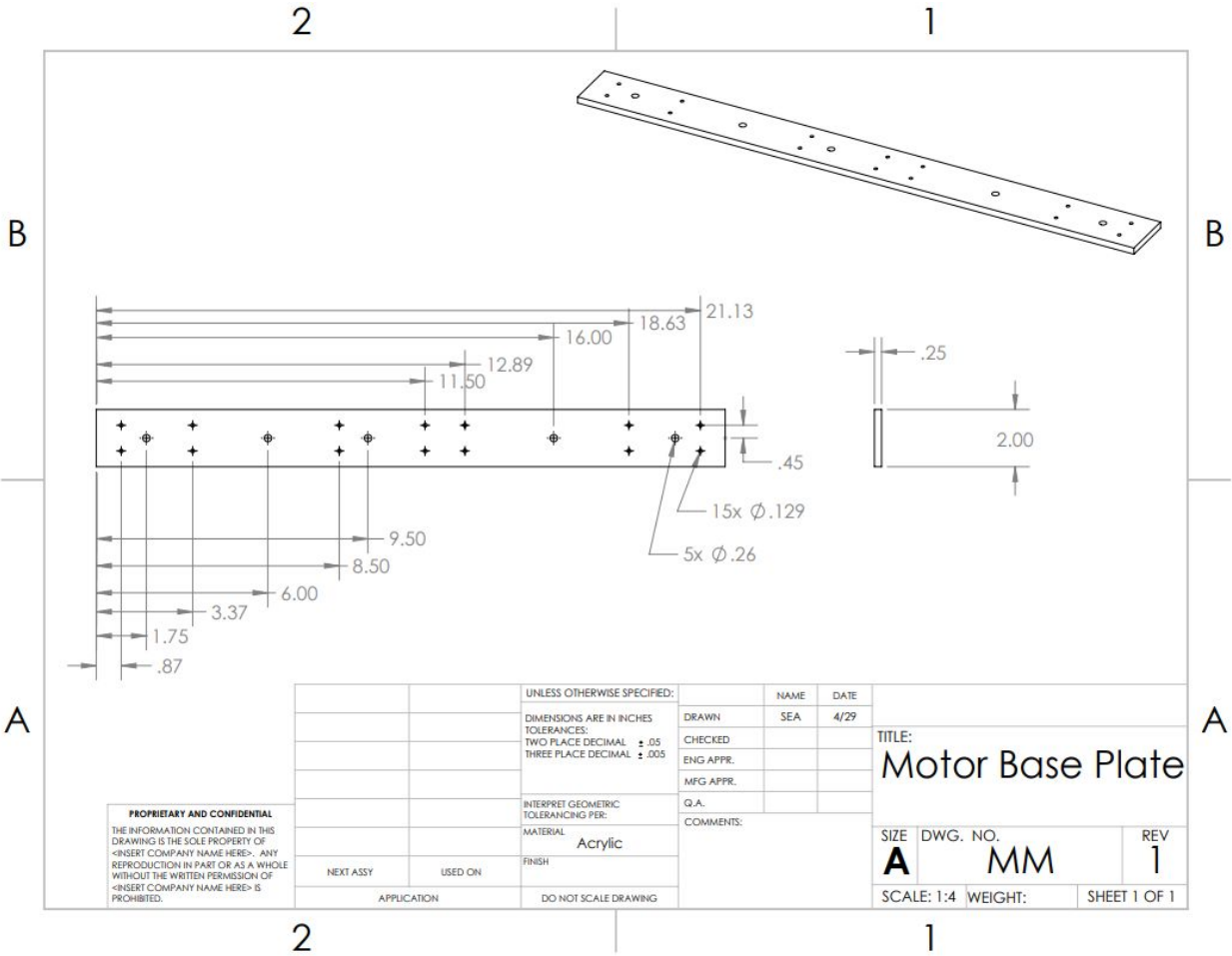


PROPRIETARY AND CONFIDENTIAL
 THE INFORMATION CONTAINED IN THIS DRAWING IS THE SOLE PROPERTY OF <INSERT COMPANY NAME HERE>. ANY REPRODUCTION IN PART OR AS A WHOLE WITHOUT THE WRITTEN PERMISSION OF <INSERT COMPANY NAME HERE> IS PROHIBITED.

		UNLESS OTHERWISE SPECIFIED:		NAME	DATE
		DIMENSIONS ARE IN INCHES		DRAWN	
		TOLERANCES:		CHECKED	
		TWO PLACE DECIMAL ± .05		ENG APPR.	
		THREE PLACE DECIMAL ± .005		MFG APPR.	
		INTERPRET GEOMETRIC TOLERANCING PER:		Q.A.	
		MATERIAL		COMMENTS:	
		FINISH			
NEXT ASSY	USED ON				
APPLICATION		DO NOT SCALE DRAWING			

TITLE:		
Electronics Box Side		
SIZE	DWG. NO.	REV
A	EB	1
SCALE: 1:2 WEIGHT:		SHEET 1 OF 1



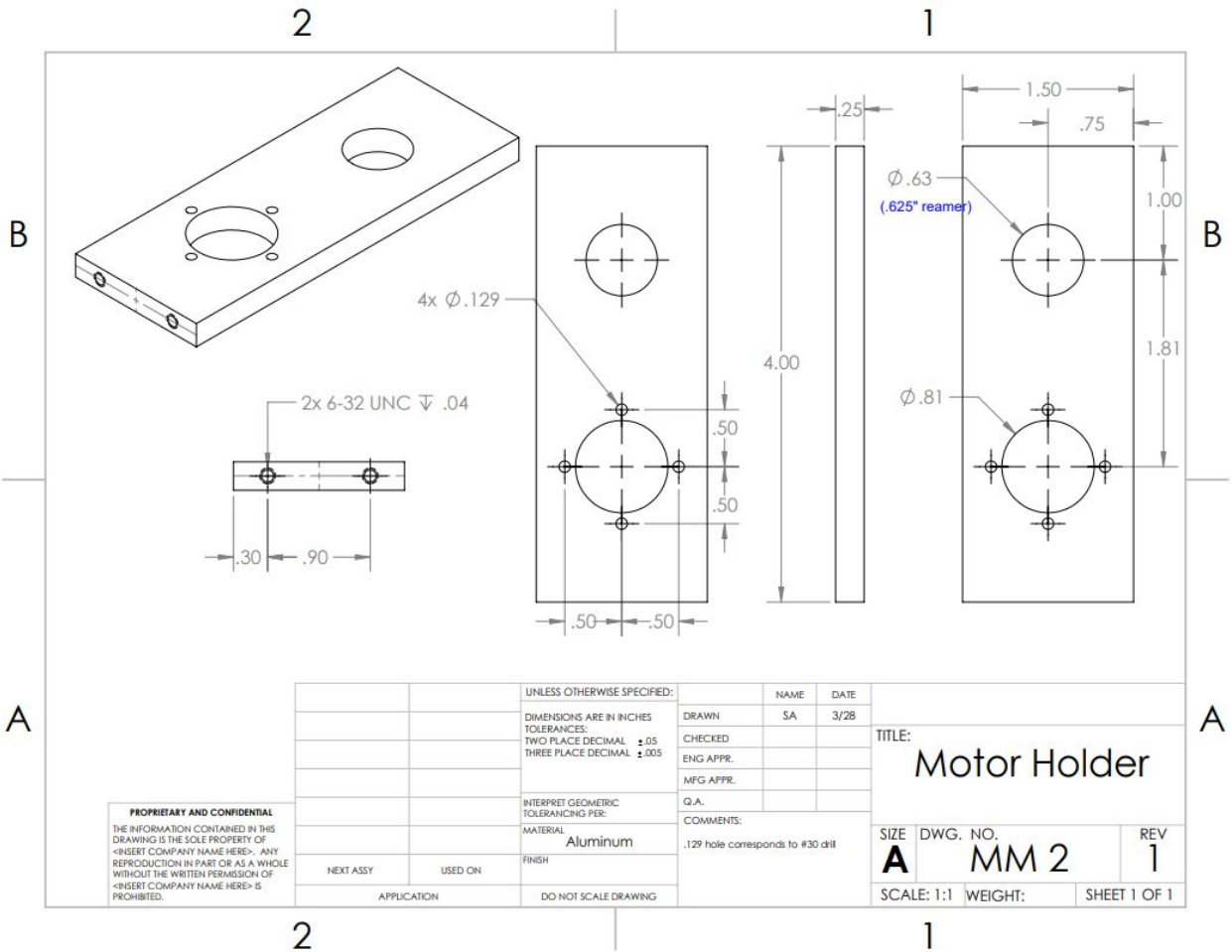


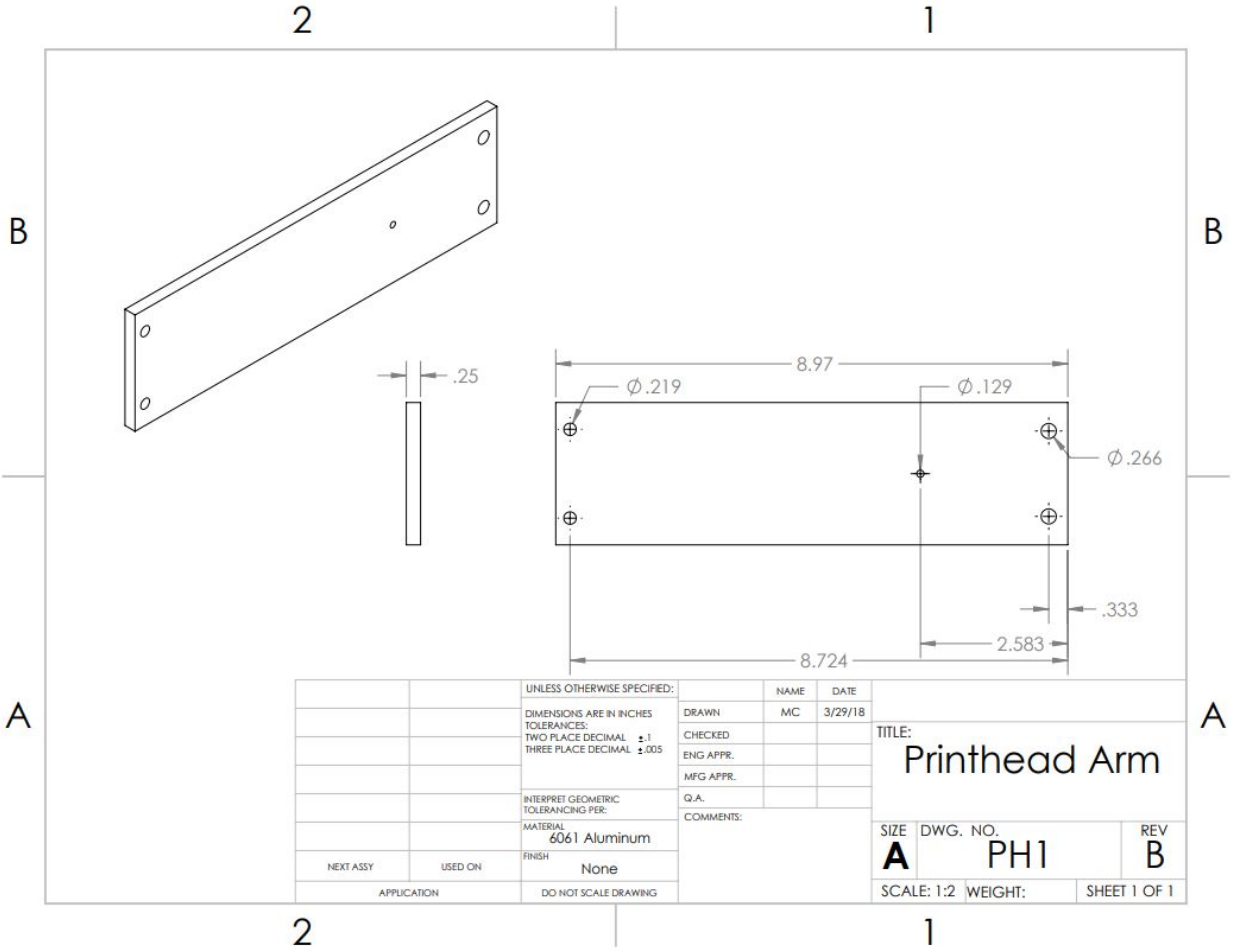
PROPRIETARY AND CONFIDENTIAL
 THE INFORMATION CONTAINED IN THIS DRAWING IS THE SOLE PROPERTY OF <INSERT COMPANY NAME HERE>. ANY REPRODUCTION IN PART OR AS A WHOLE WITHOUT THE WRITTEN PERMISSION OF <INSERT COMPANY NAME HERE> IS PROHIBITED.

		UNLESS OTHERWISE SPECIFIED:	NAME	DATE
		DIMENSIONS ARE IN INCHES	DRAWN	SEA
		TOLERANCES:	CHECKED	4/29
		TWO PLACE DECIMAL ±.05	ENG APPR.	
		THREE PLACE DECIMAL ±.005	MFG APPR.	
		INTERPRET GEOMETRIC TOLERANCING PER:	Q.A.	
		MATERIAL	COMMENTS:	
		Acrylic		
		FINISH		
NEXT ASSY	USED ON	APPLICATION	DO NOT SCALE DRAWING	

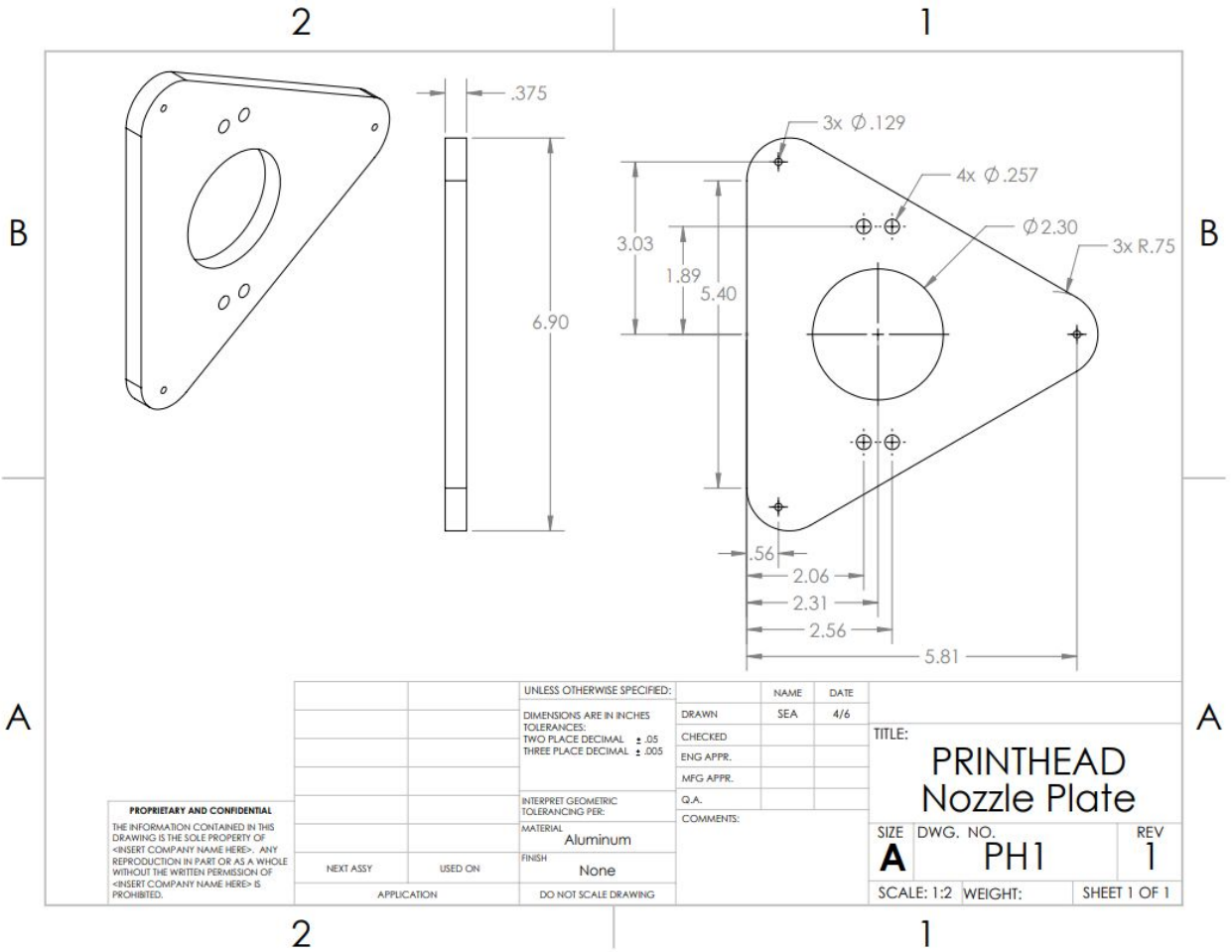
TITLE:
Motor Base Plate

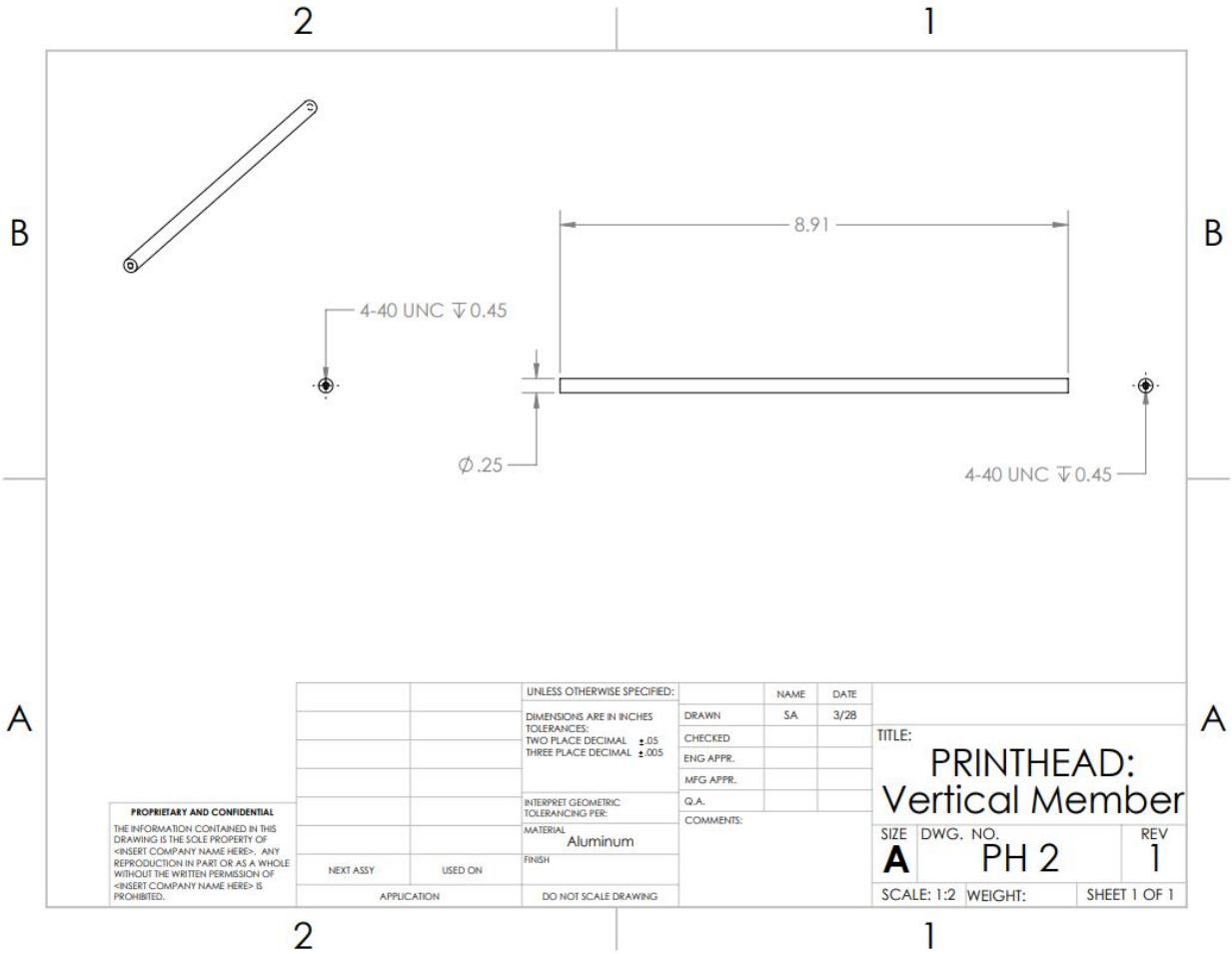
SIZE	DWG. NO.	REV
A	MM	1
SCALE: 1:4		WEIGHT:
		SHEET 1 OF 1





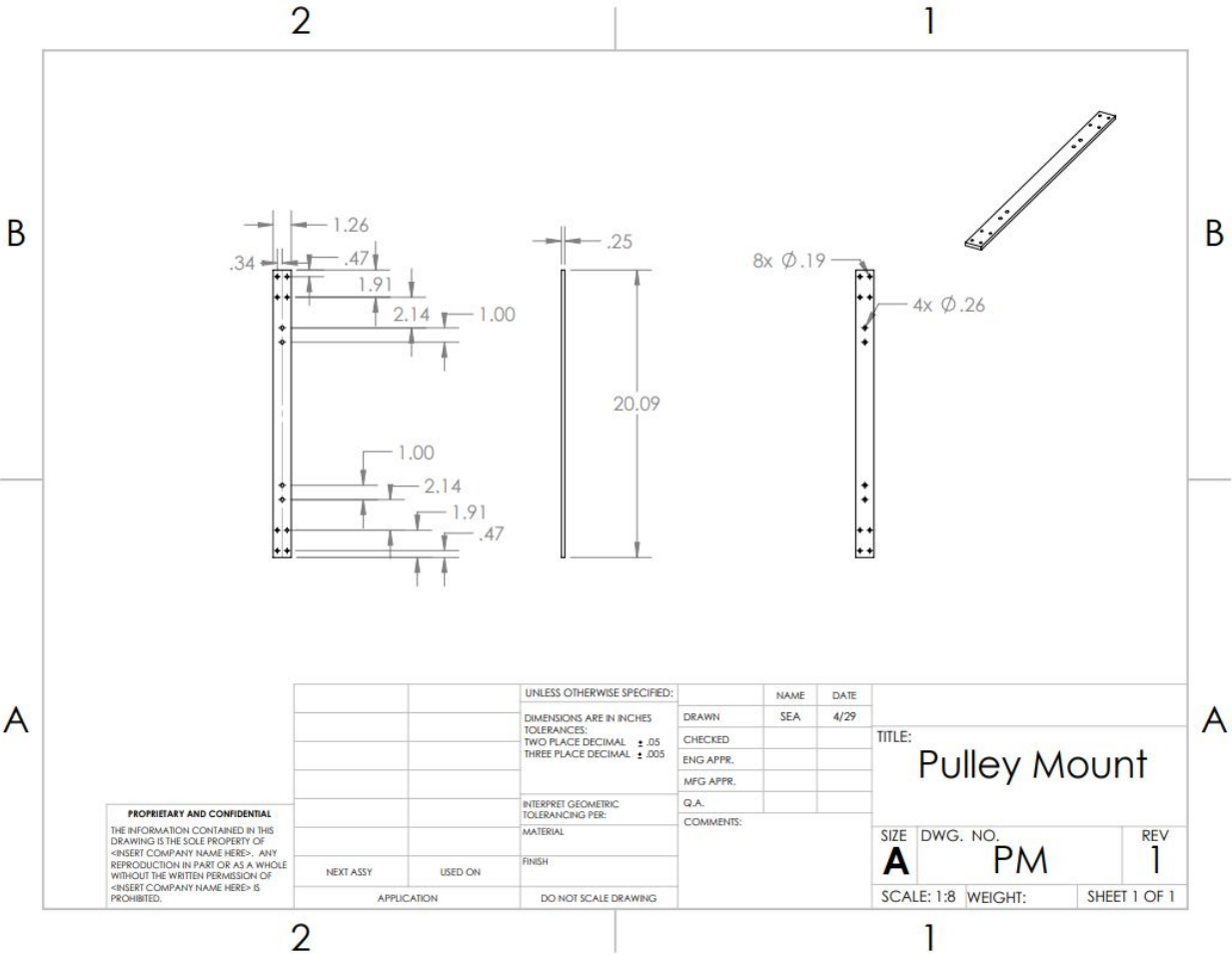
		UNLESS OTHERWISE SPECIFIED:	NAME	DATE		
		DIMENSIONS ARE IN INCHES	DRAWN	MC	3/29/18	TITLE: Printhead Arm
		TOLERANCES:	CHECKED			
		TWO PLACE DECIMAL $\pm .1$	ENG APPR.			
		THREE PLACE DECIMAL $\pm .005$	MFG APPR.			
		INTERPRET GEOMETRIC TOLERANCING PER:	Q.A.			SIZE DWG. NO. REV A PH1 B
		MATERIAL	COMMENTS:			
		5061 Aluminum				SCALE: 1:2 WEIGHT: SHEET 1 OF 1
NEXT ASSY	USED ON	FINISH				
APPLICATION		DO NOT SCALE DRAWING				

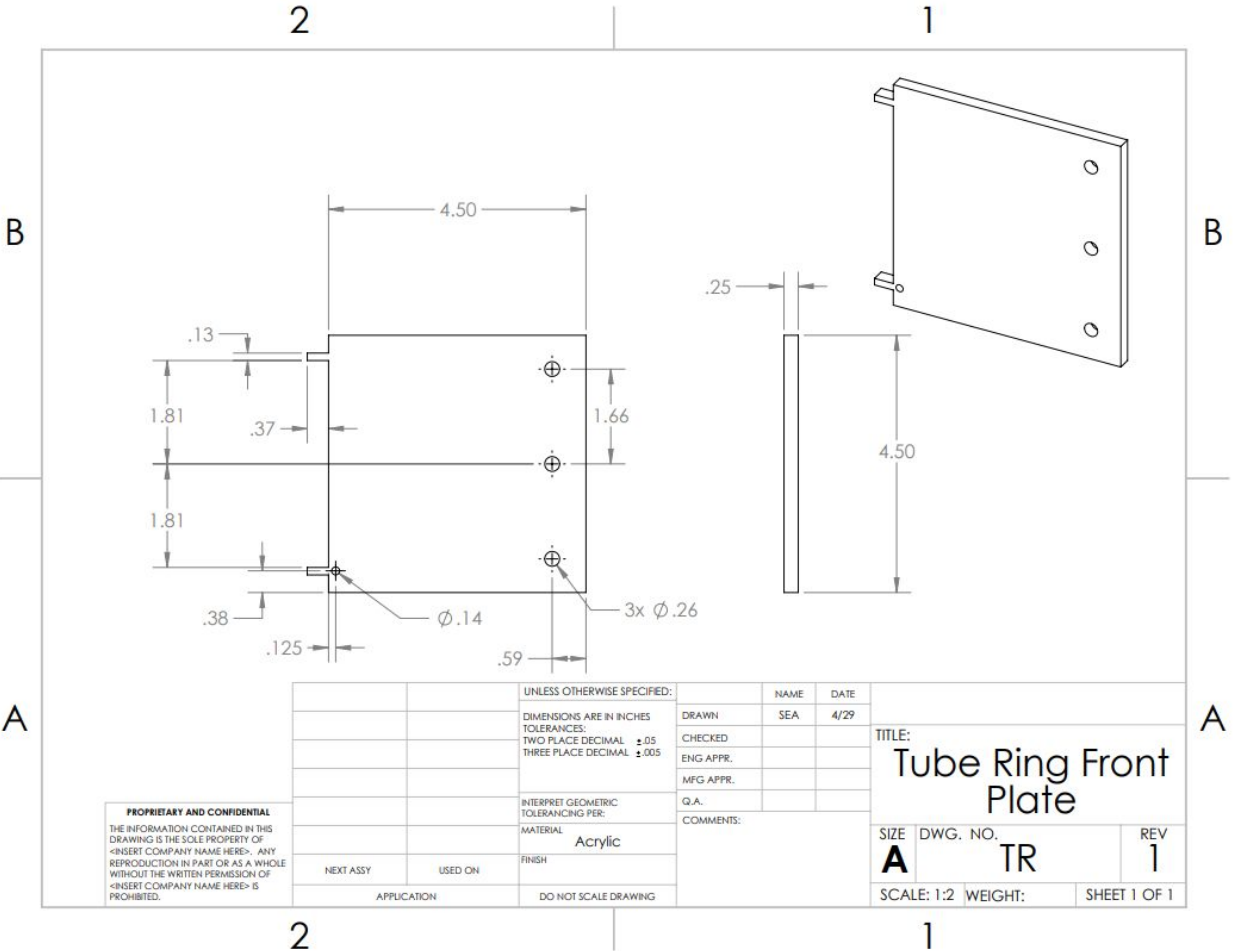




PROPRIETARY AND CONFIDENTIAL
 THE INFORMATION CONTAINED IN THIS DRAWING IS THE SOLE PROPERTY OF <INSERT COMPANY NAME HERE>. ANY REPRODUCTION IN PART OR AS A WHOLE WITHOUT THE WRITTEN PERMISSION OF <INSERT COMPANY NAME HERE> IS PROHIBITED.

		UNLESS OTHERWISE SPECIFIED:		NAME	DATE
		DIMENSIONS ARE IN INCHES		DRAWN	SA
		TOLERANCES:		CHECKED	3/28
		TWO PLACE DECIMAL ±.05		ENG APPR.	
		THREE PLACE DECIMAL ±.005		MFG APPR.	
		INTERPRET GEOMETRIC TOLERANCING PER:		Q.A.	
		MATERIAL		COMMENTS:	
		Aluminum		TITLE:	
NEXT ASSY	USED ON	FINISH		PRINTHEAD: Vertical Member	
APPLICATION		DO NOT SCALE DRAWING		SIZE	DWG. NO.
				A	PH 2
				SCALE: 1:2	WEIGHT:
					REV
					1
					SHEET 1 OF 1

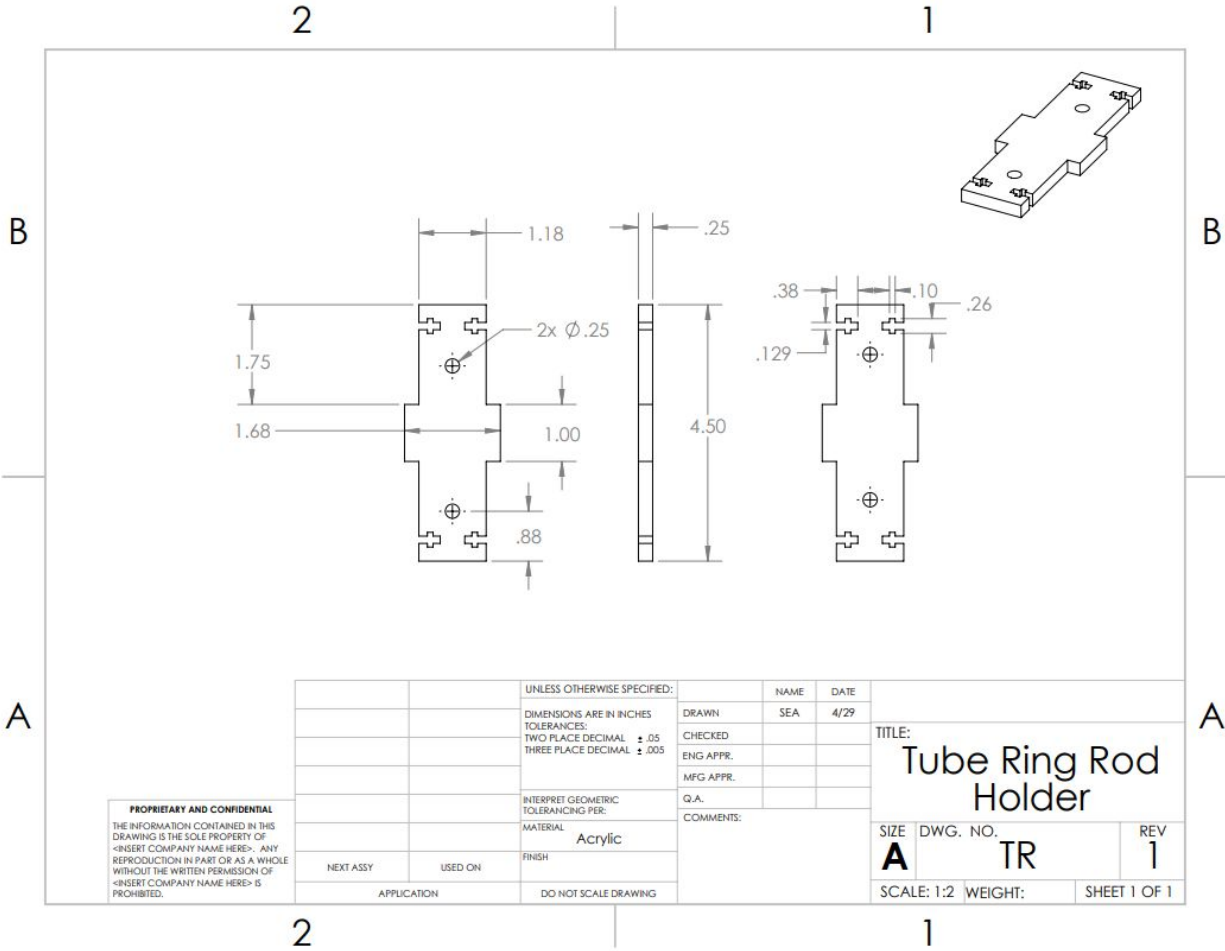




PROPRIETARY AND CONFIDENTIAL
 THE INFORMATION CONTAINED IN THIS DRAWING IS THE SOLE PROPERTY OF <INSERT COMPANY NAME HERE>. ANY REPRODUCTION IN PART OR AS A WHOLE WITHOUT THE WRITTEN PERMISSION OF <INSERT COMPANY NAME HERE> IS PROHIBITED.

		UNLESS OTHERWISE SPECIFIED:		NAME	DATE
		DIMENSIONS ARE IN INCHES		DRAWN	SEA
		TOLERANCES:		CHECKED	4/29
		TWO PLACE DECIMAL ±.05		ENG APPR.	
		THREE PLACE DECIMAL ±.005		MFG APPR.	
		INTERPRET GEOMETRIC TOLERANCING PER:		Q.A.	
		MATERIAL		COMMENTS:	
		Acrylic			
		FINISH			
NEXT ASSY	USED ON				
APPLICATION		DO NOT SCALE DRAWING			

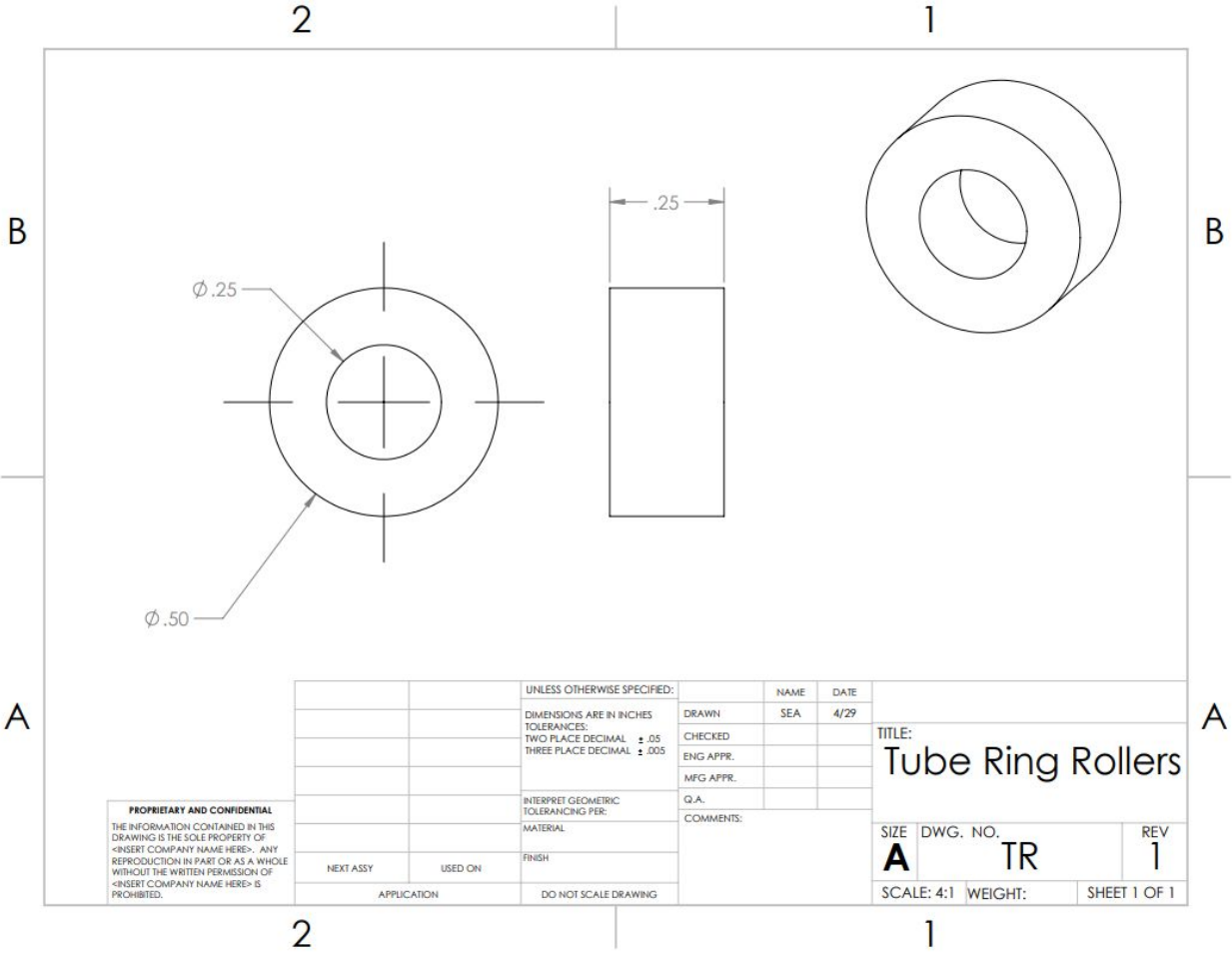
TITLE:		
Tube Ring Front Plate		
SIZE	DWG. NO.	REV
A	TR	1
SCALE: 1:2		WEIGHT:
		SHEET 1 OF 1



PROPRIETARY AND CONFIDENTIAL
 THE INFORMATION CONTAINED IN THIS DRAWING IS THE SOLE PROPERTY OF <INSERT COMPANY NAME HERE>. ANY REPRODUCTION IN PART OR AS A WHOLE WITHOUT THE WRITTEN PERMISSION OF <INSERT COMPANY NAME HERE> IS PROHIBITED.

		UNLESS OTHERWISE SPECIFIED:	NAME	DATE
		DIMENSIONS ARE IN INCHES	DRAWN	SEA
		TOLERANCES:	CHECKED	4/29
		TWO PLACE DECIMAL ±.05	ENG APPR.	
		THREE PLACE DECIMAL ±.005	MFG APPR.	
		INTERPRET GEOMETRIC TOLERANCING PER:	Q.A.	
		MATERIAL	COMMENTS:	
		Acrylic		
NEXT ASSY	USED ON	FINISH		
APPLICATION		DO NOT SCALE DRAWING		

TITLE:		
Tube Ring Rod Holder		
SIZE	DWG. NO.	REV
A	TR	1
SCALE: 1:2	WEIGHT:	SHEET 1 OF 1



PROPRIETARY AND CONFIDENTIAL
 THE INFORMATION CONTAINED IN THIS DRAWING IS THE SOLE PROPERTY OF <INSERT COMPANY NAME HERE>. ANY REPRODUCTION IN PART OR AS A WHOLE WITHOUT THE WRITTEN PERMISSION OF <INSERT COMPANY NAME HERE> IS PROHIBITED.

		UNLESS OTHERWISE SPECIFIED:		NAME	DATE
		DIMENSIONS ARE IN INCHES	DRAWN	SEA	4/29
		TOLERANCES:	CHECKED		
		TWO PLACE DECIMAL $\pm .05$	ENG APPR.		
		THREE PLACE DECIMAL $\pm .005$	MFG APPR.		
		INTERPRET GEOMETRIC TOLERANCING PER:	Q.A.		
		MATERIAL	COMMENTS:		
		FINISH			
NEXT ASSY	USED ON				
APPLICATION		DO NOT SCALE DRAWING			

TITLE:		
Tube Ring Rollers		
SIZE	DWG. NO.	REV
A	TR	1
SCALE: 4:1	WEIGHT:	SHEET 1 OF 1